

Characterizing the roles of the putative Tor1p effector, Sfp1p, in
growth and development of the fungal pathogen *Candida albicans*

Amine El Osmani

A Thesis
in
The Department
of
Biology

Presented in Partial Fulfilment of the Requirements
for the Degree of Master of Science (Biology) at
Concordia University
Montreal, Quebec, Canada

April 2013

© Amine El Osmani, 2013

CONCORDIA UNIVERSITY
School of Graduate Studies

This is to certify that the thesis prepared

By: Amine El Osmani

Entitled: Characterizing the roles of the putative Tor1p effector, Sfp1p, in growth and development of the fungal pathogen *Candida albicans*

and submitted in partial fulfilment of the requirements for the degree of

Master of Science (Biology)

complies with the regulations of the University and meets the accepted standards with respect to originality and quality.

Signed by the final Examining Committee:

Dr. Selvadurai Dayanandan Chair

Dr. Reginald Storms Examiner

Dr. Vladimir Titorenko Examiner

Dr. Michael Sacher External Examiner

Dr. Catherine Bachewich Supervisor

Approved by _____

Chair of Department or Graduate Program Director

_____ 2013

_____ Dean of Faculty

ABSTRACT

Characterizing the roles of the putative Tor1p effector, Sfp1p, in growth and development of the fungal pathogen *Candida albicans*

Amine El Osmani

C. albicans is one of the most common fungal pathogens of humans. Important virulence-determining traits include proper cell proliferation and the ability to develop into different cell types, including yeast, pseudohyphae and hyphae. Both of these processes are dependent on environmental cues such as availability and types of nutrients. It is thus important to understand how these cues are sensed and integrated with the machinery that control cell division and development. The TOR pathway plays an important role in mediating environmental conditions in many organisms, and accordingly, TOR kinase is required for cell division and the maintenance of hyphal growth in *C. albicans* (1). However, the mechanisms by which TOR regulates these processes in the pathogen are not clear. Here, we provide the first characterization of Sfp1p, an orthologue of a major downstream effector of TOR kinase in *S. cerevisiae*. Deletion of *SFPI* in *C. albicans* resulted in a decrease in cell size, which could be reduced further in the presence of poor carbon source media. The *sfp1D/sfp1D* cells grew slowly, formed small colonies, and were more sensitive to rapamycin, suggesting that Sfp1p mediates a least part of Tor1p function in *C. albicans*. Transcription profiles of the deletion strain demonstrated down-regulation of genes involved in ribosome biogenesis, translation, and amino acid synthesis,

consistent with a role in the TOR pathway. However, many hyphal-specific genes were upregulated, as well as some genes associated with the opaque cell fate, suggesting additional and novel links with development.

ACKNOWLEDGEMENTS

I would like to thank my supervisor, Dr. Catherine Bachewich, for her wisdom, guidance and encouragement, my current and past professors and committee members, Dr. Muriel Herrigton, Dr. William Zerges, Dr. Reginald Storms, Dr. Vladimir Titorenko and Dr. Michael Sacher for their valuable time and advice, Dr. Martine Raymond for the plasmid (p425 – GPD – Ca*CDR3*) and strain (CIB4 [YPB-ADHpt/CDR3]), my colleagues Amandeep Glory, Hao Huang, Bahira Hussein and Hsini Chou for their contributions, and my family and friends for their continuous support.

This study was funded by Concordia University and a CIHR Team Grant Program part of the CIHR Team in Fungal Pathogenesis.

Table of Contents

List of Figures.....	ix
List of Tables.....	x
List of Acronyms.....	xi
1.0 Introduction	1
1.1 <i>C. albicans</i> Overview.....	1
1.2 Virulence-determining trait: Morphogenesis	2
1.2.1 <i>C. albicans</i> cell types.....	2
1.2.2 Environmental regulation of morphogenesis	3
1.3 Virulence-determining trait: Cell proliferation.....	4
1.3.1 Cell cycle and G1/S regulation in <i>S. cerevisiae</i>	4
1.3.2 Cell cycle regulation in <i>C. albicans</i> : G1/S transition.....	6
1.4 The G1/S transition and its relationship with morphogenesis.....	7
1.5 Environmental sensing and cell cycle progression: the TOR pathway.....	8
1.5.1 TORC complex.....	8
1.5.2 TORC effectors.....	10
1.5.3 The nutrient sensing Split Zinc Finger Protein Sfp1p is also a target of Tor1p.....	11
1.5.4 TOR pathway and <i>C. albicans</i>	12
1.6 Objectives.....	13
2.0 Materials & Methods.....	15
2.1 Media and growth conditions	15
2.2 Strain construction.....	16
2.3 Transformation.....	18
2.4 Genomic DNA extraction.....	19
2.5 PCR screening of strains.....	20
2.6 Southern blotting.....	22

2.7 Microscopy.....	24
2.8 RNA extraction.....	25
2.9 Microarray Expression Analysis.....	26
2.10 Northern blotting.....	27
2.11 Quantitative RT-PCR.....	30
2.12 Western Blotting.....	31
3.0 Results.....	33
3.1 <i>C. albicans</i> contains an <i>SFPI</i> orthologue.....	33
3.2 Absence of <i>SFPI</i> reduces cell size and growth rate.....	34
3.3 Sfp1p is not essential for mediating cell size in response to select poor carbon sources.....	36
3.4 <i>C. albicans</i> is hypersensitive to sublethal concentrations of rapamycin in the absence of Sfp1p.....	37
3.5 Sfp1p levels increase during cell cycle progression in <i>C. albicans</i>	37
3.6 The absence of Sfp1p reduces the diameter of hyphal cells, and impairs filamentation under specific conditions.....	40
3.7 Sfp1p modulates metabolism, ribosome biogenesis, cell cycle, and development genes.....	41
4.0 Discussion.....	47
4.1 Sfp1p is important for the regulation of cell size and growth in <i>C. albicans</i> ..	47
4.2 Sfp1p may function in part through regulating ribosome biogenesis.....	49
4.3 Sfp1p may be a component of the TOR pathway in <i>C. albicans</i>	50
4.4 Sfp1p influences filament development in <i>C. albicans</i>	52
4.5 Sfp1p and the TOR pathway may be linked to the developmental state of mating in <i>C. albicans</i>	54
4.6 Sfp1p and Sch9p show more divergence in function in <i>C. albicans</i> than in <i>S. cerevisiae</i>	55
4.7 Conclusions.....	56

4.8 Future work.....	56
5.0 Figures.....	58
6.0 Tables.....	73
7.0 References.....	81
8.0 Appendix.....	90
Table S1: Length by width ratios of the <i>sfp1Δ/sfp1Δ</i> strain compared to the control strain in media containing different carbon sources.....	90
Table S2: List of modulated genes of the <i>sfp1Δ/sfp1Δ</i> microarray expression experiment.....	92

LIST OF FIGURES

- Figure 1: Signalling pathways regulating hyphal gene expression in *C. albicans*.
- Figure 2: TORC1 pathway effectors in *S. cerevisiae*.
- Figure 3: PCR gene manipulation strategies.
- Figure 4: Confirmation of the *sfp1Δ/sfp1Δ* strains by PCR and Southern Blot.
- Figure 5: Confirmation of the *MET3::SFP1-URA3/sfp1Δ::HIS1* (AM1511 & AM1512) strains by PCR.
- Figure 6: Cells depleted of Sfp1p show a reduction in size.
- Figure 7: Cells lacking Sfp1p are reduced in growth rate.
- Figure 8: Cells lacking Sfp1p can still modulate cell size in response to select poor carbon sources.
- Figure 9: Cells lacking Sfp1p are hypersensitive to sublethal concentrations of Rapamycin.
- Figure 10: Construction and confirmation of Sfp1-HA and Sfp1p-GFP strains.
- Figure 11: Sfp1p-HA levels increase during cell cycle progression.
- Figure 12: Localization of Sfp1p-GFP.
- Figure 13: The absence of Sfp1p results in a reduction in filamentation on select medium, and lack of nitrogen source suppresses the cell size defect of *sfp1Δ* cells.
- Figure 14: Distribution of transcriptionally modulated genes in the absence of Sfp1p among 26 categories of biological processes.
- Figure 15: GO Slim Mapper categories with 2% difference or more between upregulated and downregulated genes in the absence of Sfp1p.
- Figure 16: Northern blot confirmation of the expression of opaque and white phase specific genes.

LIST OF TABLES

- Table 1: *Candida albicans* strains used in this study.
- Table 2: Oligonucleotides used in this study.
- Table 3: Plasmids used in this study.
- Table 4: Length by width ratios of the *sfp1Δ/sfp1Δ* strain compared to the control strain in rich and minimal media.
- Table 5: Length by width ratios of the *sfp1Δ/sfp1Δ* strain and the control strain in media containing different carbon sources.
- Table 6: Length and width measurements of hyphae formed in the presence or absence of Sfp1p.
- Table 7: GO Slim Mapper term analysis of genes modulated in cells lacking Sfp1p in comparison to the complete list of *C. albicans* genes.

LIST OF ACRONYMS

AESBF	4-(2-aminoethyl)-benzenesulfonyl fluoride
ATP	Adenosine triphosphate
BSA	Bovine serum albumin
cAMP	3', 5'-cyclic adenosine monophosphate
CDK	Cycling-dependent kinase
cDNA	Coding DNA
CGD	Candida genome database
ChIP	Chromatin immuno-precipitation
CSPD	Chloro-5-substituted adamantyl-1,2-dioxetane phosphate
CWI	Cell wall integrity
Cy3	Cyanine 3
Cy5	Cyanine 5
DAPI	Diamidino-2-phenylindole
dCTP	Deoxycytidine triphosphate
DEPC	Diethylpyrocarbonate
DIG	Dioxigenin
DNA	Deoxyribonucleic acid
dNTP	Deoxynucleotide triphosphate
DTT	Dithiothreitol
ECL	Enhanced chemiluminescence
EDTA	Ethylenediaminetetraacetic acid
FACS	Fluorescence-activated cell sorting
FAT	<i>FRAP</i> , <i>ATM</i> and <i>TRRAP</i>
FATC	<i>FRAP</i> , <i>ATM</i> and <i>TRRAP</i> at C-terminus
FBS	Fetal bovine serum

FKBP12	FK506-binding protein
FRB	FKBP12-rapamycin binding
GAP	Guanine activating protein
gDNA	Genomic DNA
GFP	Green fluorescent protein
GO	Gene ontology
HA	Haemagglutinin
HEAT	Huntingtin, <i>EF3</i> , <i>PP2A</i> , <i>TOR1</i>
HIV	Human immunodeficiency virus
HSG	Hyphal specific genes
L	Length
MAPK	Mitogen activated protein kinase
MAPKK	MAPK kinase
MAPKKK	MAPKK kinase
MBF	<i>MLU1</i> -binding factor
MC	Methionine, Cysteine
MCB	<i>MLU1</i> cell cycle box
MM	Minimal media
MOPS	3-(N-morpholino)propanesulfonic acid
MTL	Mating type locus
MYC	<i>C-MYC</i> gene derived tag
NCR	Nitrogen catabolite repressed
OD _{600nm}	Optical density at 600 nm
PAC	Polymerase A and C
PCR	Polymerase chain reaction
PIKK	Phosphatidylinositol kinase-related kinase
PKA	Protein kinase A

PP2A	Protein phosphatase 2A
pRb	Retinoblastoma protein
PVDF	Polyvinylidene difluoride
qPCR	Quantitative PCR
RIBI	Ribosome biogenesis
RIPA	Radio Immuno Precipitation Assay
RNA	Ribonucleic acid
RP	Ribosomal protein
rRNA	Ribosomal RNA
RRPE	rRNA processing element
RT-PCR	Real time PCR
SAB	Sample application buffer
SBF	<i>SWI6</i> -binding factor
SCB	<i>SWI4/6</i> cell cycle binding box
SCF	Skp, Cullin, F-box containing complex
SDS	Sodium dodecyl sulfate
PAGE	Polyacrylamide gel electrophoresis
SLAD	Synthetic low ammonium dextrose
SR	Serine, arginine protein
SSC	Saline sodium citrate
TAP	Tandem affinity purification
TBST	Tris-Buffered Saline and Tween 20
TE	Tris, EDTA
TOR	Target of rapamycin
TORC1	TOR complex 1
TORC2	TOR complex 2
tRNA	Transfer RNA

UDG	Uracil-DNA glycosylase
UV	Ultraviolet
W	Width
YFP	Yellow fluorescent protein
YPD	Yeast extract, peptone, dextrose

1.0 INTRODUCTION

1.1 *C. albicans* Overview

Candida albicans is a multimorphic fungus present in 80% of mammals, including humans. It lives as a commensal in the gastrointestinal tract and on mucosal surfaces and its proliferation is under the tight control of the host's immune system (2). Nevertheless, this opportunistic pathogen can invade and colonize host tissues in immuno-compromised individuals, including chemotherapy and HIV patients, or following antibiotic treatments that unbalance the gastrointestinal flora. The results can be minor superficial infections of the mucosa but can reach severe life-threatening systemic infections especially when the fungus enters the bloodstream (3). Several types of drugs are available to candidiasis patients but only a few are fungicidal. Most, including azoles like fluconazole, polyenes like amphoterecin B, and allylamines like terbinafine, target the biosynthesis of ergosterols, components of the fungal cytoplasmic membrane, proving to be fungistatic. Another type, flucytosine, is converted into subproducts that inhibit RNA transcription, RNA translation, and DNA replication, but has been associated with multiple side effects on the bone marrow, gastrointestinal tract, liver, and kidneys and it has also been challenged with high rates of resistance (4). Thus, *Candida albicans* is a worldwide leading cause for fungal infections (5) and the fourth most common cause for nosocomial infections in the US with mortality rates reaching 50% (6). Due to serious side effects and increasing drug resistance, new drug targets and therapeutic strategies are needed. To this end, we require a more comprehensive understanding of the biology of *C. albicans* and its virulence-determining traits.

1.2 Virulence-determining trait: Morphogenesis

1.2.1 *C. albicans* cell types

Contributing to its pathogenesis, *C. albicans* demonstrates the ability to undergo phenotypic switching in response to environmental conditions like temperature, acidity, carbon source and nutrient availability (6, 7). Three main growth forms are distinguishable: the yeast, hyphal and pseudohyphal forms. Yeast cells grow as ellipsoid single cells with round-shaped buds that detach at the end of cytokinesis. Hyphae continuously grow in a long narrow tubular form with parallel walls and no constriction at the site of septation. Pseudohyphae consist of a thick chain of elongated yeast cells with clear constrictions at sites of septation but no detachment. A fourth growth form, the opaque state, corresponds to the mating competent form of yeast cells as opposed to the white state for mating incompetent cells. Opaque cells grow as oblong-shaped cells with a rough surface and on solid media as flat colonies, whereas white cells grow as smooth domed soft colonies with well defined sharp edges (6, 8).

Candida albicans' ability to switch between morphologies in response to environmental cues is necessary for its virulence as blocking cells in a specific form results in a significant loss of virulence (9-11). Further, plasticity in form allows *C. albicans* to exist in different environments of the host. Filamentous forms facilitate tissue invasion and evasion from the host's immune system; filaments allow the fungus to break out of macrophages, for example, and permit migration across endothelial layers and the blood-brain barrier. Yeast forms, on the other hand, might be more advantageous for colonizing tissues and travel through the bloodstream (12-15).

1.2.2 Environmental regulation of morphogenesis

Morphogenesis in *C. albicans* is regulated by a diversity of environmental cues and associated signalling pathways (Fig. 1). For example, yeast growth is favored at low temperature and low pH while hyphal growth can be induced at a higher temperature of 37°C in combination with serum, high pH or alternative carbon sources (8). The yeast-to-hyphal morphogenetic switch is well characterized. Its regulation involves many different environmental signalling pathways, including the mitogen activated protein kinase (MAPK) and the cyclic adenosine monophosphate (cAMP)/protein kinase A pathways (16), for example. The MAPK and the cAMP/PKA pathways (17) are activated by a common GTPase encoded by the *RAS1* gene (18). In the MAP kinase pathway, Ras1p transduces a signal through a cascade of kinases including Cst20p, Ste11p, Hst7p, and Cek1p resulting in the activation of Cph1p, a transcription factor required for mating and hyphal growth on solid media (19). In the cAMP/PKA pathway, Ras1p activates the adenylyl cyclase Cdc35p (also known as Cyr1p) that catalyzes the conversion of adenosine triphosphate to 3', 5'-cyclic adenosine monophosphate (cAMP). This leads to its accumulation and the activation of a cAMP dependent protein kinase (PKA), composed of a catalytic subunit (Tpk1p or Tpk2p) and a regulatory subunit (Bcy1p) (20, 21). The downstream targets of this pathway are various transcription factors including Efg1p (22), and Tec1p that are required for the regulation of hypha-specific genes. Another pathway that transduces environment signals is the pH response pathway consisting of Rim8p, and Rim20p that activate Rim101p, a transcription factor required for alkaline induced hyphal growth, and the matrix embedding pathway. The latter in turn activates Czf1p, another transcriptional regulator of hyphal growth (5). Ultimately the pathways control the physical

switch to hyphal growth as well as co-expression of hyphal-specific genes (HSG's), many of which are virulence factors (23).

1.3 Virulence-determining trait: Cell proliferation

1.3.1 Cell cycle and G1/S regulation in *S. cerevisiae*

Another aspect of the biology of *C. albicans* that is important for virulence is its ability to proliferate, which is under control of the cell cycle. In yeast like *Saccharomyces cerevisiae*, the cell cycle consists of an initial growth phase (G1) during which cells increase their content and volume in preparation for division. Once a critical cell size is attained, cells initiate budding and transition from the G1 phase to the S phase at a checkpoint referred to as Start. This is when cells become committed to budding and division. The S phase mainly consists of the duplication of the cell content including DNA replication in preparation for mitosis. A second growth phase (G2) allows the budding cell to increase in size and prepare for the transfer of the genetic material. A final stage referred to as the M phase for mitosis follows. It is preceded by a second checkpoint (G2/M) that ensures the proper replication of the genetic material and ends with the separation of the budding cell from the mother cell during cytokinesis, and entry of the new cells into G1 phase or a “dormant” phase referred to as G0. The cell cycle is regulated at many different levels, but the major players are the cyclin-dependent kinases (CDKs) (16, 24). CDKs associate with phase-specific cyclins to phosphorylate several targets that allow transition between cell cycle stages.

The G1/S transition is a crucial stage where many cell types either commit to division or exit the cell cycle to follow different developmental pathways (16). The G1/S regulatory circuitry is well defined in the model yeast *S. cerevisiae*. Here, the CDK Cdc28p associates with the G1 cyclin Cln3p and activates the SBF/MBF G1/S transcription factor complex, which is composed of ankyrin-repeat proteins specific to fungi (25, 26). SBF is composed of the DNA activating factor Swi6p in association with the DNA binding factor Swi4p (SBF), and mediates G1/S early events such as cyclin expression, budding, and cell wall deposition. MBF is composed of Swi6p in combination with the DNA binding element Mbp1p, which mediates DNA replication. SBF is activated through Cdc28p/Cln3p-mediated inactivation of Whi5p, an SBF repressor and considered the pRb functional equivalent (25, 26). The mechanisms underlying Cdc28p/Cln3p-dependent activation of MBF is unclear, but MBF is a transcriptional repressor of its targets outside G1 phase, with the assistance of a co-repressor Nrm1p, thus restricting MBF target gene expression to G1 phase (27). SBF and MBF bind SCB (Swi4/6 cell cycle binding box) and MCB (*Mlu1* cell cycle box) elements, respectively, (28). Their targets include other transcription factors and additional G1 cyclins such as *CLN1* and *CLN2* (29), for example.

The G1/S machinery and Start are coordinated with cell growth through external and internal cues. These cues dictate the critical size cells need to reach to progress through Start to the S phase. Smaller cells are the result of quicker progression through G1/S relative to growth or slower growth relative to division (30, 31). These cues include nutrient conditions (like carbon source type and amino acid availability) (24) and internal rates like ribosome biogenesis (32-34).

1.3.2 Cell cycle regulation in *C. albicans*: G1/S transition

In *C. albicans*, the cell cycle is not as well defined but a framework for the G1/S circuitry is emerging based on sequence comparisons, cell-cycle stage-specific DNA expression profiles and limited functional analyses (35-37). For example, *C. albicans* contains orthologues of the CDK Cd28p (38, 39) and G1 cyclins *CCNI* (previously known as *CLNI*) (40), *CLN3* (previously known as *CLN2*) (38), and *HGCI* (41). Yeast cells lacking *CCNI* grew more slowly, implying a cell cycle function (42), but absence of *HGCI* had no effect on yeast growth (41). In contrast, *CLN3* was essential for growth as cells lacking this factor arrested in G1 phase (43, 44). *C. albicans* also contains orthologues of the G1/S transcription complex factors Swi6p, Swi4p and Mbp1p. Cell size defects and expression profiles of cells lacking Swi4p and Swi6p suggested that these factors may constitute a single G1/S transcriptional complex that is important for the G1/S transition in *C. albicans* yeast cells (35, 37). Thus, some important players in the putative G1/S circuit have been identified in *C. albicans* but a detailed knowledge of the regulatory network is lacking. Moreover, the putative G1/S regulatory circuit in *C. albicans* shows some clear differences compared to the situation in *S. cerevisiae*. For example, *C. albicans* lacks an orthologue of the SBF repressor, Whi5p, and some G1 cyclins do not show cell cycle functions.

1.4 The G1/S transition and its relationship with morphogenesis

Intriguingly, the G1/S transition in *C. albicans* demonstrates an important and novel link with hyphal development in *C. albicans*. For example, it was found that the deletion of *CCNI* results in the inability to maintain hyphal growth under certain conditions (42). A subsequent study found that Ccn1p associates with Cdc28p to target the septin cytoskeleton protein Cdc11p required for hyphal development (45). Despite not having a yeast cell cycle function, the cyclin Hgc1p was found to be required for hyphal growth, where it interacts with the CDK Cdc28p to promote hyphal morphogenesis and prevent cell separation by sequestering some polarity proteins from the site of cytokinesis (41). In addition the same study provided evidence that *HGCI* expression was linked to the signal transduction pathway cAMP/PKA. Further, yeast cells lacking Cln3p were found to switch to hyphal and pseudohyphal growth following an extended G1 phase delay (43, 44), and cells lacking Swi4p or Swi6p also grew in a more filamentous manner (35, 37). Finally, absence of orthologues of factors that regulate the SCF ubiquitin ligase complex in *S. cerevisiae* and in turn influence G1 phase progression, including Grr1p and Cdc4p, also results in filamentation in *C. albicans* (46-49). Thus, G1 phase appears to be linked to hyphal development in *C. albicans*, although the underlying mechanisms remain unclear.

1.5 Environmental sensing and cell cycle progression: the TOR pathway

1.5.1 TORC complex

In order to ensure successful growth and division, cells must be able to sense their environment as well as transduce the signals to the cell division apparatus. Several signalling pathways function in this regard, one of which is the TOR pathway. Target of rapamycin or TOR (50) was discovered through work with the drug rapamycin, an antibiotic produced by the bacterium *Streptomyces hygroscopicus* that has novel antifungal properties as well as valuable immunosuppressive and antiproliferative activities (51). A mutation that confers resistance to this drug in *S. cerevisiae* led to the identification of Tor1p, a phosphatidylinositol kinase-related kinase (PIKK) (50). Rapamycin inhibits this kinase by forming a complex with a peptidylprolyl isomerase (rotamase), the FK506-binding protein (FKBP12). The complex then binds directly to Tor1p and blocks its activity. While rapamycin also inhibits FKBP12 enzymatic activity, it is the association with the Tor1p kinases that is behind its antifungal and immunosuppressive properties since preventing the complex from binding to the kinase confers resistance to rapamycin (52). The gene product is a large 280 kDa protein that is functionally conserved from yeast to humans. Structurally it consists of an essential serine/threonine kinase domain at its carboxy-terminal and N-terminal to the kinase domain is the FKBP12-rapamycin binding (FRB) domain. These domains are demarcated by a FAT domain, N-terminal to the FRB, and a FATC domain, C-terminal to the kinase domain. Both are not very well understood but they are exclusively found coupled in all PIKKs, suggesting an important interaction between them. The N-terminal is composed of up to 20 tandem HEAT repeats, each

consisting of an antiparallel α -helical motif and suspected to play a role in protein-protein interactions and anchoring the kinase to the plasma membrane (53, 54).

Treatment of cells with rapamycin was found to result in a response similar to the nutrient-deprivation response (55), including G1 cell cycle arrest, protein synthesis inhibition, accumulation of glycogen, and autophagy (56, 57). This has prompted many investigations of TOR's involvement in the nutrient-sensing pathway, leading to its position as a central controller of growth in response to nutrients (58, 59). The pathway is also involved in the response to other environmental conditions like temperature, energy and stress levels, as well as growth factors and pheromones (54) making it the main transducer of growth regulating environmental signals (60). Most of the factors involved in this pathway have been primarily characterized in the model yeast *Saccharomyces cerevisiae*, but the majority of them were found to have counterparts in other fungi, flies, worms, plants and mammals (61). Most eukaryotes have a single copy of the TOR kinase, but the budding yeast has two homologous copies, *ScTOR1* and *ScTOR2*. These homologues form two distinct protein complexes, TORC1 and TORC2, which mediate different aspects of the growth response. The former regulates the temporal aspects (feeding cues to the cell cycle) while the latter controls its spatial aspects (regulating actin polarization). TORC2, is insensitive to rapamycin and exclusively made of the association of the ScTor2p kinase with ScLst8p, ScAvo1p, ScAvo2p, ScAvo3p, ScBit61p and ScBit2p (62). The rapamycin sensitive complex TORC1 is formed by the association of either ScTor1p or ScTor2p with ScLst8p, ScKog1p, and ScTco89p. The functions of these components are not fully understood but they are essential for a proper transduction of the environmental cues.

1.5.2 TORC effectors

In *Saccharomyces cerevisiae*, TORC1 transduces environmental signals to factors regulating transcription, translation and ribosome biogenesis (Fig. 2). One of its direct targets is ScTap42p, a regulatory protein that associates with ScSit4p, a PP2A (protein phosphatase 2A)-related serine/threonine phosphatase involved in the G1/S transition of the cell cycle (63, 64). Under normal conditions, ScTap42p is phosphorylated, inactive, and tightly bound to TORC1 at the plasma membrane (65). When TORC1 is inactivated (by nutrient depletion or rapamycin treatment), ScTap42p is released and a number of stress-regulated, nitrogen catabolite repressed, and retrograde signalling genes are activated. An example is the transcription activator of nitrogen catabolite repressed genes, ScGln3p, which relocates from the cytoplasm to the nucleus when ScTap42p is activated (66-68). A less understood example is ScMaf1p, a negative regulator of RNA polymerase III that is dephosphorylated by PP2A resulting in its translocation from the cytoplasm to the nucleus (69, 70). Thus, ScTap42p is playing a role in the regulation of its associated phosphatase in response to TORC1 activity.

An ScTap42p-independent effector of TORC1 is ScSch9p, a protein kinase involved in the transcriptional activation of osmostress responsive genes and the regulation of progression through G1. *ScSCH9* was first identified in a screen for gene deletions that result in significant cell size effects. Cells deleted for *ScSCH9* showed one of the smallest cell size phenotypes observed in *S. cerevisiae* accompanied by a growth defect (71, 72). It is a direct substrate of TORC1, and when phosphorylated results in the induction of ribosome biogenesis (RIBI) and ribosomal protein (RP) genes (73, 74). Huber *et al.* (2011) demonstrated that the transcriptional repressors *ScSTB3*, *ScDOT6*, and *ScTOD6* are direct

targets of ScSch9p and their combined deletion results in nearly a complete loss of RIB1 and RP gene repression when ScSch9p is inhibited (74). The combined deletion also partly restored the *ScSCH9* deletion cell size and growth defect. ScSch9p was also recently found to play a role in the nutrient sensing cAMP-PKA pathway, regulating the localization of PKA's regulatory subunits, ScBcy1p (74-76).

1.5.3 The nutrient-sensing Split Zinc Finger protein Sfp1p is also a target of Tor1p

Another established effector of the TOR pathway is ScSfp1p, a split zinc finger protein discovered by Blumberg & Silver in 1991. Sfp1p was found to be required for normal yeast growth as it caused a block in the nuclear targeting of nucleolar proteins when present in high copy numbers (77). It was later found to be involved in the regulation of the G2/M transition and the DNA damage response (78). In comparison to an isogenic wild type strain, the deletion of *ScSFPI* in *S. cerevisiae* resulted in a smaller cell size, an increase in doubling time of 100 minutes, the accumulation of cells in G1, and failure to arrest at G2/M under DNA damaging conditions. This led to the conclusion that ScSfp1p plays a negative regulatory role at the G2/M transition. Subsequently, ScSfp1p was proposed to be a novel repressor of the G1/S transition that acts upstream of the G1/S transcriptional regulators SBF and MBF (71). Similar to deletion of *ScSCH9*, deletion of *ScSFPI* resulted in the smallest cell sizes observed accompanied by a significant increase in doubling time. Induction of *ScSFPI* resulted in the expression of nucleotide biosynthesis, aminoacyl tRNA synthetases, ribosome biogenesis, rRNA, transcription, translation initiation and elongation genes indicating a role in regulation of growth (79). In

addition, absence of ScSfp1p caused a decrease in the expression of a reporter gene with the RRPE and PAC promoter elements, indicating that transcription from promoter regions containing these elements is Scfp1p-dependent. Mutational analysis revealed that the PAC element serves as a repressor, the RRPE as an activator, and that the two C-terminal zinc fingers of the ScSfp1p protein are essential for its function (79). More recently, a direct interaction between ScSfp1p and Tor1p was demonstrated by immunoprecipitation. A Rab escort protein, ScMrs6p was found to be required for the nuclear localization of ScSfp1p and might be involved in the regulation of TORC1-dependent ScSch9p activity. In addition, a negative feedback mechanism was reported whereby ScSfp1p's transcriptional role leads to a reduction in the TORC1 ScSch9p activity (80, 81).

1.5.4 The TOR pathway and *C. albicans*

In *C. albicans*, a TOR pathway exists but is not fully characterized. One copy of the *TOR* gene exists with 60% sequence homology to both *S. cerevisiae* copies. Most of the TORC1 and TORC2 components have homologues in *C. albicans*, including *SIT4*, *GLN3*, *MAF1*, and *SCH9*, for example, but others such as *ScBIT61* and *ScBIT2* (52) are missing. Of the factors that have been investigated, several show conservation in function but, intriguingly, also influence filamentation (61, 63, 82, 83). For example, Sit4p plays a role in cell growth, hyphal development and virulence, and through microarray expression analysis was shown to be involved in cell wall biosynthesis and the osmotic stress response (63). Sit4p interacts with Mds3p, another member of the *C. albicans* TOR pathway involved in morphogenesis (83). Similarly, Gln3p functions downstream of the TOR

pathway and is required for filamentation on specific nitrogen sources like urea and ammonium (82, 84). Further, Liu *et al.* (2010) found that the deletion of *SCH9* resulted in a phenotype similar to the one observed in *S. cerevisiae*, where cells were reduced in size, and delayed in growth (85). In addition, absence of CaSch9p resulted in increased sensitivity of cells to several compounds including rapamycin, affected filamentation on select medium, and attenuated virulence in a mouse model of systemic candidiasis (85). In alignment with these findings, transcription profiles of *C. albicans* cells treated with sublethal doses of rapamycin demonstrated modulation of genes associated with nitrogen starvation, ribosome biogenesis, and hyphal-specific cell wall adhesions (86). Finally, recent work showed that down-regulation of the TOR pathway was required for maintaining hyphal growth, as this resulted in downregulation of the MAPK Hog1p and subsequent induction of the transcription factor Brg1p. Brg1p in turn outcompetes a repressor of hyphal growth for binding to hyphal specific genes (87).

Thus, aspects of the TOR pathway are emerging in *C. albicans*, but a detailed picture of all of the components and their mechanisms of action in regulating growth as well as development is lacking.

1.6 Objectives:

In order to obtain a better understanding of how Tor1p functions in regulating growth and development in *C. albicans*, and to gain important insights into how environmental cues such as nutrients are sensed and communicated to the cell division apparatus, we characterized an orthologue of Sfp1p, a transcription factor lying

downstream of the TOR and PKA nutrient sensing pathways in *S. cerevisiae*. We demonstrate that *C. albicans* Sfp1p has some conservation in function in regulating growth and cell size, possibly through influencing ribosomal biogenesis, but may also play a role in regulating developmental responses in the pathogen.

2.0 MATERIAL & METHODS

2.1 Media and growth conditions

Cells were grown in rich medium (YPD) (1.0% yeast extract, 2.0% peptone, and 2.0% dextrose) or complete minimal medium (MM) (0.67% yeast nitrogen base without amino acids, 2.0% dextrose, 0.15% complete amino acid mix). The complete amino acid mix consisted of 4.9% adenine; 2.5% uracil; 4.9% tryptophan; 2.5% histidine; 2.5% arginine; 2.5% methionine; 3.7% tyrosine; 3.7% isoleucine; 18.4% valine; 3.7% lysine; 6.2% phenylalanine; 12.4% glutamic acid; 24.7% threonine; 7.4% leucine. Appropriate amino acids were left out when selecting for *URA3+*, *HIS1+* and/or *ARG4+* prototrophs. For solid medium, 2.0% agar was added. To investigate the effect of different carbon sources, glucose in MM was replaced with 2.0% galactose, raffinose or glycerol. Strains carrying *SFPI* under control of the *MET3* promoter (88) were grown in MM without methionine (-MC) or with 2.5 mM methionine and 0.5 mM cysteine (+MC) to induce or repress expression, respectively. Spider medium consisted of 2.0% nutrient broth, 2.0% mannitol, and 0.4% K₂PO₄, pH to 7.2 with NaOH (89). Synthetic low-ammonium dextrose (SLAD) medium (90) consisted of a 0.17% yeast nitrogen base without amino acids and (NH₄)₂SO₄, 2.0% dextrose, and 50 μM (NH₄)₂SO₄. Rapamycin was added to YPD or MM medium from a 100 μM stock in ethanol. A similar volume of EtOH was added to control cells. For growth assays, overnight cultures of cells were diluted to an Optical Density at 600 nm (OD_{600nm}) of 0.1 and incubated at 30 °C for the indicated times. Hyphal growth was induced by the addition of 10% Fetal Bovine Serum (FBS) to YPD or MM medium and incubating at 37 °C for 2 hours. For microarray analysis, cells were inoculated in 5 ml

fresh MM media then serially diluted 5 times in 10 ml fresh MM media from 10^2 to 10^6 in order to obtain an overnight 30 °C culture of cells at an OD_{600nm} of < 0.01 , and collected the next day at an OD_{600nm} of 0.8. This was done to account for the difference in the growth rate of the *sfp1* Δ ::*URA3/sfp1* Δ ::*HIS1* mutant and the isogenic control (*SFPI/SFPI*; *URA3*; *HIS1*). Growth curves were constructed by inoculating cells in 3ml fresh MM and YPD for overnight incubation at 30 °C. Cultures were diluted next day from a stationary phase OD_{600nm} to an OD_{600nm} of 0.1 in 10ml fresh MM or YPD media and incubated at 30 °C for 10 to 12 hours. Measurements were taken every two hours starting with T_0 (at the start of incubation) and up to T_{10} or T_{12} (after 10 h or 12 h of incubation time). Values from 2 to 4 independent cultures were averaged and normalized to a T_0 OD_{600nm} of 0.1. The doubling rate of each strain was estimated from the final averaged growth curve. The *sfp1* Δ /*sfp1* Δ growth curve was also constructed with haemocytometer cell counts in order to account for potential cell size effects on the 600nm optical density measurements.

2.2 Strain construction

Strains, oligonucleotides and plasmids are listed in Tables 1-3, respectively. In order to delete *SFPI*, constructs made by PCR fusion (91, 92) were utilized. Oligonucleotides HH20F, HH20R and HH22F, HH22R amplified approximately 800 bp fragments from genomic DNA (gDNA) lying, respectively, upstream and downstream of the *SFPI* open reading frame. The PCR amplification conditions of both fragments consisted of 3 min at 94 °C; 25 cycles of 30 sec at 94 °C, 30 sec at 52 °C, and 1 min at 68 °C, followed by 7 min at 68 °C. Oligonucleotides HH30F and HH30R were used to amplify

URA3 from pBSCaURA3 at the following conditions: 94 °C for 3 min, 25 cycles of 30 sec at 94 °C, 30 sec at 45 °C, 1.5 min at 68 °C, followed by 7 min at 68 °C. The three PCR products were then combined in a 1:2:1 ratio (50 ng: 150 ng: 50 ng) with oligonucleotides HH20F and HH22R to create the final fusion construct. The PCR conditions included 2 min at 95 °C, 10 cycles of 10 sec at 95 °C, 30 sec at 46 °C, 3 min at 68 °C, 15 cycles of 10 sec at 95 °C, 30 sec at 46 °C, and 3 min at 69 °C, followed by 7 min at 69 °C. The product was purified and transformed into strain BWP17, resulting in strain HHCa20, or SN148, resulting in strain AM1401. The second copy of *SFPI* was replaced with *HIS1* using the same 5' and 3' end fragments. The middle fragment was amplified at the same PCR conditions using oligonucleotides HH30F and HH30R and plasmid pBSCaHIS1. The *HIS1*-containing construct was transformed into strains HHCa20 and AM1401 to replace the second wild type copy of *SFPI*, resulting in strains HHCa28 and AM1415 respectively.

In order to create a strain carrying a single copy of *SFPI* under control of the *MET3* promoter (88) oligonucleotides AOM1F and AOM1R were used to amplify an 824 bp fragment from gDNA, located 857 bp upstream of the *SFPI* start codon. PCR conditions consisted of 94 °C for 3 min, 30 cycles of 94 °C for 30 sec, 50 °C for 30 sec, 68 °C for 1 min, followed by 68 °C for 7 min. Oligonucleotides AOM3F and AOM3R amplified a 799 bp fragment from gDNA that included the *SFPI* start codon and downstream sequence. The PCR conditions included 94 °C for 3 min, 30 cycles of 94 °C for 30 sec, 38 °C for 30 sec, 68 °C for 1min, followed by 68 °C for 7 min. Oligonucleotides AOM2F and AOM2R were then used to amplify a *HIS1-MET3* fragment from pFA-*HIS1*-Met3p. PCR conditions included 94 °C for 3 min; 30 cycles of 94 °C for 30 sec, 50 °C for 30 sec, 68°C for 3 min, followed by 68 °C for 7 min. A final fusion PCR construct was created from the three

products at a ratio of 1:2:1 of the 5', middle, and 3' fragments (50 ng : 150 ng: 50 ng) using oligonucleotides AOM1F and AOM3R. PCR conditions included 94 °C for 3 min; 10 cycles of 94 °C for 30 sec, 45 °C for 30 sec, 68 °C for 5 min, 15 cycles of 95 °C for 30 sec, 45 °C for 30 sec, 69 °C for 5 min, followed by and finally 69 °C for 7 min. The construct was transformed into strain AM1401, resulting in strains AM1511 and AM1512.

In order to tag *SFPI* with HA, oligonucleotides AOL1F and AOL1R amplified a HA-*HIS1* cassette from plasmid pFA-HA-Ca*HIS1* using the following conditions: 94 °C for 4 min, 30 cycles of 94 °C for 1 min, 45 °C for 1 min, 68 °C for 2 min, followed by 68 °C for 7 min. The product was transformed into strain HHCa20, resulting in strain AM1213. In order to tag *SFPI* with GFP, oligonucleotides AOL3F and AOL3R amplified a GFP-*ARG4* from plasmids pFA-GFP-Ca*ARG4* using the following conditions: 94 °C for 4 min, 30 cycles of 94 °C for 1 min, 46 °C for 1 min, 68 °C for 3 min, followed by 68 °C for 7 min. The product was transformed into strain HHCa20, resulting in AM1312 and AM1317. The PCR amplification and genetic manipulation strategies are described in Fig. 3.

2.3 Transformation

Transformations were done according to Rose *et al.* (1990) with modifications (93). Briefly, 4 to 10 µg of the purified PCR product was mixed with 300 µl of an overnight cell culture grown in rich media to an OD_{600nm} of ≥ 12.0 , pelleted, washed and resuspended in 100 µl one-step-buffer (25 µl boiled salmon sperm DNA; 0.015 g DTT; 800 µl sterile 50% PEG 4000; 200 µl sterile 1M LiAc) then incubated overnight at 30°C and heat-shocked

next day at 43 °C for 1 hour before plating on solid selective media. After incubating at 30 °C for 2 days, screening of colonies was done by PCR, southern blotting, and western blotting (for HA-tagged strains).

2.4 Genomic DNA extraction

To extract gDNA, 5 ml of an overnight culture of cells were treated for 2 h at 37 °C with 100 U lyticase (10 U/μl) in 1 ml Sorbitol buffer (1 M sorbitol, 0.1 M EDTA pH 8.0) and 8 mM DTT. The lysate was then centrifuged at 13,500 rpm for 1 min and the supernatant removed. The pellet was resuspended in 200 μl of 50 mM Tris pH 8.0, 20 mM EDTA pH 8.0. After resuspension SDS was added to a final concentration of 1%, and the sample was incubated at 65 °C for 30 min. 100 μl of a 5 M KAc solution was then added to the sample, which was then incubated on ice for 60 min, and centrifuged at 13,500 rpm for 10 min. The supernatant was transferred to a new tube and gDNA precipitated by adding an equal volume of isopropanol. The pellet was washed with 70% ethanol then resuspended in 150 μl buffer of 10 mM TRIS pH 8.0. RNA was removed from the sample by adding 2 μl of 10 mg/ml RNase A (Fermentas) and incubated at 37 °C for 30 min. Samples were quantified using the Hoefer DQ300 nanospectrometer and stored at 4 °C before use.

2.5 PCR screening of strains

PCR screening of strains utilized the method of Ling *et al.* (1995) (94). Briefly, colonies growing on selective media were transferred by streaking onto fresh selective

solid media for three rounds. Single colonies were then lysed enzymatically by carrying with a sterile pipette tip and mixing with 10 μ l of a Zymolyase solution (2.5 mg/ml of Zymolyase (MP Biomedicals, LLC), 1.2 M sorbitol, 0.1 M NaPO₄). Incubation at 43 °C for 60 min allowed for the enzymatic reaction to take place and 50 μ l PCR reactions were then performed with 2 μ l of the resulting lysed cells solution, 15 μ M of oligonucleotides, 100 mM of dNTPs (Fermentas), and Expand Long Template Polymerase with Buffer 3.

For the double deletion of *SFP1*, strain HHCa28 (*sfp1 Δ ::URA3/sfp1 Δ ::HIS1*), prepared in the BWP17 wild type background, was screened using three sets of oligonucleotides along with its isogenic control, HHCa1 and the wild type strain BWP17. The first set of oligonucleotides, SFP1FS1 and SFP1FR1, flank the *SFP1* locus and would amplify a wild type fragment of 3.3 kb, a *sfp1 Δ ::URA3* fragment of 3.1 kb, and a *sfp1 Δ ::HIS1* fragment of 3.0 kb. The second oligonucleotide set used SFP1FS1 with a *URA3* embedded oligo, URA3R1 to amplify a 2.1 kb *sfp1 Δ ::URA3* fragment. Similarly, the third set consisted of SFP1FS1 and HIS1R1, a *HIS1* embedded oligo. The third set amplified a 1.4 kb *sfp1 Δ ::HIS1* fragment. All three sets were used in 50 μ l PCR reactions at the following conditions: 94 °C for 3 min; 30 cycles 94 °C for 30 sec, 40 °C for 30 sec, 68 °C for 2 min; followed by 68 °C for 7 min, and a hold at 4 °C. The double deletion of *SFP1* prepared from the wild type SN148 background and resulting in strains AM1401 (*sfp1 Δ ::URA3/SFP1*) and AM1415 (*sfp1 Δ ::URA3/sfp1 Δ ::HIS1*) were also screened using the *SFP1* locus flanking oligos, SFP1FS1 and SFP1RS1. A 3.3 kb wild type *SFP1* fragment a 3.1 kb *sfp1 Δ ::URA3* fragment, and a 3.0 kb *sfp1 Δ ::HIS1* fragment were amplified at the following PCR conditions: 94 °C for 3 min; 30 cycles 94 °C for 30 sec, 40 °C for 30 sec, 68 °C for 3.5 min; followed by 68 °C for 7 min. The AM1401 strain was also confirmed

using oligos SFP1FS1 and URA3R1 amplifying a 2.1 kb *sfp1Δ::URA3* fragment at the following conditions: 94 °C for 3 min; 30 cycles 94 °C for 30 sec, 40 °C for 30 sec, 68 °C for 3 min; followed by 68 °C for 7 min. AM1415 was also confirmed using the same set of oligos SFP1FS1 and URA3R1 for a 2.1 kb *sfp1::URA3* fragment and another set SFP1FS1 and HIS1R1 for a 1.4 kb *sfp1::HIS1* fragment at the following conditions: 94 °C for 3 min; 30 cycles 94 °C for 30 sec, 39 °C for 30 sec, 68 °C for 2.5 min; followed by 68 °C for 7 min.

The *HIS1-MET3p-SFP1/sfp1Δ::URA3* strains (AM1511 and AM1512) were screened using two sets of oligonucleotides along with wild type BWP17 strain. The first set of oligonucleotides, HH20F and CaMETr, amplify a *HIS1-MET3p* fragment of 3.7 kb, and no wild type fragment. This set was used in 50 μl PCR reactions at the following conditions: 95 °C for 1 min; 25 cycles 95 °C for 30 sec, 45 °C for 30 sec, 72 °C for 4 min; followed by 72 °C for 7 min. The second set, HH20F and CaHIS1R amplified a 1.58 kb fragment of the *HIS1* marker. Reactions (50 μl) were performed at the following conditions: 95 °C for 1 min; 25 cycles 95 °C for 30 sec, 49 °C for 30 sec, 72 °C for 2 min; followed by 72 °C for 7 min.

The AM1213 strain (*SFP1-HA-HIS1/sfp1Δ::URA3*) was confirmed using oligonucleotides SFP1FS1 and SFP1RS1 to amplify a 3.3 kb wild type fragment, a 4.8 kb *SFP1-HA-HIS1* fragment, and a 3.1 kb *sfp1Δ::URA3* fragment. PCR conditions were the following: 94 °C for 3 min; 25 cycles at 94 °C for 30 sec, 40 °C for 30 sec, 68 °C for 6 min; followed by 68 °C for 7 min, and a hold at 4 °C. Similarly strains AM1312 and AM1317 (*SFP1-GFP-ARG4/sfp1Δ::URA3*) were confirmed using the same oligo pair at

the same PCR conditions to amplify the same wild type and *sfp1Δ::URA3* fragments in addition to a 6.0 Kb *SFPI-GFP-ARG4* fragment.

2.6 Southern blotting

To confirm the genotype of the *sfp1Δ::HIS1/sfp1Δ::URA3* strains (HHCa28 and AM1415), Southern blotting was also utilized, using the DIG system (Roche Diagnostics). A 754 bp probe homologous to the 3' flank of *SFPI* was amplified by PCR using oligonucleotides HH22F and HH22R. 500 ng of the PCR product was labelled by boiling for 10 min to denature, cooling on ice for 5 min, then centrifuging and adding 10 μl of 10x hexanucleotide mix, 10 μl of 10x dNTP -DIG labelling reaction, and 25 U of Klenow in a total reaction volume of 100 μl. The reaction was incubated overnight at 37 °C and stopped the next day by adding 4 μl of 0.5 M EDTA. The labelled probe was precipitated by adding 1 μl of 20 mg/ml glycogen, 7.92 μl of 5 M LiCl, and 3 volumes 95% EtOH, then mixing and cooling at -20 °C overnight. The probe was pelleted by centrifugation at 4 °C, 13,500 rpm for 10 min, washed with 150 μl 70% EtOH, and resuspended in 50 μl TE buffer.

Genomic DNA from the *sfp1Δ::HIS1/sfp1Δ::URA3* strains AM1415, HHCa28, the *SFPI/SFPI; URA3; HIS1* isogenic control, HHCa1, and the wild type strains BWP17 and SN148, were digested with 40 U of *DraI* (NEW ENGLAND BioLabs) by mixing 4 μg gDNA with 10 μl of 10x BSA (10 mg/ml), 10 μl of 10x Buffer 4, and water and incubating overnight at 37°C. *DraI* cuts the *SFPI* locus to result in a 4191 bp fragment for the wild type *SFPI* gene, a 2968 bp fragment for *sfp1Δ::URA3*, and a 1944 bp fragment for *sfp1Δ::HIS1*. Digests were then precipitated overnight at -20 °C with 4 μl 5 M NaCl and

400 µl 95% EtOH. Samples were collected by centrifuging at 13,500 rpm for 10 min at 4 °C, washed with 70% EtOH, air-dried for 15 min, and resuspended in 20 µl TE buffer. Digested gDNA was then loaded on a 1% agarose gel containing 0.4 mg/ml Ethidium Bromide along with 10 µl of the DIG-labelled molecular weight marker and separated overnight at 25 V. The gel was washed twice for 15 min in denaturing solution (1.5 M NaCl; 0.5 M NaOH), rinsed with water, and washed twice for 15 min in neutralizing solution (3 M NaCl; 0.5 M Tris-HCl pH 8.0). The samples were then transferred overnight to a positively charged nylon membrane (Boehringer Mannheim) in 20x SSC (3 M NaCl; 300 mM Na₃C₆H₅O₇ pH 7.0). The following day, the membrane was rinsed in 2x SSC, UV crosslinked in the Stratalinker (Stratagene) and stored at 4 °C.

The membrane was then prehybridized by rotating for 1 h at 65 °C in 12 ml of preheated prehybridization solution (5x SSC, 1% blocking agent; 0.1% Sarkosyl (Sodium Lauryl Sarcosinate); 0.02% Sodium Dodecyl Sulfate (SDS)). Next, 50 ng of the probe was boiled, snap-cooled on ice, and added to 10 ml of the 65 °C preheated prehybridization solution, which was then added to the membrane. Hybridization was performed overnight at 65 °C. The following day, the membrane was washed twice for 5 min with 50 ml room temperature 2x Wash Solution (2x SSC; 0.1% SDS), twice for 15 min with 50 ml 65 °C preheated 0.1x Wash Solution (0.1x SS; 0.1% SDS), then equilibrated in Solution 1 (0.1 M Maleic Acid; 0.15 M NaCl) for 3 min. The membrane was then blocked for 1 h at room temperature in 100 ml of 1x Blocking Solution (Roche). Anti-DIG-alkaline phosphatase coupled antibody was diluted 1/10 000 in 50 ml Solution 1, added to the membrane, and incubated for 30 min with shaking. The membrane was then washed twice for 15 min at room temperature (300 µl Tween 20 in 100 ml Solution 1), equilibrated for 5 min in

Solution 3 (0.1 M NaCl; 0.1 M Tris pH 9.5), then transferred to a hybridization bag and incubated with 2 ml of Solution 3 containing 10²x diluted CSPD (chloro-5-substituted adamantyl-1,2-dioxetane phosphate) for 5 min at room temperature. The membrane was sealed, incubated for 15 min at 37 °C, and then exposed to an X-ray film for 15 min.

2.7 Microscopy

Cell microscopy was performed on a Leica DM6000B microscope (Leica Microsystems Canada Inc, Richmond Hill, ON, Canada) equipped with a Hamamatsu Orca ER digital camera (Hamamatsu Photonics, Hamamatsu City, Japan) using 63x and 100x objectives and DAPI (460 nm) filter sets. Images were captured with OpenLab software (Improvision Inc, PerkinElmer). Staining of nuclei was done by pelleting cells, washing twice with double distilled sterile water, and fixing with 70% EtOH. Pellets were then rinsed with double distilled sterile water and DNA was stained with 4'-6'-diamidino-2-phenylindole (DAPI) by incubating cells for 15 min in 100 µl of a 1 µg/ml DAPI solution. Cells were then rinsed twice with double distilled sterile water before visualization. Cell size measurement was done manually from microscope images taken under the 63x lens. A minimum of 100 yeast cells and 50 hyphal cells were measured and Microsoft Excel was used to analyse the data, calculate the mean, standard deviation, variance and standard error of the mean values. Additional statistical analyses including the normality test, the parametric student's t-test, and the non-parametric Mann-Whitney test was performed using Minitab 16 (Minitab Inc., State College, PA, USA).

2.8 RNA extraction

For microarray analysis, *SFPI/SFPI* (HHCa1) and *sfp1Δ/sfp1Δ* (HHCa28) cells were serially diluted after inoculation 2 to 6 fold in 10 ml minimal media targeting an OD_{600nm} of 0.001 in 10 ml MM. After overnight incubation at 30 °C, 3 ml and 5 ml, respectively, of the strains at an OD_{600nm} of 0.8 were collected, washed, with sterile water, and frozen at -80 °C. RNA was then extracted and purified using the MasterPure yeast RNA purification kit (Epicentre Biotechnologies). Alternatively, the hot phenol method (95) was utilized for Northern blots, since it resulted in higher yields. Cells were inoculated overnight in 10 ml minimal medium and diluted next day from a stationary phase to an OD_{600nm} of 0.1 in 100 ml of fresh culture media to be collected by centrifugation for 5 min at 3500 rpm in a 50 ml conical at an OD_{600nm} of 0.8.

Cells were resuspended in 10 ml SAB buffer Ph 5.0 (50 mM NaCH₃COO; 10 mM EDTA; 0.1% Diethylpyrocarbonate (DEPC)) and lysed by vortexing for 10 min at 65 °C with 3 g of acid washed glass beads, 1 ml of 10% SDS, and 10 ml of a 65 °C-preheated 1:1 SAB-Phenol solution. Samples were cooled down to room temperature, then centrifuged for 10 min at 3,000 rpm. The lower phase was discarded and replaced with another 10 ml 65°C-preheated 1:1 SAB-Phenol solution to vortex for another 10 min. This was repeated a total of 2 to 3 times to minimise DNA contamination and maximise purity. The upper phase was then transferred to a new tube and mixed by vortexing for 2 min with 10 ml chloroform, then centrifuging for 4 min at 3,000 rpm. The upper phase was transferred to a clean conical and vortexed with 10 ml of a 24:1 chloroform-isoamylalcohol solution, then centrifuged for 4 min at 3,000 rpm. The upper phase was transferred again and RNA

precipitated by adding 1 ml of 3 M NaCH₃COO and 30 ml of 95% EtOH. After incubating overnight at -20°C, the extracted RNA was collected by centrifuging at 3,500 rpm for 15 min, washed with 70% EtOH, resuspended in 100 µl DEPC treated water, and stored at -80 °C.

2.9 Microarray Expression Analysis

In order to determine the transcription profiles of cells lacking Sfp1p, total RNA from strains HHCa1 and HHCa28 was reverse transcribed and directly labelled with dCTP-Cy5 or dCTP-Cy3 (96, 97). Briefly, 40 µg of total RNA was mixed with 1.5 µl 100 pmol/µl AncT mRNA primer and incubated at 70 °C for 10 min followed by another 10 min incubation at room temperature. The samples were then mixed with 3 µl 6.67 mM dGTP, dATP, dTTP mix; 1 µl 2 mM dCTP; 4 µl 0.1 M DTT; 8 µl 5x First Strand Buffer and 2 µl SuperScript II reverse transcriptase. In addition 2 µl of 1 mM Cy3 was added to the Cy3 sample, and 1 µl of 1 mM Cy5 with 1 µl DEPC H₂O to the Cy5 sample. RNA was then reverse transcribed at 42 °C for 2 h, after which an additional 1 µl of reverse transcriptase was added to each sample and reverse transcription extended for an additional 1 h. Next, 1 µl of 10 mg/ml RNase A and 1µl (0.05 U) of RNase H were added to each tube and incubated at 37 °C for 30 min. The reaction samples were then topped up to 50 µl with DEPC H₂O and purified using Qiagen columns.

C. albicans microarray gene chips were obtained from the National Research Council - Biotechnology Research Institute (NRC-BRI) in Montreal, Quebec. Chips were prehybridized for 1 h in a moist chamber at 42 °C with 50 µl of prehybridization solution

(400 µl DIG EASY HYB buffer; 20 µl 10 mg/ml yeast tRNA; 20 µl 10 mg/ml salmon sperm DNA) that was previously incubated at 95 °C for 3 min. The cDNA samples were concentrated to a 3 µl volume, combined, and topped to 30 µl with the same buffer. After heating at 95 °C for 3 min, the sample was kept in a 42 °C bath until use. The chips were washed in preheated distilled water, dried by centrifuging for 2 min at 2000 rpm, and hybridized overnight with the 30 µl of sample at 42 °C. The chips were then washed once for 10 min in 42 °C 1x SSC, 0.2% SDS after removal of the cover slips, twice for 10 min at 37 °C in 0.1x SSC, 0.2% SDS, then once for 5 min in 0.1x SSC at room temperature. The chips were subsequently rinsed six times in 0.1x SSC before drying. Arrays were scanned using a GenePix 4000B scanner (Axon Instruments) and the data was analysed with GeneSpring v.9.0 software (Silicon Genetics, Redwood City, CA). Significantly modulated genes were identified based on a 1.5 fold cut-off and a t-test with $p < 0.05$.

2.10 Northern blotting

Northern blotting probes were designed to be fragments of the exonic gene sequence amplifiable by PCR using the Expand Long Template PCR System (Roche). The 50µl reaction mix was composed of 50 to 100 ng of gDNA (extracted as described in the southern blotting section) mixed with 1x buffer 3 (Roche), 400 µM dNTP, 0.6 µM of each of the forward and reverse gene specific oligonucleotides (Table 2), 0.75 µl of the enzyme mix, and topped with water.

In order to investigate the expression levels of developmental genes in the absence of *SFPI*, probes for an opaque specific gene, *CDR3* and a white specific gene, *WH11* were

designed. A 341 bp fragment from the 5' end of the *CDR3* locus was amplified by PCR using oligos HHCDR3F and HHCDR3R (98) at the following conditions: 94 °C for 3 min; 30 cycles of 94 °C for 30 sec, 38 °C for 30 sec, 68 °C for 1 min; followed by 68 °C for 7 min, and a hold at 4 °C. The full *CDR3* sequence was also used as a probe in a 1.35 kb fragment restriction digested with HindIII from plasmid p425-*GPD-CDR3* obtained from Dr. Martine Raymond. The plasmid was transformed into *E. coli* competent cells by mixing 1 µl of the 10 ng/µl plasmid preparation to 50 µl of the competent cells and leaving on ice for 30 min. The cells were then heat-shocked at 42 °C for 2min and cooled on ice for 5 min before incubating at 37 °C in 900 µl of 2YT media for 1 hour. Cells were then plated on 2YT plates with ampicillin (100 µg/ml) and incubated overnight at 37 °C. Colonies growing on these plates were transferred to fresh liquid 2YT media with 100 µg/ml ampicillin and incubated overnight at 37 °C before DNA extraction by mini-prep. Restriction digests with 2 µl of HindIII (New England Biolab) and 3 µg of the plasmid preparation were done in 30 µl reactions by mixing with 0.3 µl of 100 x BSA, 3 µl of Buffer #2, and topping with sterile water. Digests were performed overnight at 37 °C. The *WH11* probe was prepared by PCR amplification of a 200 bp long fragment using oligos HHWH11F and HHWH11R at the following conditions: 94 °C for 3 min; 30 cycles of 94 °C for 30 sec, 38 °C for 30 sec, 68 °C for 1 min; followed by 68 °C for 7 min, and a hold at 4 °C.

In order to separate RNA fragments, 20 µg of the extracted and purified RNA was mixed with 3.5 µl 10x MOPS (pH 7.2; 0.4 M MOPS 0.1 M NaAcetate; 10 mM EDTA), 3.5 µl formaldehyde, 10 µl formamide, and topped to 20 µl with DEPC-treated water. RNA samples were denatured by heating to 65 °C for 15min then 2 µl loading buffer (1 mM

EDTA; 50% Glycerol; 0.02% Bromophenol blue) and 2 μ l 10% Ethidium Bromide were added and the samples loaded on a RNA agarose gel (1% Agarose; 1% MOPS; 20% Formaldehyde; prepared in DEPC treated water). RNA fragments were separated by electrophoresis in 1x MOPS at 100 V for 3 h then washed with distilled water 4x 15 min, verified under a UV transilluminator and transferred overnight to a Zeta-Probe membrane in 10x SSC buffer (pH 7.0; 1.5 M NaCl; 150 mM NaCitrate).

The membrane was prehybridized in 20 ml 500 mM NaPO₄ pH 7.2; 1 mM EDTA; 7% SDS; 1% BSA; 0.01% salmon sperm DNA by rotating for 4 h in a hybridization oven at 65 °C. The purified PCR product probe was then diluted to a concentration of 50 ng in 45 μ l of RNase free TE buffer (10 mM Tris pH 8.0; 1 mM EDTA). It was then denatured by boiling for 5 min, snap cooled for 5 min, added to a reaction tube from the RediPrime II labelling system (GE healthcare Life Sciences), with 5 μ l Redivue dCTP³² and incubated at 37 °C for 45 min. The reaction was stopped with 2 μ l 0.5M EDTA and the radioactive probe purified with a G-50 ProbeQuant micro column (GE healthcare Life Sciences). The probe was then boiled for 5 min, snap cooled on ice for another 5 min, then added to the prehybridization solution to hybridize overnight at 65 °C. The membrane was then washed for 10 min in 20 ml 65 °C preheated wash buffer 1 (40 mM NaPO₄ pH 7.2; 5% SDS; 1 mM EDTA; 0.5% BSA), followed by a 20 min wash in 65 °C preheated wash buffer 2 (40 mM NaPO₄ pH 7.2; 1% SDS; 1 mM EDTA). The membrane was then exposed to a phosphor image for 4 h and scanned in a Typhoon Trio (GEhealth Biosciences).

2.11 Quantitative RT-PCR

RNA used for the real time RT-PCR was extracted using the hot phenol method and the MasterPure RNA extraction kit (Epicentre Biotechnologies) method as described. However in order to minimize DNA contamination, DNase I treatment with the Epicentre kit was extended to 45 min. 5 µg of the hot phenol extracted RNA was treated for 45 min at 37 °C as well with 5 U of the Fermentas DNase I enzyme and buffer. The DNase I-treated RNA was reverse transcribed by adding 1.5 µl of the 500 µg/ml Oligo dT primer, and 1 µl of the 10 mM dNTP mix to 500 ng RNA and topping the reaction volume up to 12 µl with DEPC-H₂O. RNA was denatured by heating the reaction to 65 °C for 5 min then quickly cooled on ice and mixed with 4 µl of the 5x first strand buffer, and 2 µl of the 0.1 M DTT provided with the SuperScript II reverse transcriptase (Invitrogen Cat. #18064022). The reaction was heated to 42 °C for 2 min before adding 1 µl of the reverse transcriptase and incubating at 42 °C for 50 min. The enzymes were heat inactivated at 70 °C for 15 min and RNA removed at 37 °C for 20 min after the addition of 1 µl of the 10 mg/ml RNase A (Roche Cat. # 10109142001) and 0.5 µl of the 1 U/µl RNase H (Roche). As a reverse transcription contamination control (NoRT), a similar reaction was prepared for each RNA sample without adding the SuperScript II reverse transcriptase.

Five serial dilutions (10x to 1000x) of the reverse transcribed RNA samples, and the NoRT controls were prepared in sterile H₂O. 5 µl of each dilution was mixed with 12.5 µl of the Maxima SYBR Green/ROX qPCR Master Mix (Fermentas) 0.3 µM of each primer, and completed to a 25 µl reaction volume with nuclease-free water. These reactions were prepared in a 96 well plate and loaded in the ABI Prism at the following settings : UDG pretreatment at 50 °C, for 2min; initial denaturation at 95 °C for 10 min; and 40

cycles of denaturation at 95 °C for 15 sec, annealing at 60 °C for 30 sec, and extension at 72 °C for 30 sec.

2.12 Western Blotting

Cells were grown overnight in YPD media, diluted next day to an OD_{600nm} of 0.1 in 5 ml of the same media and collected at an OD_{600nm} of 1.0 by centrifugation for 5 min. Pellets were lysed by adding 20 µl of a RIPA (Radio Immuno Precipitation Assay) buffer (10 mM NaH₂PO₄; 0.1% SDS; 10 mM EDTA; 150 mM NaCl; 1% Triton; 1 mM AESBF; 2 µg/ml Leupeptin; 5 µg/ml Aprotinin), and 200 µl of acid washed glass beads (Sigma) then homogenized for 1 min in a Mini-BeadBeater-8 (BioSpec Products). The extract was collected after adding an additional 200 µl of the RIPA buffer, and centrifuged for 5 min at 4 °C, 13,500 rpm. The protein concentration of the extract was estimated with a Bradford assay, and 30 µg was prepared in 25 µl of a 1X sample buffer (50 mM Tris pH 6.8; 2% SDS; 10% Glycerol; 100 mM DTT; 0.01% Bromophenol Blue), boiled for 10 min, then loaded on a 10% SDS-PAGE mini gel with a 4% stacking top and separated electrophoretically at 75 V for 30 min, then 150 V for 1 h in running buffer (25 mM Tris, 192 mM Glycine, 0.1% SDS). Proteins were transferred onto a PVDF membrane (pre-treated with methanol for 10 min) overnight under a constant 30 V, at 4 °C in transfer buffer (pH 8.3; 25 mM Tris; 192 mM Glycine; 0.1% Methanol). The membrane was then dried for 5 min, blocked for 2 h in a 5% skimmed milk; 0.05% Tween 20 solution prepared in TBST buffer (pH7.6; 50 mM Tris; 150 mM NaCl; 0.05% Tween 20), washed 3x 15 min in TBST, incubated in primary solution for 1.5 h, washed 3x 15 min in TBST, incubated

in secondary for 1.5 h, washed 3x 15 min in TBST, then reacted with a 1 ml ECL solution, exposed, and developed.

3.0 RESULTS

3.1 *Candida albicans* contains an *SFPI* orthologue.

In *S. cerevisiae*, Sfp1p was first identified as a factor that blocks nuclear transport at high copy numbers (77). It was later found to play a role in the DNA damage checkpoint (78) and negatively influence the G1/S and G2/M transitions (71, 78, 99). Sfp1p also acts as a sensor of the environment as it mediates in part the effects of the environmental sensor kinase Tor1p (80, 81), as well as PKA (99, 100). In *C. albicans*, little is known about how environmental signals impinge on cell proliferation (101). A *TOR1* orthologue was found to be essential for growth and play an important role in influencing hyphal development and morphogenesis (82-84, 86, 102-104). However, only a few downstream effectors of Tor1p in *C. albicans* have been characterized, including Sit4p (63, 83), Gln3p (84), Gat1p (82) and Sch9p (85), for example. In order to further our understanding of how cell proliferation is mediated by environmental cues, and gain insights on the mechanisms by which Tor1p may function in *C. albicans*, we explored the role of another potential Tor1p mediator, Sfp1p. Based on the sequence assembly 21 of the *Candida albicans* genome (<http://www.candidagenome.org>), there are two uncharacterized ORF's annotated as *SFPI*. The first, *orf19.872*, has no significant similarity to the well characterized *S. cerevisiae* *SFPI* (YLR403W), and is indicated as being a possibly spurious ORF. The second, *orf19.5359*, has a total sequence identity of 45% to its orthologue in *S. cerevisiae* (YLR403W), with 73% nucleotide sequence identity at the 3' end and 79% amino acid sequence identity at the C-terminus, which contains two conserved zinc finger motifs.

3.2 Absence of *SFPI* reduces cell size and growth rate

In *S. cerevisiae*, the *SFPI* null phenotype has been described as one of the most abnormally small “whi” mutants and shows an increase in yeast doubling rate (71). In order to characterize *C. albicans SFPI*, the alleles of *orf19.5359* were sequentially replaced with *URA3* and *HIS1* markers (Fig. 3) in strains BWP17 and SN148, resulting in strains HHCa28 and AM1415 (*sfp1Δ::HIS1/sfp1Δ::URA3*), respectively. PCR and Southern blot screening confirmed the deletion of both alleles (Fig. 4). In order to ensure that any effects were due to absence of Sfp1p, a strain carrying a single copy of *SFPI* under control of the *MET3* promoter was constructed resulting in strain AM1511 (*HIS1-MET3p-SFPI/sfp1Δ::URA3*), allowing for the induction or repression of *SFPI* in the absence or presence of 2.5 mM methionine and 0.5 mM cysteine, respectively (88) (Fig. 5). As an isogenic control, strain BWP17 was transformed with pBSCa*URA3* and pBSCa*HIS1*, resulting in strain HHCa1 (*SFPI/SFPI*, *URA3+*, *HIS1+*).

When strains were grown on minimal complete medium for 2 days at 30 °C, colonies lacking Sfp1p (HHCa28) were reduced in size compared to the control strain (HHCa1) (Fig. 6A). Reduced colony size was also observed on YPD medium, and when *SFPI* was deleted in a different strain background (AM1415; data not shown). When *MET3::SFPI/sfp1Δ* (AM1511) cells were plated on repressing medium, they also showed a reduction in cells size, unlike on inducing medium (Fig. 6A), confirming that the effect was due to the absence of Sfp1p. Some heterogeneity in size was observed for *MET3::SFPI/sfp1Δ* colonies on repressing medium, but the size was always reduced relative to colonies on inducing medium. In contrast, the control strain (HHCa1) formed colonies of normal and similar size on repressing and inducing medium (Fig. 6A). When

overnight cultures of strains HHCa1 and HHCa28 were diluted into fresh liquid medium and incubated for 7 h, length (L) by width (W) measurements of cells lacking Sfp1p revealed a significant size reduction compared to control cells in either MM (Fig. 6B) or YPD medium (Table 4). After 24 h of incubation, differences in cell size were more prominent in both media, where *sfp1Δ/sfp1Δ* cells were 23% or 29% reduced in MM and YPD, respectively, relative to control cells. Comparing length x width ratio distributions at 24 h, none of the cells lacking Sfp1p reached the largest cell size categories attained by 44% of wild type cells (Fig. 6C). In contrast, 70% fell within the smallest cell size categories, compared to 25% of wild type cells (Fig. 6C). Thus, there is a clear shift towards a smaller size in the distribution of cells lacking Sfp1p.

When yeast cell doubling rate was quantified using OD_{600nm} measurements, cells lacking Sfp1p showed a significant increase relative to control strains. The isogenic control strain HHCa1 demonstrated a mean doubling rate of 110 min, while *sfp1Δ/sfp1Δ* cells (HHCa28) doubled in 161 min (Fig. 7A), representing an increase of 46%. Strains made in a different background (AM1415) showed similar growth defects. To eliminate the effects of possible cell size differences on OD_{600nm} measurements, cell numbers were scored using a haemocytometer at each time point. The results are consistent with OD_{600nm} measurements, and confirm a reduction in doubling rate in the absence of Sfp1p (Fig. 7B). Thus, *sfp1Δ/sfp1Δ* cells show a reduction in cell size and growth rate, suggesting that Sfp1p may play a role in cell size and growth regulation in *C. albicans*, similar to the situation in *S. cerevisiae*.

3.3 Sfp1p is not essential for mediating cell size in response to select poor carbon sources.

Jorgensen *et al.* (2004) reported cells of *S. cerevisiae* lacking *SFP1* or *SCH9* failed to adjust size in response to poor carbon sources; *sfp1Δ* cells were at the minimum size and did not reduce further when incubated in poor carbon source media, unlike control cells. In order to determine whether *C. albicans* Sfp1p was also critical for mediating nutrient modulation of cell size, *sfp1Δ/sfp1Δ* cells were incubated in liquid MM containing either 2% glucose, galactose, raffinose, or glycerol for 10 or 24 h, and fixed. Based on mean width-by-length ratios, wild type *C. albicans* yeast cells were reduced in size when incubated in the presence of galactose, glycerol and raffinose carbon sources relative to glucose (Fig. 8, Table 5), similar to that observed for *S. cerevisiae* cells. However, unlike the situation in *S. cerevisiae*, the mean length-by-width ratios of *sfp1Δ/sfp1Δ* cells of *C. albicans* could still reduce in response to raffinose, galactose and glycerol, although the changes were less dramatic than those seen in control cells, and were more evident after 24 h incubation (Fig. 8, Table 5). The final length x width ratios at 24 h were the same for wild-type and *sfp1pΔ/sfp1Δ* cells incubated in raffinose, suggesting that this value may reflect the minimum cell size (Table S1). When growth rates were determined for the strains in different carbon source media, wild-type cells showed a reduction in glycerol. The rate was similar to cells lacking Sfp1p grown in glucose, raffinose or galactose (Fig. 8C). However, the growth rate was reduced further in *Δsfp1/Δsfp1* cells grown in the presence of glycerol (Fig. 8C). Collectively, these results suggest that *Δsfp1/Δsfp1* cells are not at a minimum cell size, and that Sfp1p is not essential for mediating the effects of select nutrients on the critical cell size threshold, in contrast to the situation in *S. cerevisiae*.

3.4 *C. albicans* is hypersensitive to sublethal concentrations of rapamycin in the absence of Sfp1p.

Sfp1p is an established effector of the TOR pathway and a direct target of the Tor1p kinase in *S. cerevisiae* (81). However, in *C. albicans*, few elements of the TOR pathway have been characterized (83, 85, 86, 104-107). In order to determine whether *C. albicans* Sfp1p participates in the TOR pathway, *sfp1Δ/sfp1Δ* (HHCa28) and control (HHCa1) cells were incubated on solid medium containing 0 ng/ml or 10 ng/ml of rapamycin, which binds to Fkbp12p to form a complex with Tor1p and block its activity. Although high concentrations (≥ 100 ng/ml) of rapamycin are lethal (51, 52, 108), 10 ng/ml of the drug allows growth, indicating that Tor1p function is not completely blocked (51). When incubated on YPD plates for 2 to 3 days at 30 °C in the presence of 10 ng/ml of rapamycin, strain HHCa1 showed a slight sensitivity to rapamycin at a dilution of 10^3 (Fig. 9). However, cells lacking Sfp1p (HHCa28) showed enhanced growth sensitivity, suggesting that reduced Tor1p activity is dependent on Sfp1p. Thus, *C. albicans* Sfp1p may be a downstream effector of the TOR signalling pathway.

3.5 Sfp1p levels increase during cell cycle progression in *C. albicans*.

In *S. cerevisiae*, Sfp1p is regulated at the transcriptional level in part through either increased expression or stability, as its levels vary with cell cycle stages, peaking at G2 phase of the mitotic cell cycle (78). Spellman *et al.* (1998) through microarray analysis of cells synchronized by elutriation found that the *SFPI* transcript accumulates at later stages

of the cell cycle corresponding to a peak at G2 (109). In order to investigate the regulation of *C. albicans* Sfp1p, we tagged it at the C-terminus in strain HHCa20 (*SFP1/sfp1Δ::URA3*) with 3 copies of the hemagglutinin (HA) epitope, resulting in strain AM1213 (*SFP1-HA-HIS1/sfp1Δ::URA3*) (Fig. 10). In order to determine whether Sfp1p-HA was functional, the growth rate was investigated, and found to be similar to that of control strain SN148 (Fig. 10C). Strain AM1213 was then incubated overnight in YPD medium at 30°C to stationary phase, when most cells are in G1 phase and unbudded. After collecting samples at this time “0”, the remaining cells were diluted into fresh medium, collected at subsequent time intervals, and processed for Western blotting. A separate sample at each time point was also collected, fixed, sonicated and scored for the proportion of budding cells to determine the approximate degree of cell cycle progression. From time 0 to 60 min, when the majority of cells were unbudded, the levels of Sfp1p were detectable but low (Fig. 11). At later time points, when more cells were budded and thus were progressing into the cell cycle, Sfp1p levels were enriched (Fig. 11). Sfp1p levels were lower at 120 vs. 90 min, despite the former having a higher proportion of budded cells, but the PSTAIRE (Cdc28p cyclin dependent kinase) loading control signal indicated unequal loading. Since it is difficult to obtain synchronized cells in *C. albicans* (36), it was not possible to determine the precise cell cycle stage in which Sfp1p levels peaked. However, the general pattern of expression is consistent with an increase during later stages of the cell cycle as seen in *S. cerevisiae* (78, 109).

In *S. cerevisiae*, Sfp1p is also regulated at the posttranslational level via localization. Jorgensen *et al.* (2004) measured the variation in abundance and localization of the YFP (Yellow Fluorescent Protein) tagged Sfp1p, and found that the protein is located

in the nucleus under normal conditions but quickly exits to the cytoplasm in the presence of rapamycin or following starvation (99). Similar results were also reported by Marion *et al.* (2004) for a GFP-tagged Sfp1p protein under the control of its native promoter (100). Sfp1p levels are also regulated by proteasomal degradation since protein nuclear concentrations increase upon nutrient deprivation in the absence of the proteasome activator Blm10p (110). However rapamycin and carbon starvation did not affect total protein abundance and electrophoretic mobility of a MYC-tagged version of Sfp1p implying that environmental signals do not affect protein levels nor result in protein modifications (99). In order to gain more insight into the regulation of Sfp1p in *C. albicans*, the protein was tagged at its amino-terminus with GFP (Green Fluorescent Protein) in an *SFP1/sfp1Δ* strain (HHCa20), resulting in strains AM1312 and AM1317 (*SFP1-GFP-ARG4/sfp1Δ::URA3*) (Fig. 10). The tagged protein was found to be functional since the growth rate of the *SFP1-GFP/sfp1Δ* strains was indistinguishable from that of the wild type strain (Fig. 10C). In order to determine the localization pattern, strains AM1312, AM1317, the parental strain HHCa20 and the wild type strains BWP17 and SN148 were incubated in minimal or YPD medium at 30 °C to an OD_{600nm} of 0.8, washed with sterile water, mounted on a slide, and examined immediately. No specific GFP signal was detected (Fig. 12). However, this could be due to limitations of microscope sensitivity coupled with expression levels of the protein.

Thus, Sfp1p in *C. albicans* shows some similarity to its orthologue in *S. cerevisiae* with respect to cell-cycle-dependent levels of expression. *C. albicans* Sfp1p appears to accumulate at later stages of the cell cycle corresponding with the G2 and M phases.

3.6 The absence of Sfp1p reduces the diameter of hyphal cells, and impairs filamentation under specific conditions

Since Tor1p was shown to be important for hyphal development (82-84, 86, 102-104), as well as its downstream effector Sch9p (85), we asked whether Sfp1p also influenced hyphal growth. Strains HHCa1 and HHCa28 were inoculated on several hyphal and pseudohyphal inducing media, including YPD supplemented with 10% fetal bovine serum (FBS), synthetic low-ammonium dextrose (SLAD), and Spider medium, and incubated at 37 °C for several days. After 3 days in the presence of 10% FBS, colonies from control strain HHCa1 were wrinkled, indicating extensive filamentation. In contrast, *sfp1Δ/sfp1Δ* colonies were smooth (Fig. 13). A similar result was observed after longer incubation (5 days), indicating that the absence of filaments in *sfp1Δ/sfp1Δ* colonies was not simply due to a slower growth rate, and suggesting that Sfp1p is required for hyphal growth on serum-containing solid medium. On solid Spider medium, control and *sfp1Δ/sfp1Δ* colonies showed a similar degree of filamentation (Fig. 13). However on solid SLAD medium, colonies lacking Sfp1p showed reduced filamentation compared to control colonies. Surprisingly, *sfp1Δ/sfp1Δ* colonies were also no longer reduced in size on this medium (Fig. 13), indicating that some aspect of SLAD medium suppressed the growth defect.

In order to determine whether Sfp1p influenced hyphal formation under liquid growth conditions, strains HHCa1 and HHCa28 were incubated in YPD medium at 37°C supplemented with 10% serum for 1.5 h. Cells lacking Sfp1p (HHCa28) were able to form hyphae, but the filaments' average length ($9.27 \mu\text{m} \pm 0.45 \mu\text{m}$) and width ($1.41 \mu\text{m} \pm 0.05$

μm) were smaller compared to those of control cells (length: $15.17 \mu\text{m} \pm 1.23 \mu\text{m}$; width: $1.74 \mu\text{m} \pm 0.05 \mu\text{m}$) (Table 6). Differences in length may be due to the slower growth rate, or a failure in the ability to maintain hyphal growth. However, the concomitant reduction in hyphal diameters suggests that the hyphal cells are smaller in size, much like the yeast form, in the absence of Sfp1p. Thus Sfp1p is involved in the regulation of *C. albicans* yeast and hyphal growth as its absence results in size reduction of both and is required for filamentation under select conditions. While many investigations have identified factors important for hyphal growth, the hyphal feature that is analyzed is presence/absence of length/morphology of hyphal filaments (41, 42, 111). This is the first report of a reduction in hyphal width as well as length, and thus suggests that Sfp1p plays an important role in influencing hyphal cell size and not just growth rate or morphology.

3.7 Sfp1p modulates metabolism, ribosome biogenesis, cell cycle, and development genes.

In *S. cerevisiae*, Sfp1p plays a major role in regulating the expression of ribosomal protein and ribosome biogenesis genes (71, 99). Direct binding of Sfp1p to the promoters of ribosomal protein genes has been reported (100) and conserved promoter elements were found to be common in ribosome biogenesis genes induced by this transcription factor indicating weak binding or the activation through co-factors (79, 99). In fact, Gertz et al., (2005) found, through ChIP analysis and the comparison of gene expression levels, that Stp2p is a potential co-factor of Sfp1p (112). In order to identify potential targets of *C. albicans* Sfp1p and further understand its functions, the transcription profiles of *sfp1* Δ

sfp1Δ cells were obtained. Strains HHCa28 and HHCa1 were grown to an OD_{600nm} of 0.8 in minimal medium at 30 °C, and collected. Total RNA was extracted, reverse transcribed, and directly labelled with Cyanine 5 or 3. Four different *C. albicans* gene chips were hybridized with independently prepared and labelled samples. Significantly modulated genes were selected based on a 1.5 fold expression cut-off coupled with a *t*-test function using $p < 0.05$ confidence. In the absence of Sfp1p, 374 genes were found to be up-regulated and 370 were repressed (Table S2). Pie chart distributions of the total set of modulated genes were produced by manually sorting genes into single, select categories (Fig. 14). Based on this method 3.2% of the downregulated gene set was involved in ribosome biogenesis, 7.6% in the regulation of the cell cycle, and 2% in nucleus organization while percentages shift to 0.8%, 4%, and 0.5% in the list of upregulated genes, respectively (Fig. 14). The data was also sorted according to biological processes using the GO Slim Mapper at CGD (<http://www.candidagenomedatabase.org>). Of the total number of modulated genes 36.5% are involved in transport, 26.6% in the response to chemical stimulus, 23.7% in the response to stress, 20.4% in filamentous growth, 15.1% in the response to drug, 12.3% in the cell cycle, 8.3% in cell wall organization, 7.5% in signal transduction, 7% in translation and 3.8% in ribosome biogenesis (Fig. 15). Using the Fisher exact test and a cutoff value of $p < 0.05$, we identified seven GO Slim Mapper categories for which the ratio of genes from our dataset was significantly different from the ratio of genes in the genome. These were ribosome biogenesis, transport, response to chemical stimulus and drug, cytokinesis, nucleus and cell wall organization (Table 7). While the identified 46 cell cycle genes modulated in the absence of Sfp1p did not represent a significant ratio, some of these genes were associated with the G1/S transition, suggesting an influence of Sfp1p on START.

These are *MBP1*, a putative component of the MBF G1/S transcription complex, *GRR1*, an orthologue of the F-box protein component of the SCF ubiquitin ligase complex, *HCMI*, an orthologue of the *S. cerevisiae* forkhead transcription factor that regulates S-phase specific expression of spindle and chromosome segregation-associated genes, *RNR1*, a ribonucleotide reductase, and *HTA3*, the putative histone H2A subunit. Comparing the ratios of upregulated and downregulated genes associated with the same category, we identified 13 categories with a 2% difference or more. A higher proportion of downregulated genes were found to be associated with ribosome biogenesis, translation, organelle organization, the response to chemical stimulus, stress, and drug, RNA, DNA and lipid metabolism, interspecies interaction and pathogenesis. A higher proportion of upregulated genes were associated with the signal transduction and protein modification processes (Fig. 15). These results are in agreement with findings in *S. cerevisiae*, where Sfp1p regulates the expression of multiple ribosome biogenesis and ribosomal protein genes in response to nutrient conditions (Jorgensen *et al.* 2002). In addition, as a direct target of TOR (80, 81) and the Ras/PKA pathway (99), Sfp1p is involved in the transduction of and response to multiple environmental signals. Thus, our results suggest that Sfp1p plays may play a similar role in *C. albicans*. The manual examination of our dataset revealed other potential effects of the absence of Sfp1p. Multiple cell wall ergosterol genes involved in the uptake, sensitivity, and resistance to certain drugs (113) were found to be modulated (*ERG3*, *ERG5*, *ERG6*, *ERG10*, *ERG11*, *ERG13*, *ERG25*, *ERG252*). Transport genes including the downregulation of 9 genes involved in the ER to Golgi transport and the upregulation of 18 vacuolar transport genes were also found. Thus, Sfp1p may also be involved in the cell wall organization and intracellular transport in *C.*

albicans, either directly through its transcription factor role or indirectly as a secondary effect to its ribosome biogenesis regulation role. In support of these findings, previous studies linked cell wall integrity (102) adhesion gene expression (86), and vesicular transport (114) to the TOR pathway in *Candida albicans*.

Since Tor1p was shown to be important for hyphal development (82-84, 86, 102-104) and its putative downstream effectors Sch9p (85) and Sfp1p also influenced hyphal formation under certain conditions, we predicted that hyphal-specific genes may also be modulated in the absence of Sfp1p. Based on the GO Slim Mapper results, a few genes associated with hyphal growth were modulated in the absence of Sfp1p in *C. albicans*. The expression of 5 genes (*MED20*, *SRB9*, *SLR1*, *RGA2*, and *PMR1*) was upregulated while 3 genes (*ABG1*, *ALS1* and *CDC42*) were downregulated. Among these, *MED20* and *SRB9* both encode subunits of the RNA polymerase II mediator complex and are involved in filamentous growth (115). *SLR1* encodes a protein similar to the mammalian SR-like RNA splicing factor and is also involved in filamentous growth (116). *PMR1*, encoding a putative secretory pathway P-type ATPase, is required for hyphal oscillation on semisolid media (117). *Abg1p*, a vacuolar membrane protein, is required for normal hyphal branching (118) and *Als1p* is an adhesin expressed on the surface of hyphae (119). Interestingly, *Cdc42p* a Rho-type GTPase required for budding and hyphal growth was downregulated 2.18 times, while its putative GTPase-activating protein, *Rga2p*, which represses hyphal development (120, 121), was upregulated 3.73 times. Thus, absence of Sfp1p influences expression of some hyphal specific and regulatory genes.

Interestingly, genes involved in other developmental pathways, including mating, were modulated in the absence of Sfp1p. *CDR3*, encoding an opaque-specific multidrug

resistance transporter, was upregulated 3.16 times; *OBPA*, which encodes a mating locus oxysterol-binding protein, was upregulated 2.37 times; and *KAR4*, encoding an opaque-specific transcription factor similar to a pheromone induced protein, was upregulated 1.51 times. The modulation of opaque-developmental genes in the absence of Sfp1p was novel and unexpected, because these genes are normally only expressed when the Mating Type Locus (MTL) switches from the normal heterozygous to a homozygous state. This in turn requires chromosome 5 loss or mitotic recombination (122). To date, there is only one other report of a simple genetic change in a heterozygous MTL background resulting in induction of mating type genes (123). Since multiple studies have linked the TOR pathway to mating and meiosis in both the fission yeast *S. pombe* and the budding yeast, *S. cerevisiae* (1, 67, 124-129), we were interested in confirming whether Sfp1p function was linked to the expression of mating-type genes. GO Slim Mapper categorization of our microarray data revealed that 22 significantly modulated genes fell under the conjugation and cell development categories. Particularly, *STE11* and *STE50*, which are involved in the mating response in *S. cerevisiae* (130, 131) and *CST20* encoding a protein kinase required for mating efficiency and virulence (132) were found to be upregulated in the absence of Sfp1p.

In order to validate the microarray results, we used Northern blotting and qPCR. Cells of strains HHCa28, HHCa1, and CIB4 [YPB-ADHpt/CDR3] (*cdr3::hisG/cdr3::hisG*, YPB-ADHpt/CDR3) were grown to an OD_{600nm} of 0.8 in minimal medium at 30 °C, collected, and 20 µg of RNA was loaded onto gels for Northern blotting. Probing for *CDR3* did not reveal induction in *sfp1Δ/sfp1Δ* cells (Fig. 16). This may be due to the fact that it was only induced 3 fold, according to the microarray data. However, we

also did not detect *CDR3* in opaque phase cells under our conditions. The only strain showing *CDR3* was CIB4 [YPB-ADHpt/*CDR3*], which overexpressed the gene (Fig. 16A). We next attempted qPCR to test for induction of *CDR3*. The experiment was repeated three times but signal was detected in control samples with no template indicating contamination (data not shown). Furthermore, we investigated the differences in expression levels of *WH11*, a white-specific gene, in *sfp1Δ/sfp1Δ* cells compared to the isogenic *SFP1/SFP1* control. *WH11* transcript levels were found to be higher in the control cells but loading as measured by *ACT1* levels was unequal (Fig. 16B). Thus the results are not conclusive.

Intriguingly, however, in a separate investigation in collaboration with another member of the lab, *C. albicans* yeast cells were exposed to rapamycin at concentrations that completely block TOR function, and a master regulator of the opaque state, *WOR2*, was found to be highly upregulated via Northern blotting (Fig. 16C). Thus, TOR may negatively regulate opaque-specific genes and perhaps sexual development, but it is not entirely clear whether this also involves Sfp1p function.

4.0 DISCUSSION

The ability of *C. albicans* cells to sense and respond to their environment has crucial implications for growth, development, and virulence. The TOR pathway plays an important role in mediating environmental conditions in many organisms, and accordingly, TOR kinase is required for cell division and maintenance of hyphal growth in *C. albicans* (1, 83, 86, 104). However, the mechanisms by which TOR regulates these processes in the pathogen are not clear. Here, we provide the first characterization of Sfp1p, an orthologue of a major downstream effector of TOR kinase in *S. cerevisiae*. Deletion of *SFP1* in *C. albicans* resulted in a decrease in cell size, which could be reduced further in the presence of poor carbon source media. The *sfp1Δ/sfp1Δ* cells grew slowly, formed small colonies, and were more sensitive to rapamycin, suggesting that Sfp1p mediates at least part of Tor1p function in *C. albicans*. Transcription profiles of the deletion strain demonstrated down-regulation of genes involved in ribosome biogenesis, translation and amino acid synthesis, consistent with a role in the TOR pathway. However, many hyphal-specific genes were upregulated, as well as some genes associated with the opaque cell fate, suggesting additional and novel links with development.

4.1 Sfp1p is important for the regulation of cell size and growth in *C. albicans*.

Cell size is the result of a fine balance between growth and division, established in response to environmental conditions like nutrient status and internal factors like ribosome biogenesis (32, 33). In yeast such as *S. cerevisiae*, this balance is mainly coordinated at the

G1/S transition, where cells commit to division when a critical cell size is attained. Since *sfp1Δ* cells in *S. cerevisiae* were small and grew slowly, Sfp1p was proposed to function in cell size and growth regulation (71, 133). Here, we show that Sfp1p in *C. albicans* may play a similar role, since cells depleted of Sfp1p were reduced in size and growth rate relative to control cells. Similar to *S. cerevisiae* cells, *C. albicans* cells show nutrient modulation of the critical cell size threshold, since the size of wild type cells was reduced when incubated in poor carbon sources. However, the extent of involvement of Sfp1p in mediating this response in *C. albicans* is not clear, since *sfp1Δ/sfp1Δ* cells were not “blind” to poor carbon source, and could reduce their size even further. In contrast, the size of *sfp1Δ* cells of *S. cerevisiae* was at a near minimum and barely reduced in response to poor carbon sources (99). Thus, additional factors may be involved in mediating nutrient effects on cell size in *C. albicans*, either in a redundant or more prominent manner. Absence of another downstream effector of Tor1p, Sch9p, also resulted in a small cell phenotype in *C. albicans* (85, 134), but individual sizes in response to poor carbon sources were not reported. However, *sch9Δ/sch9Δ* colonies on medium containing galactose or glycerol as the sole carbon source did not show any growth defects (85), unlike *sfp1Δ/sfp1Δ* cells. Thus, nutrient modulation of cell size in *C. albicans* is not mediated in an identical manner as in *S. cerevisiae*, and may only partly involve Sfp1p.

Our results suggest that Sfp1p’s role in regulating growth and cell size also extends to hyphal cells. When *Δsfp1/Δsfp1* cells were incubated in liquid YPD containing 10% serum at 37°C, hyphae could form but were reduced in length. While this may simply reflect a reduced growth rate, hyphal diameters also decreased, suggesting a global size defect. This result is novel as previous studies on growth regulation in *C. albicans* hyphae

have only reported effects on length (6) and the issue of hyphal size control has not been fully addressed. Despite the differences in cell geometry, our results suggest that at least some similar mechanisms may underlie size control in yeast and hyphal cells, and that this could involve Sfp1p function.

4.2 Sfp1p may function in part through regulating ribosome biogenesis.

In *S. cerevisiae*, Sfp1p is a transcriptional activator of ribosome biogenesis genes and functions via RRPE promoter elements (79, 135). It also activates ribosomal protein genes directly and indirectly through intermediate transcription factors like Fhl1p, Ifh1p, and Rap1p (71, 99). Our findings suggest that Sfp1p in *C. albicans* may also function in regulating ribosome biogenesis and protein gene expression. Go Slim Mapper analysis showed that “Ribosome biogenesis” genes represented one of the most enriched groups of modulated genes in *C. albicans* cells lacking Sfp1p. Although significant, the full complement of ribosome biogenesis and ribosomal protein genes were not modulated, unlike in *Δsfp1* cells of *S. cerevisiae* (71, 99). The difference may reflect a more limited involvement of Sfp1p in these processes in *C. albicans*. Alternatively, this may be due to technical issues associated with our microarray experiments, including large variability between slides that resulted in several genes not meeting the significance criteria. Future work involving ChIP-chip approaches to identify Sfp1p targets will help. The modulated expression of several key G1/S-associated cell cycle genes in *C. albicans* cells lacking Sfp1p also supports a role for Sfp1p in ribosome biogenesis. In *S. cerevisiae*, inhibition of ribosome biogenesis results in Whi5p-mediated repression of the G1/S transcriptional

activator SBF (136), thus preventing passage through Start. However, the mechanisms by which Whi5p “senses” ribosome biogenesis are not clear. Further, overexpression of the CDK inhibitor Far1p in *S. cerevisiae* results in an upregulation of RNA and protein content in a manner that is dependent on Sfp1p function (137). Of the significantly-modulated genes in *C. albicans* cells lacking Sfp1p, 46 fell within the cell cycle category. This was not a significant enrichment relative to the total number of genes in the genome associated with this category (Fisher’s exact test), but this could be due to asynchrony of the cell populations, which would dilute the effect of gene expression patterns associated with any cell cycle delay. Although expression patterns of specific genes require confirmation via qPCR, it is noteworthy that some key G1/S-associated genes were modulated, including *MBP1*, *GRR1*, *HCM1*, *RNR1* and *HTA3*. The influence of ribosome biogenesis on the G1/S transition has not been investigated in *C. albicans*, but if a similar relationship exists as that observed in *S. cerevisiae*, this data further suggests a potential role for Sfp1p in ribosome biogenesis.

4.3 Sfp1p may be a component of the TOR pathway in *C. albicans*.

The hypersensitivity of *C. albicans* *sfp1Δ/sfp1Δ* cells to sub-lethal concentrations of rapamycin suggests that Sfp1p may be a potential target of the TOR pathway, as reported in *S. cerevisiae* (81). A similar approach was utilized to link several other factors to the TOR pathway in *C. albicans*, including Gln3p (82), Gat1p (82), Rhb1p (102, 106), Sch9p (73, 85, 134), and Hog1p (104, 138).

Additional lines of evidence supporting the involvement of Sfp1p in the TOR pathway in *C. albicans* stem from the transcription profiles of *sfp1Δ/sfp1Δ* cells. For example, another study showed that *C. albicans* cells treated with sub-lethal doses of rapamycin down-regulate genes associated with ribosomal proteins, rRNA processing, translation initiation and elongation, and amino acid biosynthesis, and induce genes associated with nitrogen catabolite repression and amino acid starvation, for example (86). In *C. albicans Δsfp1/Δsfp1* cells, similar groups of genes were modulated. Further, an orthologue of the Tor effector *TAP42* was induced 1.75 fold, and one of the most highly-repressed genes was *SSK2*, a MAPKKK regulator of the Hog1p pathway that was recently shown to be downstream of TOR signalling during hyphal development in *C. albicans* (104, 138, 139). The *sfp1Δ/sfp1Δ* cells also showed modulation of genes associated with cell wall organization/synthesis and the cell wall integrity (CWI) pathway, including the protein kinase C *PKC1* and Rho1p GTPase-activator *SAC7*, which are connected with the TOR pathway in *S. cerevisiae* (65, 140). A link between the TOR and CWI pathways in *C. albicans* is not yet clear, but Tor1p is connected to expression of cell-wall-containing adhesions in *C. albicans* (86).

Intriguingly, the small colony size phenotype of *sfp1Δ/sfp1Δ* cells was suppressed when cells were plated on solid SLAD, a nitrogen-limiting medium that induces filamentous growth in both *S. cerevisiae* and *C. albicans* (101, 141). The mechanisms underlying this suppression are not yet clear, but it is interesting to note that the TOR kinase activity is activated by rich nutrient media, but reduced in nutrient poor medium, including nitrogen-limiting conditions. Further, Sfp1p has a repressive effect against TORC-dependent phosphorylation of Sch9p in *S. cerevisiae*; *Δsfp1* cells have elevated TOR

activity and hyperphosphorylated Sch9p (81). It is not known if a similar circuit exists in *C. albicans*, but if so, it is possible that plating *sfp1Δ/sfp1Δ* cells on SLAD reduces otherwise elevated TOR activity and Sch9p phosphorylation to a level that is more optimal for cell growth, leading to suppression of the growth defects.

4.4 Sfp1p influences filament development in *C. albicans*

Our results suggest that Sfp1p contributes to the developmental process of hyphal growth, but in a nutrient-dependent manner. On solid media, Sfp1p is important for filamentation on SLAD, a medium characterized by a low concentration of ammonium that induces the nitrogen limitation response (102, 106, 142-144). This in turn activates the cAMP/PKA and TOR pathways, leading to filamentous growth. Hsu *et al.*, (2013) recently reported that a downstream target of the Tor1p pathway that regulates filamentation in response to nitrogen limitation is the CCAAT binding complex, a heteromeric transcriptional regulation complex that acts on the CCAAT motif in gene promoters (145). This complex links TOR signalling with the Mep2p-PKA-MAPK pathway. Disruption of the CCAAT binding complex prevents nitrogen limitation-induced filamentation, but induces multiple ribosome biogenesis, transcription, translation and RNA processing genes in the presence of rapamycin. Thus, it is possible that Sfp1p contributes to the mediation of the nitrogen limitation response in *C. albicans*, possibly through its putative connection to the TOR pathway.

Serum and high temperature represent one of the strongest inducers of hyphal growth (101) in *C. albicans*, and are mediated in part via cAMP and TOR signalling (58,

146). Serum is proposed to initially activate the cAMP pathway, which leads to removal of a repressor from the promoters of hyphal-specific genes. Serum also results in a reduction in TOR signalling, which in turn down-regulates the MAPK Hog1p, leading to activation of the transcription factor *BRG1*. Brg1p in turn binds hyphal-specific gene promoters and prevents the repressor from re-binding (104). The effects of Tor1p on Hog1p are thought to be mediated by the Tor1p effector phosphatases Ptp2p and Ptp3p. However, the fact that *sfp1Δ/sfp1Δ* cells are defective in hyphal formation on solid-serum-containing medium suggests that Sfp1p may also lie in this pathway. In this case, Sfp1p does not appear to be acting as a direct repressor of filamentation or mediate all of the effects of TOR down-regulation on hyphal development and hyphal-specific gene expression, as *C. albicans* cells treated with a non-lethal dose of rapamycin showed a much stronger and extensive induction of hyphal genes (86) compared to *sfp1Δ/sfp1Δ* cells. Sch9p, another effector of Tor1p, is also required for serum-induced hyphal growth on solid medium (85), suggesting that Tor1p activity in response to serum may be mediated by several factors.

In contrast, cells lacking Sfp1p were not defective in filamentation on Spider medium, which contains 2% mannitol as a carbon source. The filamentous response to this medium is mainly transduced by the cAMP/PKA pathway that involves Gpr1p, a plasma membrane G-protein receptor, and Gpa2p, a G-protein alpha subunit, and subsequent activation of the downstream Efg1p transcription factor (147, 148). The MAPK pathway is also in part responsible for filamentation on this medium (149). Although expression of *GPA2* and the MAPK component *CST20* were upregulated in the absence of Sfp1p (1.66 and 1.78 fold respectively), the ability of *sfp1Δ/sfp1Δ* cells to form normal filaments on

Spider medium suggests the existence of some redundancy or that Sfp1p is not playing a significant role in these pathways.

Notably, transcription profiles of *sfp1Δ/sfp1Δ* cells also demonstrated a twofold downregulation in *CDC42* expression. Cdc42p activity is required for the concentrated delivery of vesicles to the hyphal tip and was recently shown to be required for the maintenance of hyphal growth (150). Further, expression of *RGA2*, a GAP for Cdc42p and negative regulator of hyphal growth, was induced 3.7 fold. It is however not clear how Sfp1p may influence these expression patterns-whether it is a direct role or if the modulation is a response to the down-regulation of ribosomal gene expression. However, if confirmed by qPCR and similar modulation is observed under certain hyphal-inducing conditions, this may also explain the defects in hyphal formation.

4.5 Sfp1p and the TOR pathway may be linked to the developmental state of mating in *C. albicans*.

In *C. albicans*, a morphogenetic switch of the white mating incompetent cells to the opaque mating competent form of growth is regulated by the mating type locus (MTL). In order for mating to proceed, the locus must switch from being heterozygous to homozygous or hemizygous, which requires the deletion of an allele or the loss of a copy of chromosome 5 during duplication (151). Our results thus suggest that Sfp1p and possibly Tor1p function may also influence the mating pathway. The expression of several members of the MAPK cascade including *CST20*, *STE11* and *STE50* was upregulated in the absence of Sfp1p. We also noted the induction of several opaque-specific and pheromone response

genes in cells lacking Sfp1p, including *CDR3*, *OBPA*, *FIG1*, *CST20*, *STE11*, *STE50*, *KAR4*, and the downregulation of one white specific gene (*RME1*). We were not able to validate induction of *CDR3*, for example, using qPCR or Northern blots, but this could be due to technical issues as we were also not able to detect expression of *CDR3* in a positive control strain. These expression patterns were intriguing since the only other example of induction of mating responses/genes in a strain that is otherwise heterozygous at the MTL occurs in the absence of *HBR1*, a factor involved in the response to hemoglobin (123). Intriguingly, we found strong induction of the opaque-specific regulator *WOR2* in cells treated with high doses of rapamycin. Since TOR is involved in regulating development in other systems (127, 128, 152), it is conceivable that the TOR pathway, possibly involving Sfp1p function, may influence the developmental mating pathway in *C. albicans*.

4.6 Sfp1p and Sch9p show more divergence in function in *C. albicans* than in *S. cerevisiae*.

A comparison of the *sfp1Δ/sfp1Δ* phenotype with that of *sch9Δ/sch9Δ* cells in *C. albicans* reveals some important insights on the functions of these factors. Sfp1p and Sch9p play parallel and redundant roles in *S. cerevisiae* (73, 99). In *C. albicans*, both influence the regulation of filamentous growth on solid YPD medium supplemented with 10% serum at 37°C, but are differentially required for filamentation on SLAD (85). Further, *sfp1Δ/sfp1Δ* cells grew slowly on galactose and glycerol, while *sch9Δ/sch9Δ* cells, at least on a colony level, did not appear to have growth defects (85). Thus, our results suggest that Sfp1p and Sch9p may have less redundant functions in *C. albicans*. They may act in

parallel branches of the TOR pathway, but with a different involvement in select nutrient-sensing pathways. This highlights differences in the regulatory circuitry governing growth in the two organisms, and underscores the need to study these processes in the pathogen itself.

4.7 Conclusions

In summary, we have shown that Sfp1p of *C. albicans* is important for controlling growth and size of both yeast and hyphal cells, and influences hyphal development under specific conditions. We also provide evidence that Sfp1p may function in part through regulating ribosome biogenesis, and may lie downstream of the TOR pathway. However, we cannot rule out Sfp1p-independent effects and the possibility that it may lie in additional pathways. Future experiments are aimed at addressing this question. Finally, we provide preliminary evidence suggesting for the first time that the Tor pathway may also be linked to the developmental mating pathway in *C. albicans*. Our results reveal new insights on factors required for regulating growth, cell size and development in an important fungal pathogen of humans, *C. albicans*.

4.8 Future work

To validate our findings future work will include the confirmation of Sfp1p targets through promoter analysis, co-immunoprecipitation, ChIP-chip analysis, and qPCR/Northern blotting of genes within the ribosome biogenesis, G1/S transition, filamentous growth, and mating response categories. Cell size measurements will be

further supported by FACS analysis and the extent of the divergence between Sfp1p and Sch9p's roles will be evaluated by constructing and characterizing a double deletion strain lacking both genes. The involvement of Sfp1p in other signalling pathways can be studied by measuring the effects of constitutive activation and/or repression of these pathways on *SFPI*'s expression and function.

5.0 FIGURES

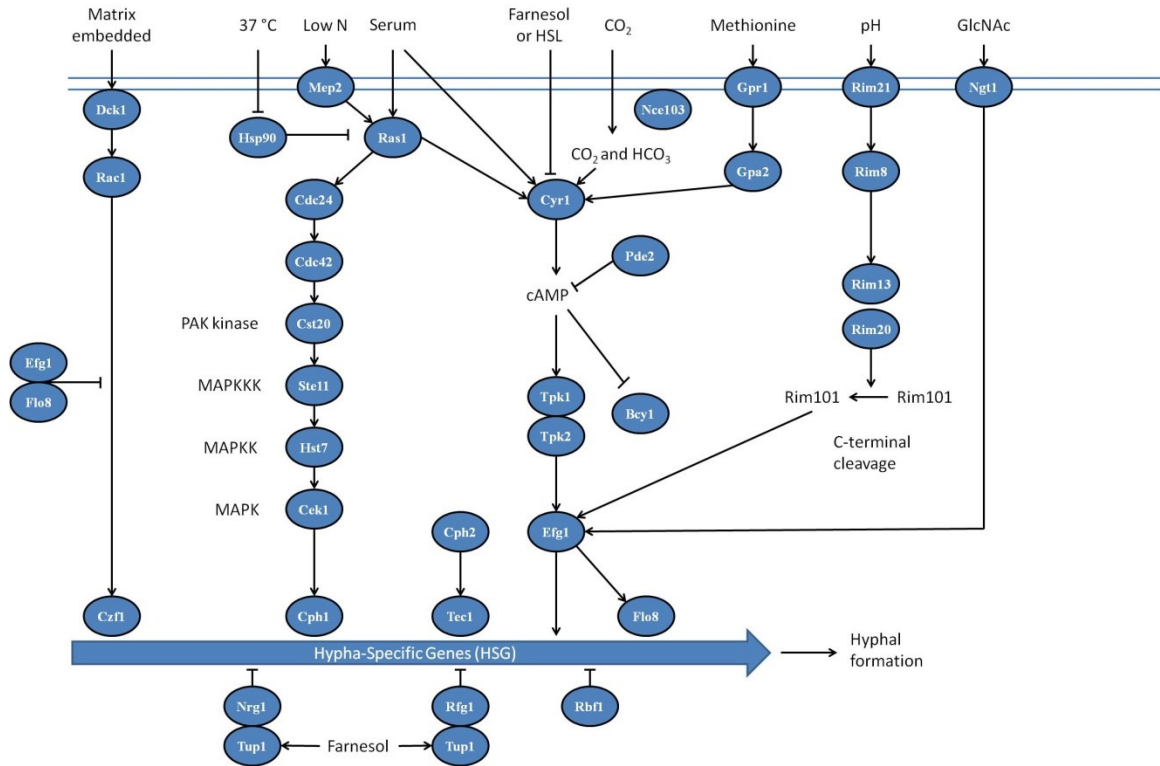


Figure 1: Signalling pathways regulating hyphal gene expression in *C. albicans*. Several pathways in *C. albicans* are influencing the expression of hypha-specific genes in response to multiple environmental conditions including temperature, pH, serum, high CO₂ levels, and low nitrogen (N).

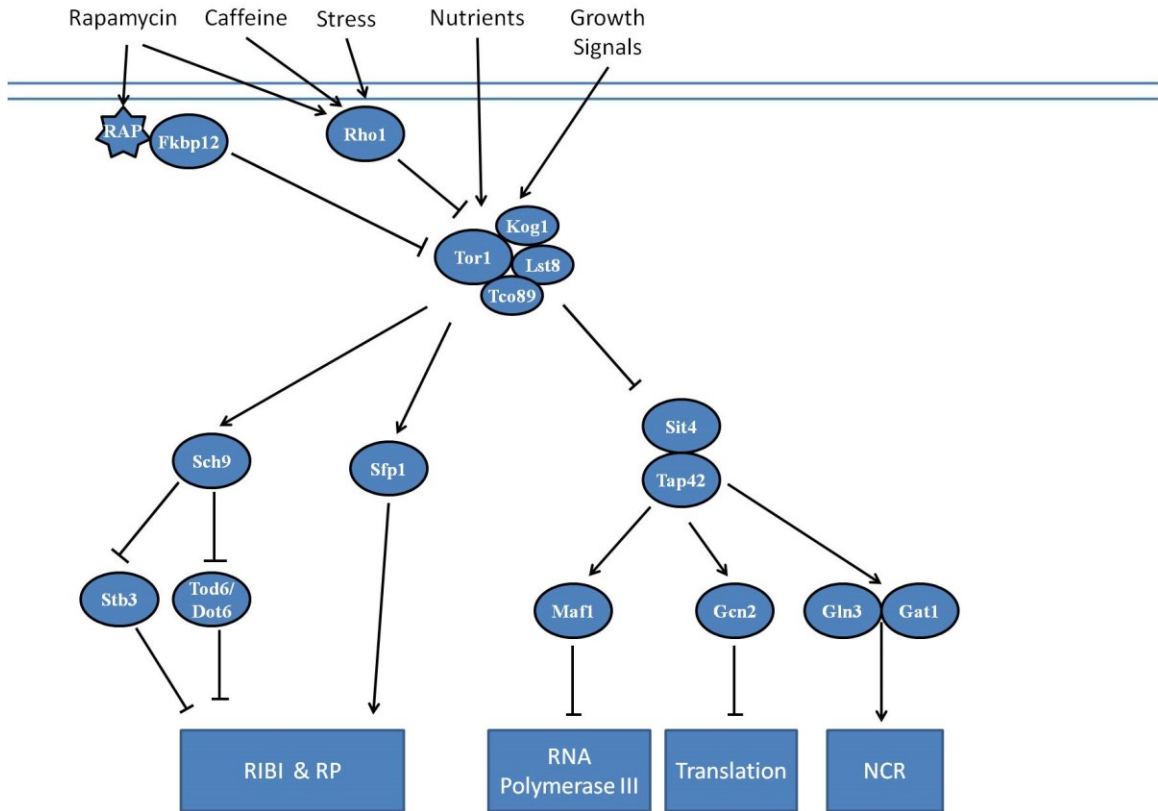


Figure 2: TORC1 pathway effectors in *S. cerevisiae*. The TORC1 pathway responds to multiple signals including nutrient conditions, growth factors, stress, rapamycin and caffeine to regulate the activity of effector proteins involved in several cellular functions including ribosome biogenesis (RIBI) and ribosomal protein (RP) gene expression, repression of RNA Polymerase III, translation, and the expression of nitrogen catabolite repressed (NCR) genes.

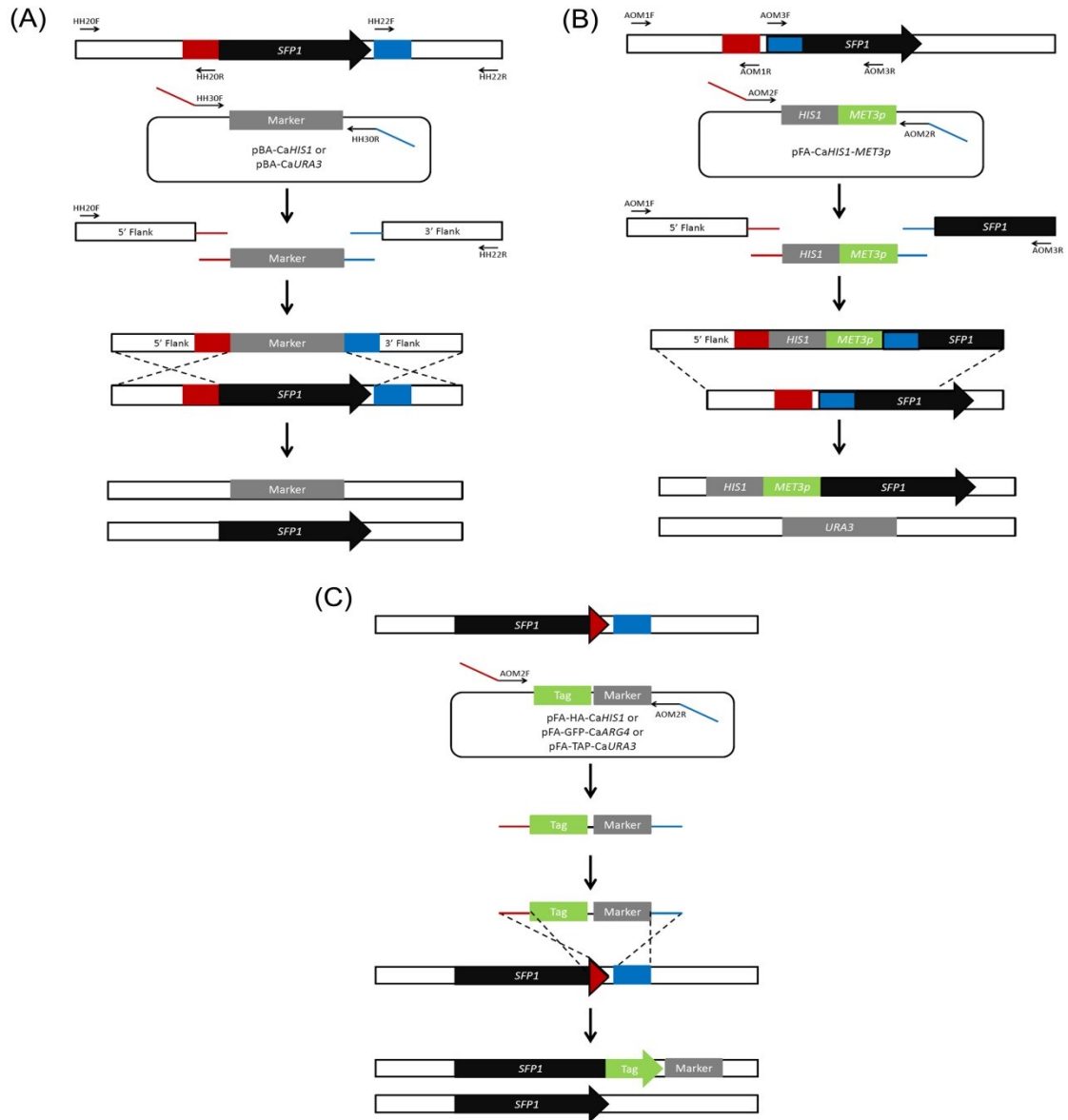


Figure 3: PCR gene manipulation strategies. (A) Gene knock-out strategy used to replace gene coding region with a selectable marker amplified from a plasmid. (B) *MET3* promoter insertion strategy for the conditional regulation of *SFP1*. (C) Epitope tagging strategy for the Sfp1p protein.

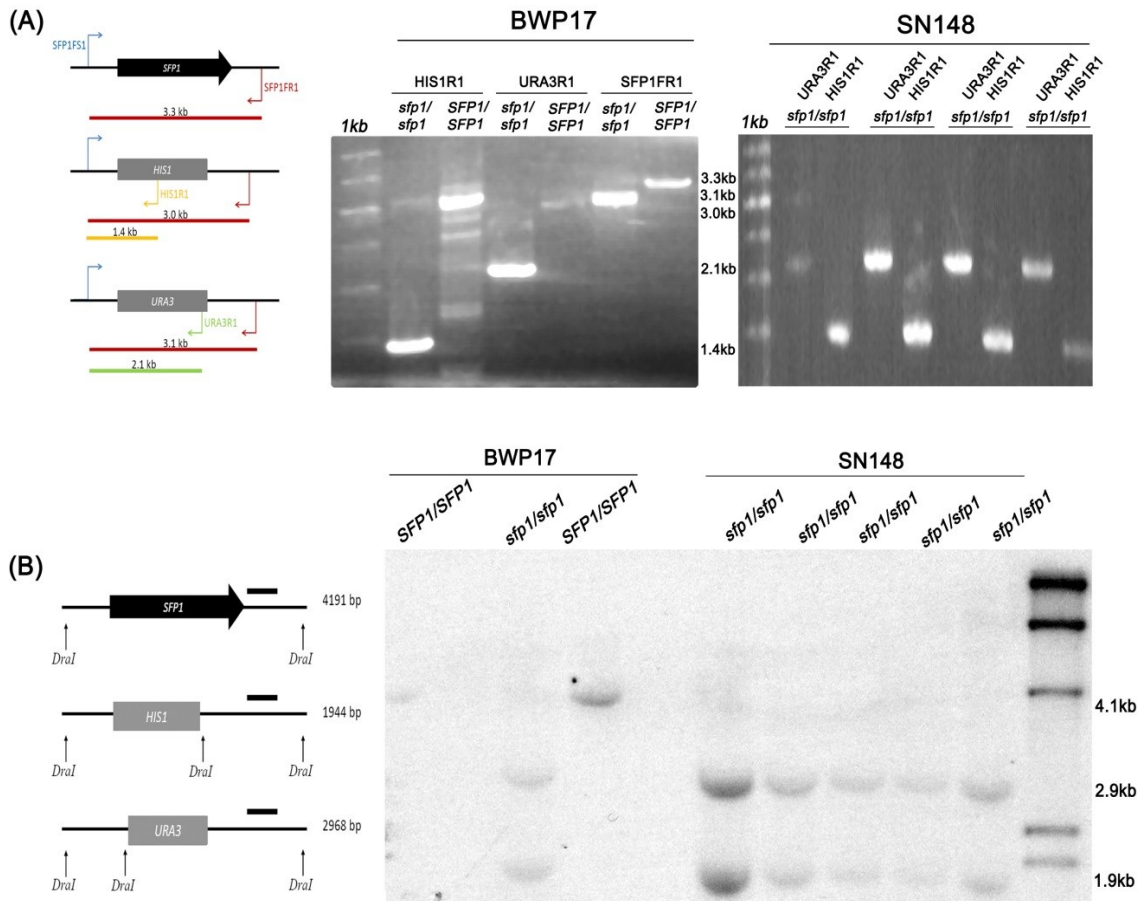


Figure 4: Confirmation of the *sfp1Δ/sfp1Δ* strains by PCR and Southern Blot. (A) The *sfp1/sfp1* strains constructed in two different backgrounds (BWP17, and SN148) were confirmed by amplifying the *SFP1* gene region using a combination of two flanking primers (flanking) and a combination of one flanking primer and one embedded in the selective marker (*HIS1* or *URA3*). Fermentas GeneRuler 1kb DNA ladder standard sizes shown are 4 kb, 3.5 kb, 3 kb, 2.5 kb, 2 kb, 1.5 kb, 1 kb, 0.75 kb, 0.5 kb & 0.25 kb (B) The same strains were also confirmed by probing for the *SFP1* gene region with a DIG-labelled 754 bp probe after digesting with *DraI*. Roche DIG-labeled, molecular weight marker II shown are 9.4 kb, 6.5 kb, 4.3 kb, 2.3 kb & 2 kb.

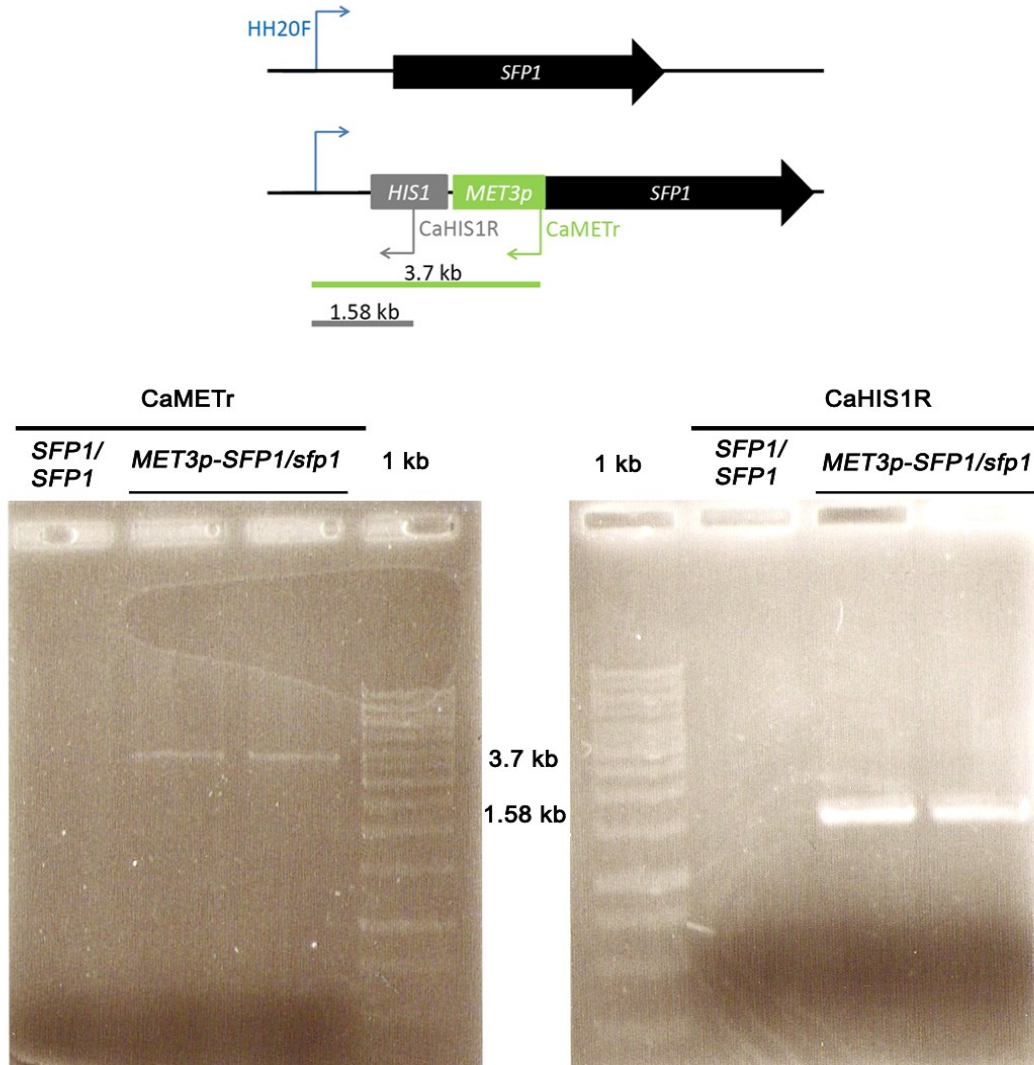


Figure 5: Confirmation of the *MET3::SFP1-URA3/sfp1Δ::HIS1* (AM1511 & AM1512) strains by PCR. Map and gel of PCR screen, showing integration of a *HIS1-MET3* -containing construct at the 5' end of *SFP1* in strain AM1401 (*SFP1/sfp1Δ::URA3*). The *HIS1-MET3* was confirmed in two PCR reactions as a complete 3.7 kb fragment and a partial 1.58 kb fragment corresponding to the *HIS1* marker. Fermentas GeneRuler 1kb DNA ladder standard sizes are 10 kb, 8 kb, 6 kb, 5 kb, 4 kb, 3.5 kb, 3 kb, 2.5 kb, 2 kb, 1.5 kb, 1 kb, 0.75 kb, 0.5 kb & 0.25 kb.

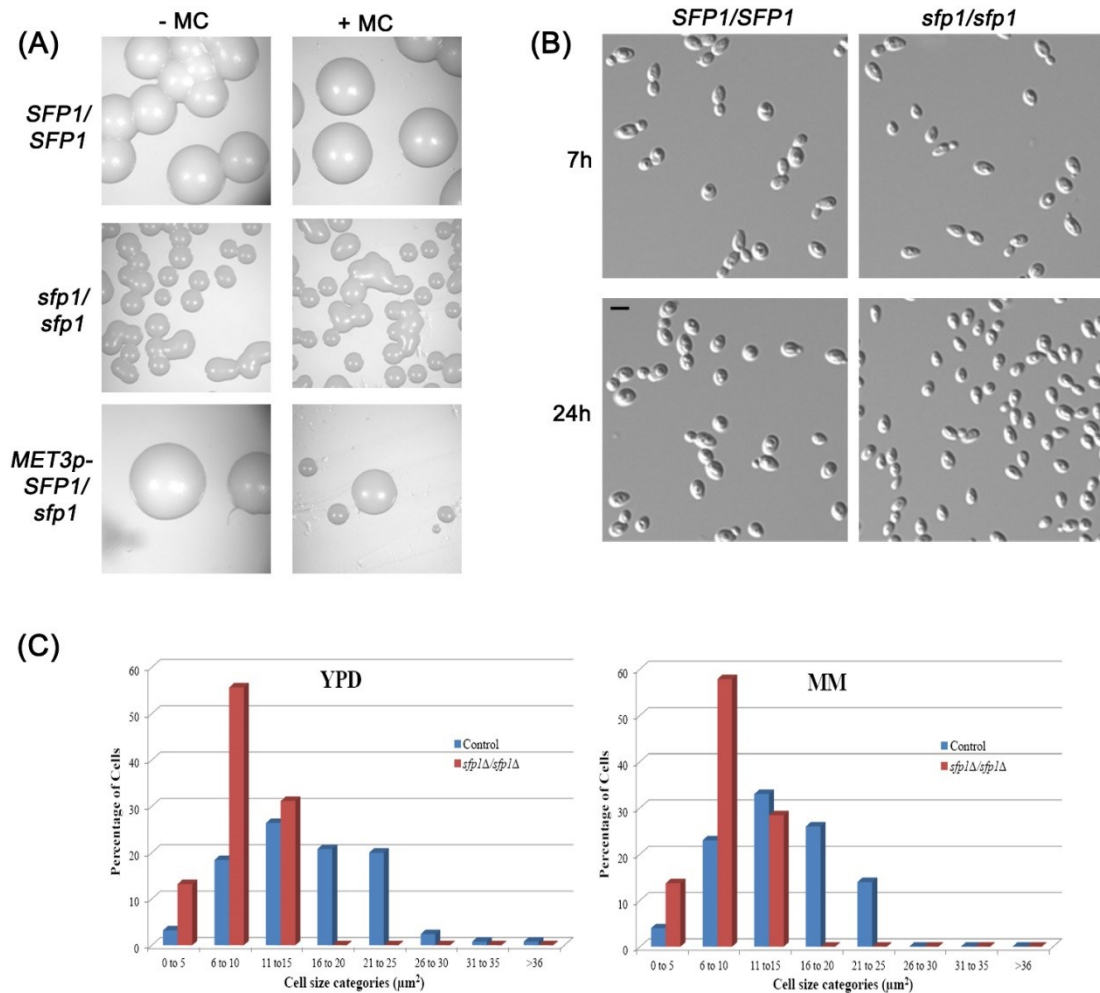


Figure 6: Cells and colonies depleted of Sfp1p show a reduction in size. (A) Cells of strain HHCa28 (*sfp1Δ::HIS1/sfp1Δ::URA3*), the isogenic control HHCa1 (*SFP1/SFP1, URA3+, HIS1+*) and the conditional AM1511 (*MET3::SFP1-URA3/sfp1Δ::HIS1*) were plated on SD+MC or SD-MC medium, and incubated at 30°C for 48 h. (B) Cells of strains HHCa1 and HHCa28 were incubated in minimal medium at 30°C overnight, diluted to an OD_{600nm} of 0.2 in fresh minimal medium and incubated for 7 or 24 h. Bar: 10 μm . (C) Cell size measurements, represented by width x length values, of strains HHCa1 and HHCa28 grown in YPD or MM medium for 24 h.

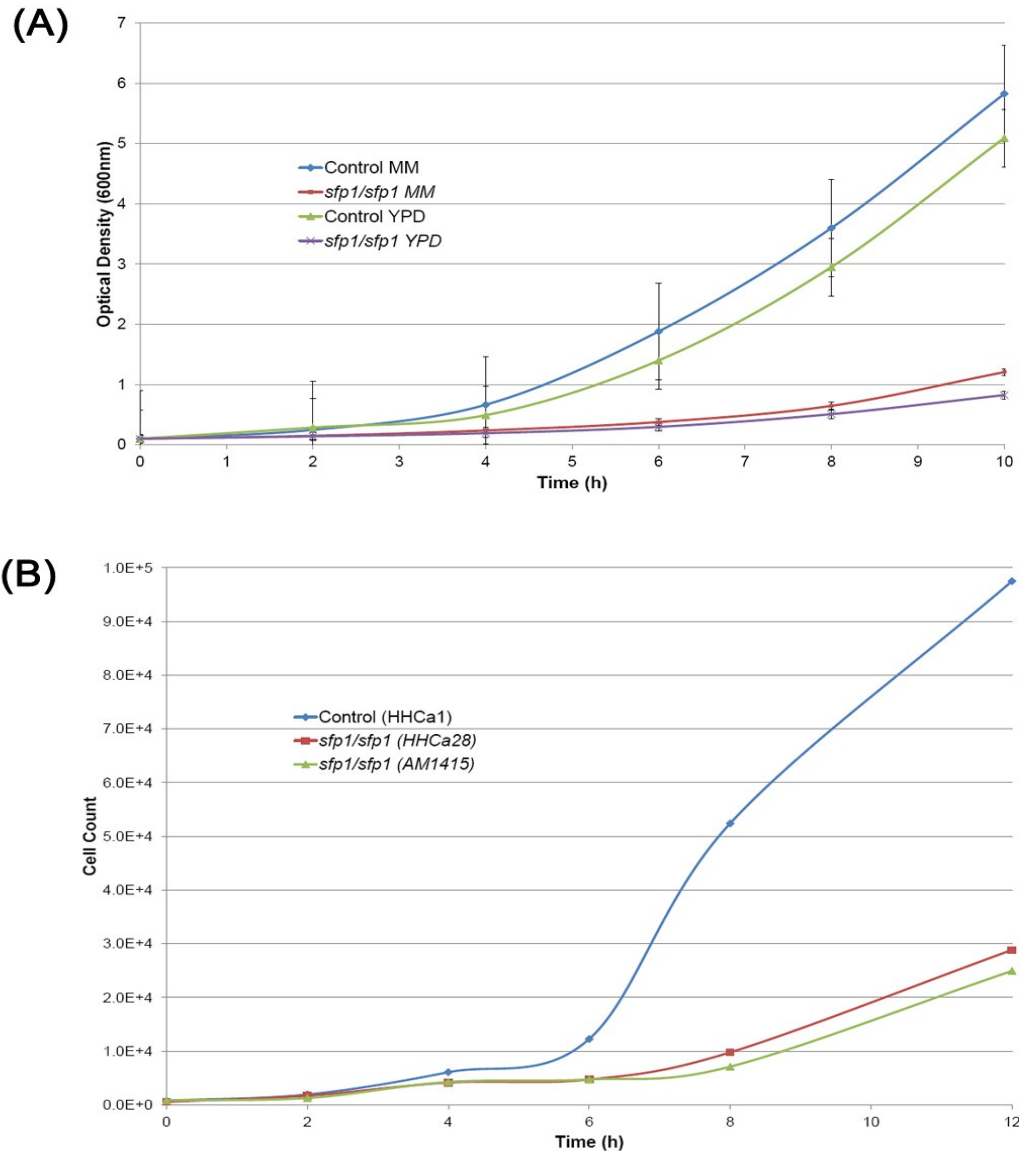


Figure 7: Cells lacking Sfp1p are reduced in growth rate. (A) Cells of strain HHCa28 (*sfp1* Δ ::*HIS1/sfp1* Δ ::*URA3*) and the isogenic control HHCa1 (*SFP1/SFP1*, *URA3*+, *HIS1*+) were incubated in SD or YPD medium at 30°C overnight, and diluted to an OD_{600nm} of 0.1 in fresh medium. Cells were incubated and the OD_{600nm} was recorded every 2 h. Growth curves and error bars are based on the average optical density measurements from four independent cell cultures normalized to a starting OD_{600nm} of 0.1. Growth rates are calculated for the segment between the T₄ to T₁₀ giving a doubling time of 1.8 h for the control versus 2.7 h for the mutant. (B) Number of cells were quantified for strains in (A), including AM1415 (*sfp1* Δ ::*HIS1/sfp1* Δ ::*URA3*) at each time point.

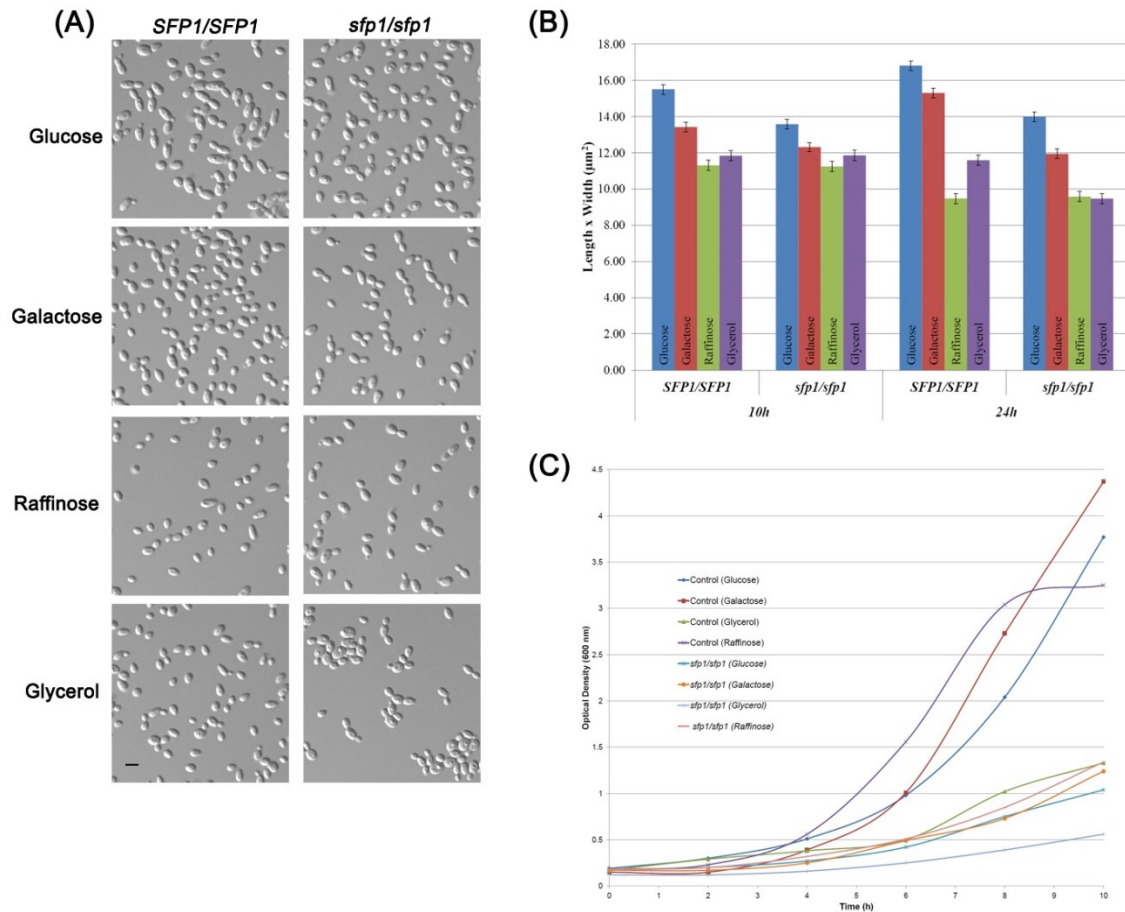


Figure 8: Cells lacking Sfp1p can still modulate cell size in response to select poor carbon sources. Cells of strains HHCa28 (*sfp1* Δ ::*HIS1/sfp1* Δ ::*URA3*) and the isogenic control HHCa1 (*SFP1/SFP1*, *URA3*⁺, *HIS1*⁺) were incubated in minimal medium containing either glucose, galactose, glycerol or raffinose overnight at 30°C, diluted to an OD_{600nm} of 0.1 in fresh medium, and incubated for 10 or 24 h. (A) Cells at 10 h were fixed for imaging. Bar: 10 μm . (B) Cells at 10 or 24 h were fixed and length x width measurements were recorded as an indication of cell size. (C) Growth of strains was investigated by recording the OD_{600nm} every 2 h during incubation in the different carbon source media.

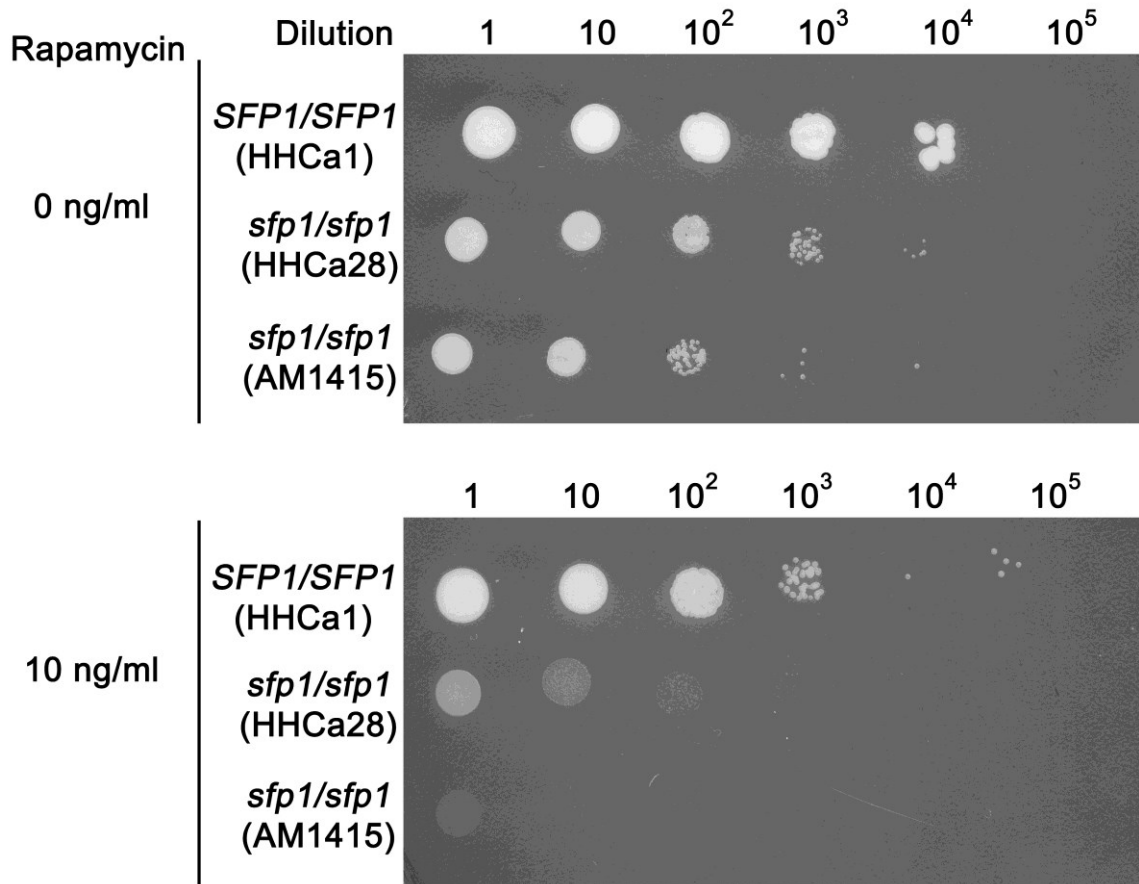


Figure 9: Cells lacking Sfp1p are hypersensitive to sublethal concentrations of Rapamycin. Strains HHCa28, AM415 (*sfp1*Δ::*HIS1/sfp1*Δ::*URA3*) and isogenic control HHCa1 (*SFP1/SFP1*, *URA3*⁺, *HIS1*⁺) were incubated overnight in YPD medium at 30°C, diluted to an OD_{600nm} of 1, serially diluted 5 times and spotted (2 μl) on solid media containing either 0 or 10 ng/ml Rapamycin. Plates were incubated at 30°C for 3 days.

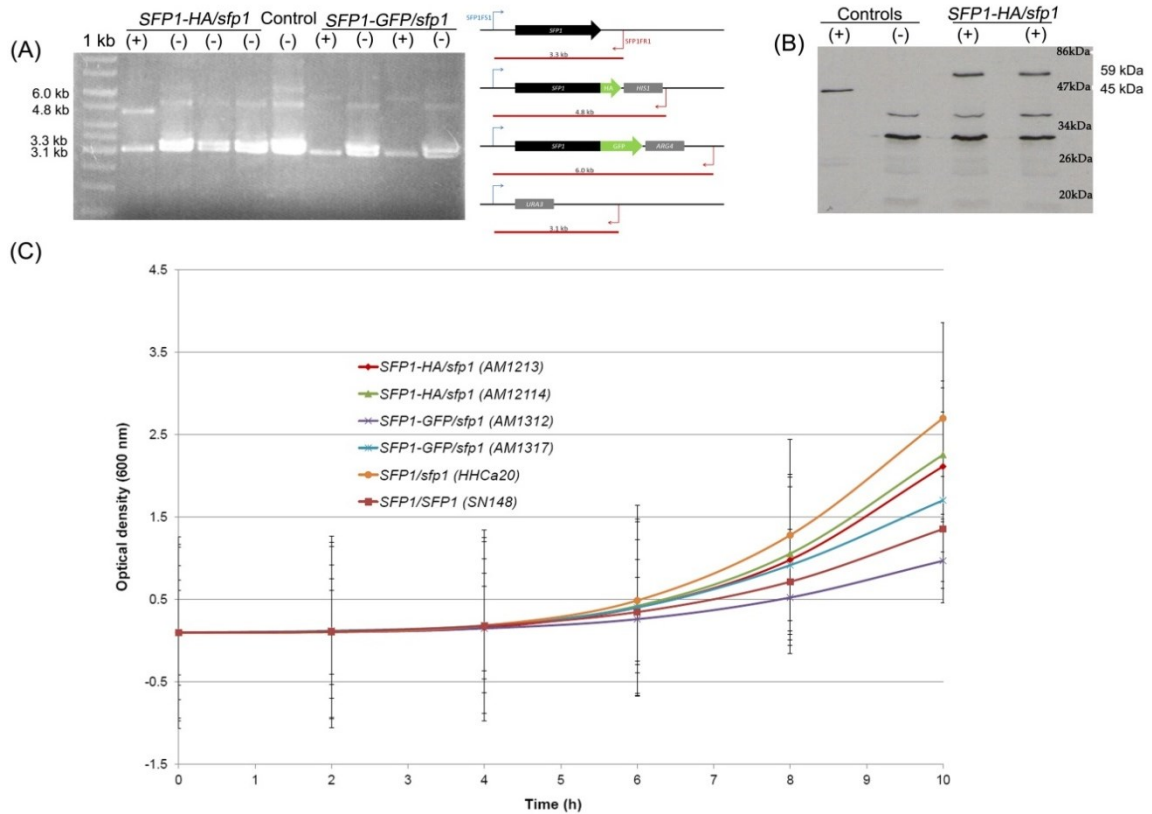


Figure 10: Construction and confirmation of Sfp1-HA and Sfp1p-GFP strains. (A) MAP and PCR screen showing *SFPI-HA-HIS1/sfp1Δ* (AM1213) and *SFPI-GFP-ARG4/sfp1Δ* (AM1312; AM1317) strains alongside the parental *SFPI/sfp1Δ::URA3* strain (HHCa20). A 6.0 kb fragment corresponded to *SFPI-GFP-ARG4*, a 4.8 kb fragment for *SFPI-HA-HIS1*, a 3.3 kb fragment for *SFPI*, and a 3.1 kb fragment for *sfp1::URA3*. (B) Western blot confirmation of two *SFPI-HA-HIS1/sfp1* strains (AM1213; AM12114) alongside the parental *SFPI/sfp1::URA3* strain (HHCa20) and an *S. cerevisiae* strain with a 45 KDa HA tagged protein, as negative and positive controls, respectively. (C) Growth rate of HA and GFP-tagged Sfp1p strains. Strains AM1213, AM12114, AM1312, AM1317, SN148 and HHCa20 were incubated in YPD medium overnight at 30°C, diluted to an OD_{600nm} of 0.1 in fresh medium, and incubated for the indicated times, at which OD_{600nm} was recorded. Graphs are the result of 4 separate experiments. Average standard errors are ±0.64 for SN148, ±1.16 for HHCa20, ±1.04 for AM1213, ±0.81 for AM12114, ±0.51 for AM1312 and ±1.07 for AM1317.

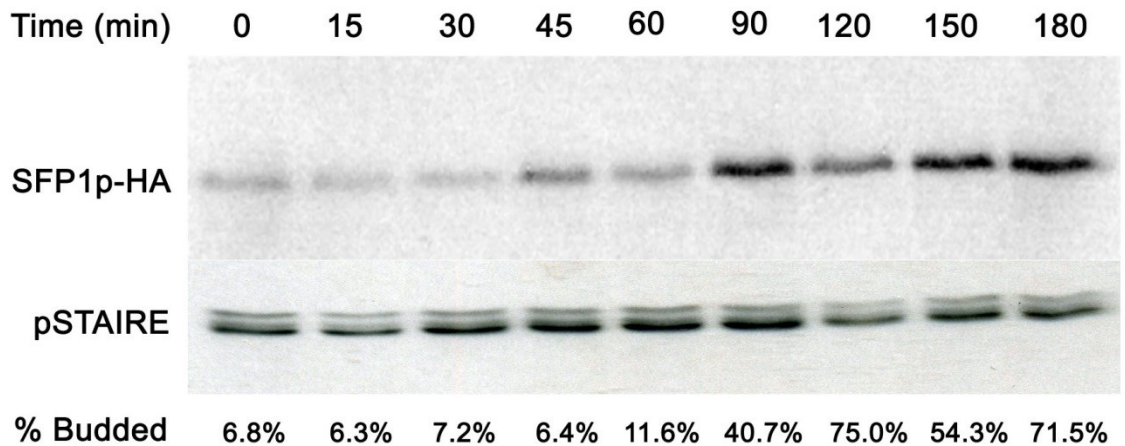


Figure 11: Sfp1p-HA levels increase during cell cycle progression. (A) Strain AM1213 (*SFP1-HA-HIS1/sfp1Δ-URA3*) was incubated overnight in YPD medium at 30°C, diluted to an OD_{600nm} of 0.2 in 500 ml of fresh YPD. At the indicated times, 50 ml of culture were collected for protein extraction. A portion of cells were also fixed and stained with DAPI in order to determine the budding ratio. PSTAIRE (Cdc28p) was used as a loading control.

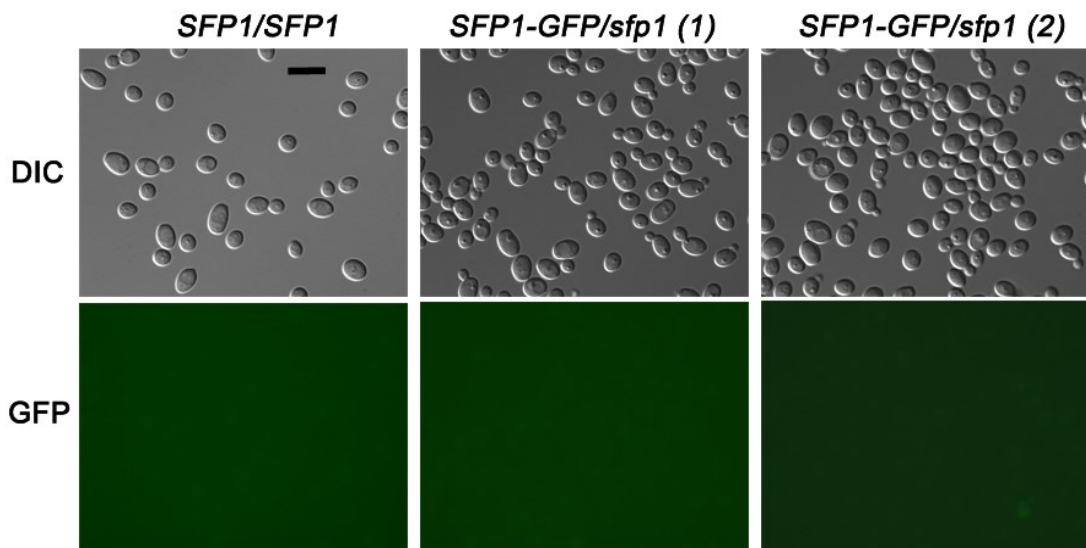


Figure 12: Localization of Sfp1p-GFP. Strains AM1312 (*SFP1-HA-HIS1/sfp1Δ-URA3*), AM1317 (*SFP1-HA-HIS1/sfp1Δ-URA3*), and HHCa20 (*SFP1-HA-HIS1/sfp1Δ-URA3*) were incubated overnight in YPD medium at 30°C, diluted to an OD_{600nm} of 0.2 in 500 ml of fresh YPD. Cells were collected (750 μl) at an OD_{600nm} of 0.8, washed and prepared for DIC and GFP microscopy. Bar: 10 μm.

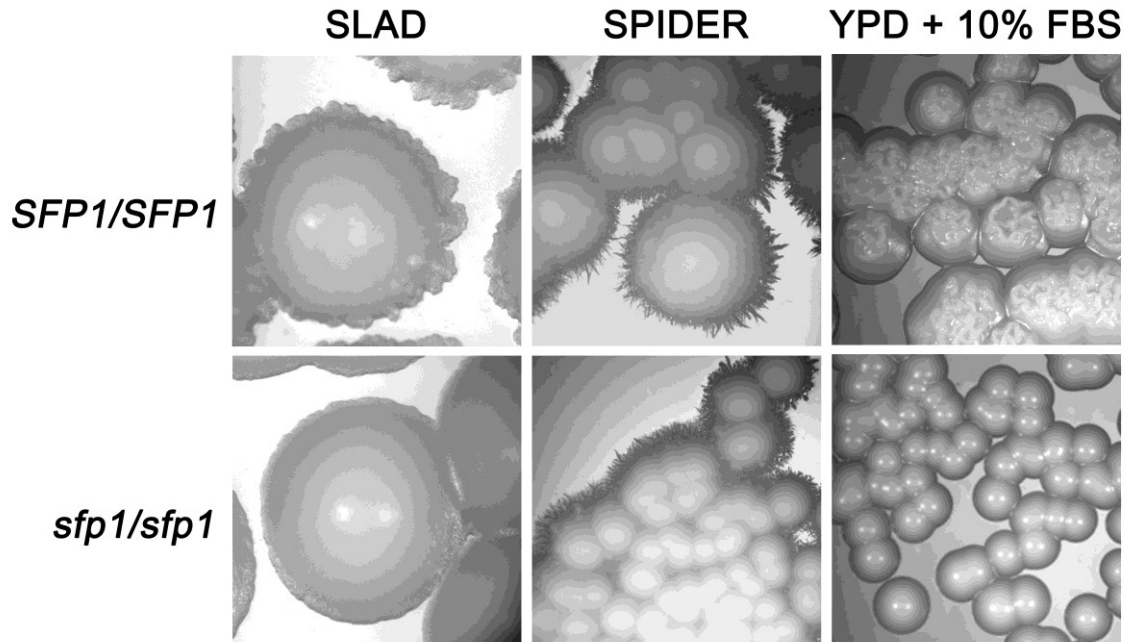


Figure 13: The absence of Sfp1p results in a reduction in filamentation on select medium, and lack of nitrogen source suppresses the cell size defect of *sfp1*Δ cells. Strains HHCa28 (*sfp1*Δ::*HIS1*/*sfp1*Δ::*URA3*) and HHCa1 (*SFP1/SFP1*, *URA3*⁺, *HIS1*⁺) were incubated in minimal media overnight, and diluted to an OD_{600nm} of 0.01 before streaking on solid media. Plates were incubated at 37°C for 3 to 5 days for the 10% FBS plates, and 5 to 7 days for the SLAD and SPIDER plates.

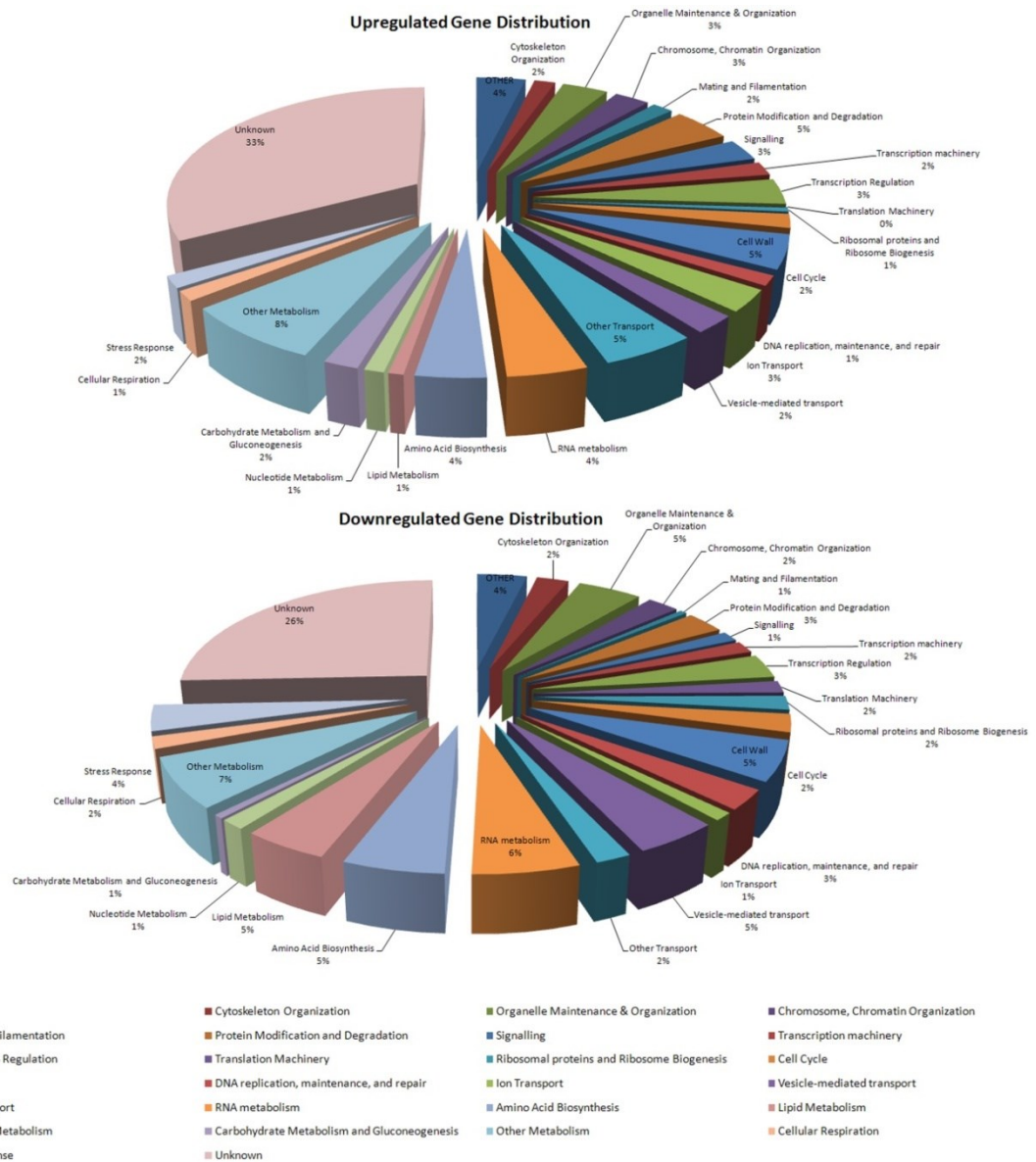


Figure 14: Distribution of genes differentially modulated between the *sfp1Δ/sfp1Δ* strain and its *SFP1/SFP1* isogenic control. Four independent gene microarray chips were analyzed to obtain 374 upregulated and 370 downregulated genes that were differentially modulated between the *sfp1/sfp1* strain and its *SFP1/SFP1* isogenic control while satisfying the 1.5x expression cutoff level and a t-test p value <0.05. Genes were manually organized into 26 categories based on their CGD (Candida Genome Database) as well as GeneSpring descriptions.

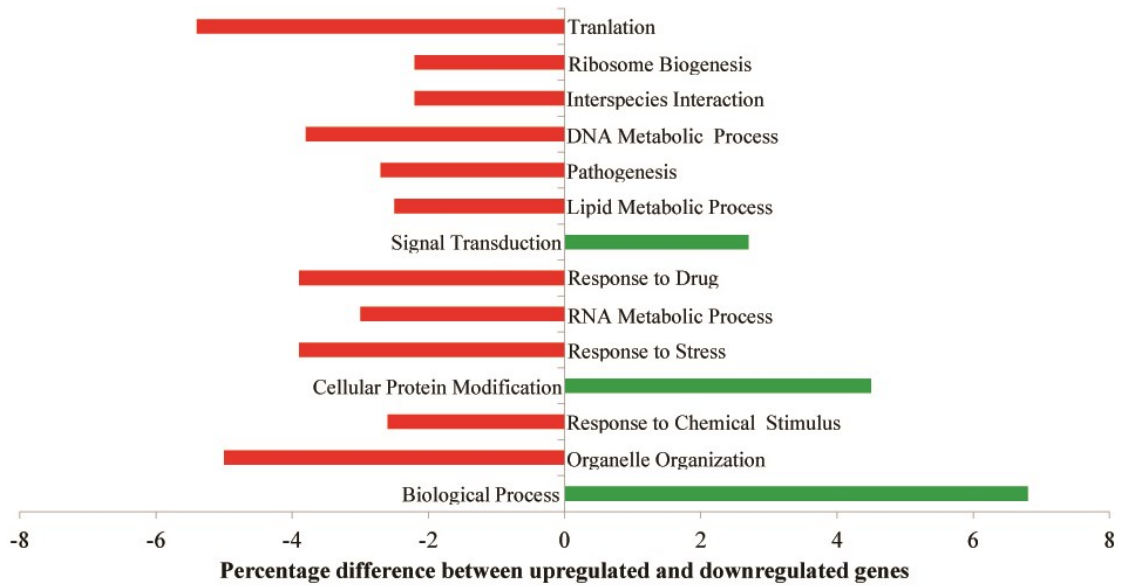


Figure 15: GO Slim Mapper categories with 2% difference or more between upregulated and downregulated genes in the absence of Sfp1p. Significantly upregulated and downregulated genes from microarray analysis of the *sfp1Δ/sfp1Δ* strain (HHCa28) were categorized by biological process using GO Slim Mapper. The percentages of upregulated and downregulated genes associated with each category were subtracted (upregulated-downregulated) to determine categories with 2% or more difference.

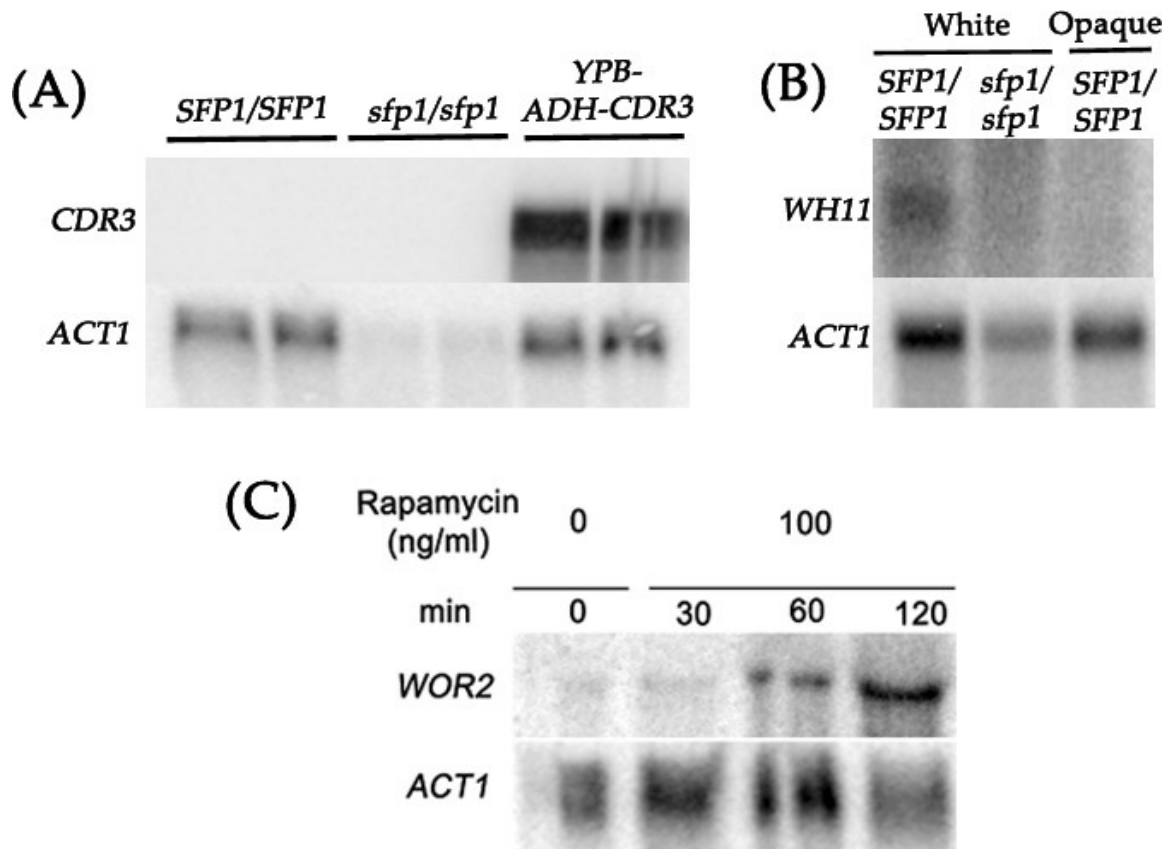


Figure 16: Northern blot confirmation of the expression of opaque and white phase specific genes. (A) The *CDR3* transcript, encoding an opaque specific gene, could not be detected in both the control *SFP1/SFP1* (BWP17) and the mutant *sfp1Δ/sfp1Δ* (HHCa28) strains unlike the *YPB-ADH-CDR3* transformed strain overexpressing the *CDR3* gene. The loading control gene *ACT1* indicates unequal loading for the *sfp1Δ/sfp1Δ* strain. (B) The *WH11* transcript encoding a white phase specific gene could be detected in the BWP17 (*SFP1/SFP1*) control strain but not in the *sfp1Δ/sfp1Δ* (HHCa28) and opaque phase *SFP1/SFP1* cells. The loading control gene *ACT1* indicates unequal loading for the *sfp1Δ/sfp1Δ* strain. (C) Rapamycin treatment results in the overexpression of *WOR2*, an opaque transcriptional regulator. Cells were diluted from an overnight stationary culture to an OD_{600nm} of 0.1 in 300ml of YPD and grown to an OD_{600nm} of 0.8 - 1.0 before adding 100ng/ml. RNA was extracted from 100ml cell pellets at 0min before the addition of rapamycin and at 30, 60, and 120min after the addition of rapamycin.

6.0 TABLES

Table 1: *Candida albicans* strains used in this study

Strains	Genotype	Source
BWP17	<i>ura3Δ::imm⁴³⁴/ura3Δ::imm⁴³⁴</i> <i>his1Δ::hisG/his1Δ::hisG</i> <i>arg4Δ::hisG/arg4Δ::hisG</i>	Fonzi & Irwin, 1994
SN148	<i>arg4Δ/arg4Δ leu2Δ/leu2Δ his1Δ/his1Δ</i> <i>ura3Δ::imm⁴³⁴/ura3Δ::imm⁴³⁴</i> <i>iro1Δ::imm⁴³⁴/iro1Δ::imm⁴³⁴</i>	Noble & Johnson, 2005
HHCa1	<i>SFPI/SFPI ura3Δ::im⁴³⁴/URA3</i> <i>his1Δ::hisG/HIS1 arg4Δ::hisG/arg4Δ::hisG</i>	This study
HHCa20	<i>SFPI/sfp1Δ::URA3</i>	This study
HHCa28	<i>sfp1Δ::HIS1/sfp1Δ::URA3</i>	This study
AM1213	<i>SFPI-HA-HIS1/sfp1Δ::URA3</i>	This study
AM130	<i>SFPI-GFP-HIS1/SFPI</i>	This study
AM1312	<i>SFPI-GFP-ARG4/sfp1Δ::URA3</i>	This study
AM1317	<i>SFPI-GFP-ARG4/sfp1Δ::URA3</i>	This study
AM1401	<i>SFPI/sfp1Δ::URA3</i>	This study
AM1415	<i>sfp1Δ::HIS1/sfp1Δ::URA3</i>	This study
AM1511	<i>HIS1-MET3p-SFPI/sfp1Δ::URA3</i>	This study
AM1512	<i>HIS1-MET3p-SFPI/sfp1Δ::URA3</i>	This study
CIB4 [YPB-ADHpt/CDR3]	<i>cdr3Δ::hisG/cdr3Δ::hisG</i> , YPB-ADHpt/CDR3	(98)

Table 2: Oligonucleotides used in this study.

Oligonucleotides	Sequence (5' to 3')
CaURA3R	TTC AAA TAA GCA TTC CAA CC
CaHIS1R	ACT GGG ATA TCA GCT GCA GG
CaMETr	TGG GGA GGG TAT TTA CTT TTA AAT
SFP1FS1	CAG GTA GTG TAC TTG AGT AT
SFP1RS1	ATT CTA CTC TGC CAA GCA AC
HH20F	ATA TGA AAT CAC CTC TTC TCA CTC CCA TTC
HH20R	AGG TTT CGA TAG AAC GTA AAT CGA GAT TAG
HH30F	CTA ATC TCG ATT TAC GTT CTA TCG AAA CCT TAT AGG GCG AAT TGG AGC TC
HH30R	AAG CTC GCT CTC GTC ATA CAC AAG TAT GGA GAC GGT ATC GAT AAG CTT GA
HH22F	TCC ATA CTT GTG TAT GAC GAG AGC GAG CTT
HH22R	TAT GTT GGT TTT GAT GGA AGA TCT TCT AGC
HH23F	AAG TTC AAA GTT CCT ACA TTG AAT GAT TTG
HH23R	ATT AGG GCT AGT GCT ATT GGA TAC AGG TTA
HH24F	TAA CCT GTA TCC AAT AGC ACT AGC CCT AAT GGT GCT GGC GCA GGT GCT TC
HH24R	GAA CAT GAT ATT GTG GAA TAG TTA GAA TCA TCA TCG ATG AAT TCG AGC TC
HH25F	TGA TTC TAA CTA TTC CAC AAT ATC ATG TTC
HH25R	CAA CAA CAA ACA AAT TCT ACG ATA TGA TAG
AOL3F	AAC CAT ATA GAT GTG AGG TAT GTG GTA GAG GAT ATA AGA ATC TCA ATG GAT TGA AAT ACC ATC GTG CTG GCG CAG GTG CTT C

AOL3R	AGT TAT TCT TGC CAA TCA GAT GGT TAC AAC AAT GTA CTA GAC GCT TGA AGA AGA AGA CCA AGT AGG CAT CAA TTC GGT AGT CAT CGA TGA ATT CGA GCT C
AOM1F	GAG AAA GCG ATC CTT AAA GAA GCG CA
AOM1R	TCT CCA CTA GAT AGG GTG GCG GTT GT
AOM2F	ACA ACC GCC ACC CTA TCT AGT GGA GA GGA TCC TGG AGG TGG AGG ATG AGG
AOM2R	TTT TCA AAT ATC TTG GTA TTA AAC AT CAT GTT TTC TGG GGA GGG TAT TTA
AOM3F	ATG TTT AAT ACC AAG ATA TTT GAA AA
AOM3R	GAT CAT GTT GCT GAA GTA TCT GAT GG
HHWOR2F	CCT CTG TAC CAA CAC CAC CA
HHWOR2R	CCA GCA CCA CCA ACT ATT GA
HHWH11F	TCC GAC TTA GGT AGA AAA GA
HHWH11R	TTT GGA GTC ACC AAA AAT AG
HHACT1F	TGG CTA ACT TCA ATG TAT CTG
HHACT1R	CGT CGT CAC CGG CAA AA
HHACT1q1F	ACG GTG AAG TTG CTG CTT TAG TT
HHACT1q1R	CGT CGT CAC CGG CAA AA
HHCDR3q1F	GCT GTA CAA AAT GAA TTG CAT CGT
HHCDR3q1R	GCT TGG TTG GTA TCT GGT TCC T
HHCDR3q2F	TCT TGG TAT TAT CCT GTT GGG TTG T
HHCDR3q2R	GAT TAA CCA CAT CAA TAC ACC ACG AT
HHCDR3F	CCA AGA CAT CAC AAG CAG
HHCDR3R	GCA ACA CCT AAT TTA CCT

Table 3: Plasmids used in this study.

Plasmid	Description	Source
pBS – <i>CaURA3</i>	pBlueScript <i>CaURA3</i>	A. J. P. Brown
pBS – <i>CaHIS1</i>	pBlueScript <i>CaHIS1</i>	C. Bachewich
pFA – TAP- <i>CaARG4</i>	pFA-TAP- <i>CaARG4</i>	(153)
pFA – GFP – <i>CaARG4</i>	pFA-GFP- <i>CaARG4</i>	(153)
pFA – HA – <i>CaHIS1</i>	pFA-HA- <i>CaHIS1</i>	(153)
pFA – <i>MET3p</i> - <i>CaHIS1</i>	pFA – <i>MET3p</i> - <i>CaHIS1</i>	(153)
p425 – GPD – <i>CaCDR3</i>	P425-GPD- <i>CaCDR3</i>	M. Raymond

Table 4: Length by width ratios ¹ of the *sfp1/sfp1* strain compared to the control strain in rich and minimal media.

Strain	Medium	Incubation Time (h)	Mean LxW ² (μm^2) \pm S.E.M.	W value ³	P value ⁴
HHCa1 (n= 110)	MM	7	12.97 \pm 0.25	14218	p < 0.0001
HHCa28 (n= 104)			11.08 \pm 0.20		
HHCa1 (n= 100)		24	14.18 \pm 0.34	12856	p < 0.0001
HHCa28 (n= 102)			10.95 \pm 0.25		
HHCa1 (n= 104)	YPD	7	12.62 \pm 0.29	13371.5	p = 0.0001
HHCa28 (n= 117)			11.11 \pm 0.23		
HHCa1 (n= 125)		24	13.21 \pm 0.28	19024.5	p < 0.0001
HHCa28 (n= 106)			9.33 \pm 0.23		

¹ Strains HHCa1 (*SFP1/SFP1*, *URA3*, *HIS1*) and HHCa28 (*sfp1::URA3/sfp1::HIS1*) were incubated in media for 7 or 24 h at 30°C, after which they were fixed in 70% EtOH, and length and width measurements were recorded.

² A minimum of 100 cells were measured, and values represent mean length by width ratios.

³ Mann-Whitney test W value for statistical analysis of non-normally distributed samples

⁴ Mann-Whitney test P value for difference between control and knockout samples.

Table 5: Length by width ratios of the *sfp1/sfp1* strain and the control strain in media containing different carbon sources¹.

Strain	Carbon Source	Incubation Time (h)	Mean LxW ² (μm^2) \pm S.E. M.	W value ³	P value ⁴
HHCa1 (n= 113)	Glucose		15.49 \pm 0.23	Reference	
HHCa1 (n= 118)	Galactose	10	13.41 \pm 0.27	9715.0	p < 0.001
HHCa1 (n= 114)	Raffinose		11.30 \pm 0.31	10785.5	p < 0.001
HHCa1 (n= 114)	Glycerol		11.83 \pm 0.28	10605.0	p < 0.001
HHCa1 (n= 101)	Glucose		16.81 \pm 0.34	Reference	
HHCa1 (n= 109)	Galactose	24	15.30 \pm 0.31	7009.0	p < 0.001
HHCa1 (n= 111)	Raffinose		9.47 \pm 0.33	10383.5	p < 0.001
HHCa1 (n= 105)	Glycerol		11.58 \pm 0.28	9305.5	p < 0.001
HHCa28 (n= 114)	Glucose		13.57 \pm 0.24	Reference	
HHCa28 (n= 116)	Galactose	10	12.31 \pm 0.19	8684.0	p < 0.001
HHCa28 (n= 113)	Raffinose		11.24 \pm 0.21	9780.5	p < 0.001
HHCa28 (n= 102)	Glycerol		11.85 \pm 0.34	7705.0	p < 0.001
HHCa28 (n= 105)	Glucose		13.97 \pm 0.24	Reference	
HHCa28 (n= 112)	Galactose	24	11.94 \pm 0.27	8415.0	p < 0.001
HHCa28 (n= 110)	Raffinose		9.58 \pm 0.25	10292.5	p < 0.001
HHCa28 (n= 104)	Glycerol		9.56 \pm 0.26	9718.0	p < 0.001

¹ Strains HHCa1 (*SFPI/SFPI*, *URA3*, *HIS1*) and HHCa28 (*sfp1::URA3/sfp1::HIS1*) were incubated in MM medium containing either 2% glucose, galactose, raffinose or glycerol, incubated for 10 or 24 h at 30°C, fixed in 70% EtOH, and length and width measurements were recorded from images. Results represent two separate trials.

² A minimum of 100 cells were measured, and values represent mean length by width ratios.

³ Mann-Whitney test W value for statistical analysis of non-normally distributed samples

⁴ Mann-Whitney test P value for difference between control and knock-out samples.

Table 6: Length and width measurements of hyphae formed in the presence or absence of Sfp1p¹.

Strain	Mean Length²	Mean Width³
	(μm) \pm S.E. M.	(μm) \pm S.E. M.
HHCa1 (n= 50)	15.17 \pm 1.23	1.74 \pm 0.05
HHCa28 (n= 52)	9.27 \pm 0.45	1.41 \pm 0.05

¹ Strains HHCa1 (*SFP1/SFP1*, *URA3*, *HIS1*) and HHCa28 (*sfp1::URA3/sfp1::HIS1*) were incubated in YPD medium overnight, diluted to an O.D._{600nm} of 0.1 into fresh YPD supplemented with 10% fetal bovine serum (FBS), and incubated for 1.5 hours at 37°C. Cells were fixed and widths and lengths were recorded from images.

² Statistical analysis of length measurements (non-normally distributed) was performed using the Mann-Whitney test and the values were $W = 2420.0$ and $p = 0.0001$

³ Statistical analysis of width measurements (non-normally distributed) was performed using the Mann-Whitney test and the values were $W = 2514.5$ and $p < 0.0001$

Table 7: GO Slim Mapper term analysis of genes modulated in cells lacking Sfp1p in comparison to the complete list of *C. albicans* genes¹.

GO Slim Mapper Process Category ²	P value ³	GO genes in set ⁴ (Total 744)	GO genes in genome ⁵ (Total 6810)
Transport	1.54E-02	1011	136
Response to chemical stimulus	1.45E--3	645	99
Response to drug	1.39E-02	360	56
Ribosome biogenesis	1.39E-03	283	14
Cell wall organization	1.07E-02	168	31
Cytokinesis	3.77E-02	110	20
Nucleus organization	4.34E-02	48	11
Other	3.57E-03	472	74
Not yet annotated	9.29E-06	594	32

¹ Genes significantly modulated by the absence of Sfp1p were obtained by microarray expression analysis of the *sfp1::URA3/sfp1::HIS1* strain (HHCa28) and the *SFPI/SFPI, URA3, HIS1* strain (HHCa1). GO Term classifications were carried out using the tool at <http://www.candidagenomedatabase.org>

² GO Terms with significant differences between the two samples.

³ Fisher exact test p value with a cut-off set at $p < 0.05$

⁴ Number of genes modulated by the absence of Sfp1p and associated with a GO Term category.

⁵ Number of genes in the genome associated with a GO Term category.

7.0 REFERENCES

1. Rohde JR, Cardenas ME. Nutrient signaling through TOR kinases controls gene expression and cellular differentiation in fungi. *Current topics in microbiology and immunology*. 2004;279:53-72.
2. Cheng SC, Joosten LA, Kullberg BJ, Netea MG. Interplay between *Candida albicans* and the mammalian innate host defense. *Infection and immunity*. 2012;80(4):1304-13.
3. Cole GT, Halawa AA, Anaissie EJ. The role of the gastrointestinal tract in hematogenous candidiasis: from the laboratory to the bedside. *Clinical infectious diseases : an official publication of the Infectious Diseases Society of America*. 1996;22 Suppl 2:S73-88.
4. Kaufman D. Fungal infection in the very low birthweight infant. *Current opinion in infectious diseases*. 2004;17(3):253-9.
5. Berman J, Sudbery PE. *Candida Albicans*: a molecular revolution built on lessons from budding yeast. *Nature reviews Genetics*. 2002;3(12):918-30.
6. Sudbery P, Gow N, Berman J. The distinct morphogenic states of *Candida albicans*. *Trends in microbiology*. 2004;12(7):317-24.
7. Alby K, Bennett RJ. Stress-induced phenotypic switching in *Candida albicans*. *Molecular biology of the cell*. 2009;20(14):3178-91.
8. Berman J. Morphogenesis and cell cycle progression in *Candida albicans*. *Current opinion in microbiology*. 2006;9(6):595-601.
9. Lo HJ, Kohler JR, DiDomenico B, Loebenberg D, Cacciapuoti A, Fink GR. Nonfilamentous *C. albicans* mutants are avirulent. *Cell*. 1997;90(5):939-49.
10. Bassilana M, Blyth J, Arkowitz RA. Cdc24, the GDP-GTP exchange factor for Cdc42, is required for invasive hyphal growth of *Candida albicans*. *Eukaryotic cell*. 2003;2(1):9-18.
11. Saville SP, Lazzell AL, Monteagudo C, Lopez-Ribot JL. Engineered control of cell morphology in vivo reveals distinct roles for yeast and filamentous forms of *Candida albicans* during infection. *Eukaryotic cell*. 2003;2(5):1053-60.
12. Jong AY, Stins MF, Huang SH, Chen SH, Kim KS. Traversal of *Candida albicans* across human blood-brain barrier in vitro. *Infection and immunity*. 2001;69(7):4536-44.
13. Lorenz MC, Bender JA, Fink GR. Transcriptional response of *Candida albicans* upon internalization by macrophages. *Eukaryotic cell*. 2004;3(5):1076-87.
14. McKenzie CG, Koser U, Lewis LE, Bain JM, Mora-Montes HM, Barker RN, et al. Contribution of *Candida albicans* cell wall components to recognition by and escape from murine macrophages. *Infection and immunity*. 2010;78(4):1650-8.
15. Wachtler B, Citiulo F, Jablonowski N, Forster S, Dalle F, Schaller M, et al. *Candida albicans*-epithelial interactions: dissecting the roles of active penetration, induced endocytosis and host factors on the infection process. *PloS one*. 2012;7(5):e36952.
16. Whiteway M, Bachewich C. Morphogenesis in *Candida albicans*. *Annual Review of Microbiology*. 2007;61:529-53.
17. Bassilana M, Hopkins J, Arkowitz RA. Regulation of the Cdc42/Cdc24 GTPase module during *Candida albicans* hyphal growth. *Eukaryotic cell*. 2005;4(3):588-603.
18. Leberer E, Harcus D, Dignard D, Johnson L, Ushinsky S, Thomas DY, et al. Ras links cellular morphogenesis to virulence by regulation of the MAP kinase and cAMP signalling pathways in the pathogenic fungus *Candida albicans*. *Molecular microbiology*. 2001;42(3):673-87.

19. Liu H, Kohler J, Fink GR. Suppression of hyphal formation in *Candida albicans* by mutation of a STE12 homolog. *Science (New York, NY)*. 1994;266(5191):1723-6.
20. Cloutier M, Castilla R, Bolduc N, Zelada A, Martineau P, Bouillon M, et al. The two isoforms of the cAMP-dependent protein kinase catalytic subunit are involved in the control of dimorphism in the human fungal pathogen *Candida albicans*. *Fungal genetics and biology : FG & B*. 2003;38(1):133-41.
21. Maidan MM, De Rop L, Serneels J, Exler S, Rupp S, Tournu H, et al. The G protein-coupled receptor Gpr1 and the Galpha protein Gpa2 act through the cAMP-protein kinase A pathway to induce morphogenesis in *Candida albicans*. *Molecular biology of the cell*. 2005;16(4):1971-86.
22. Stoldt VR, Sonneborn A, Leuker CE, Ernst JF. Efg1p, an essential regulator of morphogenesis of the human pathogen *Candida albicans*, is a member of a conserved class of bHLH proteins regulating morphogenetic processes in fungi. *The EMBO journal*. 1997;16(8):1982-91.
23. Dhillon NK, Sharma S, Khuller GK. Signaling through protein kinases and transcriptional regulators in *Candida albicans*. *Critical reviews in microbiology*. 2003;29(3):259-75.
24. Wang X, Proud CG. Nutrient control of TORC1, a cell-cycle regulator. *Trends in cell biology*. 2009;19(6):260-7.
25. Costanzo M, Nishikawa JL, Tang X, Millman JS, Schub O, Breitzkreuz K, et al. CDK activity antagonizes Whi5, an inhibitor of G1/S transcription in yeast. *Cell*. 2004;117(7):899-913.
26. de Bruin RA, McDonald WH, Kalashnikova TI, Yates J, 3rd, Wittenberg C. Cln3 activates G1-specific transcription via phosphorylation of the SBF bound repressor Whi5. *Cell*. 2004;117(7):887-98.
27. de Bruin RA, Kalashnikova TI, Chahwan C, McDonald WH, Wohlschlegel J, Yates J, 3rd, et al. Constraining G1-specific transcription to late G1 phase: the MBF-associated corepressor Nrm1 acts via negative feedback. *Molecular cell*. 2006;23(4):483-96.
28. Breeden L. Start-specific transcription in yeast. *Current topics in microbiology and immunology*. 1996;208:95-127.
29. Horak CE, Luscombe NM, Qian J, Bertone P, Piccirillo S, Gerstein M, et al. Complex transcriptional circuitry at the G1/S transition in *Saccharomyces cerevisiae*. *Genes & development*. 2002;16(23):3017-33.
30. Hartwell LH. *Saccharomyces cerevisiae* cell cycle. *Bacteriological Reviews*. 1974;38(2):164-98.
31. Johnston GC, Pringle JR, Hartwell LH. Coordination of growth with cell division in the yeast *Saccharomyces cerevisiae*. *Experimental cell research*. 1977;105(1):79-98.
32. Jorgensen P, Tyers M. How cells coordinate growth and division. *Current biology : CB*. 2004;14(23):R1014-27.
33. Cook M, Tyers M. Size control goes global. *Current opinion in biotechnology*. 2007;18(4):341-50.
34. Dosil M. Ribosome synthesis-unrelated functions of the preribosomal factor Rrp12 in cell cycle progression and the DNA damage response. *Molecular and cellular biology*. 2011;31(12):2422-38.
35. Ofir A, Hofmann K, Weindling E, Gildor T, Barker KS, Rogers PD, et al. Role of a *Candida albicans* Nrm1/Whi5 homologue in cell cycle gene expression and DNA replication stress response. *Molecular microbiology*. 2012;84(4):778-94.
36. Cote P, Hogues H, Whiteway M. Transcriptional analysis of the *Candida albicans* cell cycle. *Molecular biology of the cell*. 2009;20(14):3363-73.

37. Hussein B, Huang H, Glory A, Osmani A, Kaminskyj S, Nantel A, et al. G1/S transcription factor orthologues Swi4p and Swi6p are important but not essential for cell proliferation and influence hyphal development in the fungal pathogen *Candida albicans*. *Eukaryotic cell*. 2011;10(3):384-97.
38. Sherlock G, Bahman AM, Mahal A, Shieh JC, Ferreira M, Rosamond J. Molecular cloning and analysis of CDC28 and cyclin homologues from the human fungal pathogen *Candida albicans*. *Molecular & general genetics : MGG*. 1994;245(6):716-23.
39. Senn H, Shapiro RS, Cowen LE. Cdc28 provides a molecular link between Hsp90, morphogenesis, and cell cycle progression in *Candida albicans*. *Molecular biology of the cell*. 2012;23(2):268-83.
40. Whiteway M, Dignard D, Thomas DY. Dominant negative selection of heterologous genes: isolation of *Candida albicans* genes that interfere with *Saccharomyces cerevisiae* mating factor-induced cell cycle arrest. *Proceedings of the National Academy of Sciences of the United States of America*. 1992;89(20):9410-4.
41. Zheng X, Wang Y, Wang Y. Hgc1, a novel hypha-specific G1 cyclin-related protein regulates *Candida albicans* hyphal morphogenesis. *The EMBO journal*. 2004;23(8):1845-56.
42. Loeb JDJ, Sepulveda-Becerra M, Hazan I, Liu H. A G1 Cyclin Is Necessary for Maintenance of Filamentous Growth in *Candida albicans*. *MolCellBiol*. 1999;19(6):4019-27.
43. Bachewich C, Whiteway M. Cyclin Cln3p links G1 progression to hyphal and pseudohyphal development in *Candida albicans*. *Eukaryotic cell*. 2005;4(1):95-102.
44. Chapa y Lazo B, Bates S, Sudbery P. The G1 cyclin Cln3 regulates morphogenesis in *Candida albicans*. *Eukaryotic cell*. 2005;4(1):90-4.
45. Sinha I, Wang YM, Philp R, Li CR, Yap WH, Wang Y. Cyclin-dependent kinases control septin phosphorylation in *Candida albicans* hyphal development. *Developmental cell*. 2007;13(3):421-32.
46. Atir-Lande A, Gildor T, Kornitzer D. Role for the SCF_{CDC4} ubiquitin ligase in *Candida albicans* morphogenesis. *Molecular biology of the cell*. 2005;16(6):2772-85.
47. Li WJ, Wang YM, Zheng XD, Shi QM, Zhang TT, Bai C, et al. The F-box protein Grr1 regulates the stability of Ccn1, Cln3 and Hof1 and cell morphogenesis in *Candida albicans*. *Molecular microbiology*. 2006;62(1):212-26.
48. Shieh JC, White A, Cheng YC, Rosamond J. Identification and functional characterization of *Candida albicans* CDC4. *Journal of Biomedical Science*. 2005;12(6):913-24.
49. Tseng TL, Lai WC, Jian T, Li C, Sun HF, Way TD, et al. Affinity purification of *Candida albicans* CaCdc4-associated proteins reveals the presence of novel proteins involved in morphogenesis. *Biochemical and biophysical research communications*. 2010.
50. Heitman J, Movva NR, Hall MN. Targets for cell cycle arrest by the immunosuppressant rapamycin in yeast. *Science (New York, NY)*. 1991;253(5022):905-9.
51. Vezina C, Kudelski A, Sehgal SN. Rapamycin (AY-22,989), a new antifungal antibiotic. I. Taxonomy of the producing streptomycete and isolation of the active principle. *The Journal of antibiotics*. 1975;28(10):721-6.
52. Cruz MC, Goldstein AL, Blankenship J, Del Poeta M, Perfect JR, McCusker JH, et al. Rapamycin and less immunosuppressive analogs are toxic to *Candida albicans* and *Cryptococcus neoformans* via FKBP12-dependent inhibition of TOR. *Antimicrobial Agents and Chemotherapy*. 2001;45(11):3162-70.
53. Crespo JL, Hall MN. Elucidating TOR signaling and rapamycin action: lessons from *Saccharomyces cerevisiae*. *Microbiology and molecular biology reviews : MMBR*. 2002;66(4):579-91, table of contents.

54. Wullschleger S, Loewith R, Hall MN. TOR signaling in growth and metabolism. *Cell*. 2006;124(3):471-84.
55. Matsuo T, Otsubo Y, Urano J, Tamanoi F, Yamamoto M. Loss of the TOR kinase Tor2 mimics nitrogen starvation and activates the sexual development pathway in fission yeast. *Molecular and cellular biology*. 2007;27(8):3154-64.
56. Hall MN. The TOR signalling pathway and growth control in yeast. *Biochemical Society transactions*. 1996;24(1):234-9.
57. Aspuria PJ, Sato T, Tamanoi F. The TSC/Rheb/TOR signaling pathway in fission yeast and mammalian cells: temperature sensitive and constitutive active mutants of TOR. *Cell cycle (Georgetown, Tex)*. 2004;6(14):1692-5.
58. Cutler NS, Pan X, Heitman J, Cardenas ME. The TOR signal transduction cascade controls cellular differentiation in response to nutrients. *Molecular biology of the cell*. 2001;12(12):4103-13.
59. Rohde JR, Bastidas R, Puria R, Cardenas ME. Nutritional control via Tor signaling in *Saccharomyces cerevisiae*. *Current opinion in microbiology*. 2008;11(2):153-60.
60. Nakashima A, Maruki Y, Imamura Y, Kondo C, Kawamata T, Kawanishi I, et al. The yeast Tor signaling pathway is involved in G2/M transition via polo-kinase. *PLoS ONE*. 2008;3(5):e2223.
61. De Virgilio C, Loewith R. The TOR signalling network from yeast to man. *The international journal of biochemistry & cell biology*. 2006;38(9):1476-81.
62. Loewith R, Jacinto E, Wullschleger S, Lorberg A, Crespo JL, Bonenfant D, et al. Two TOR complexes, only one of which is rapamycin sensitive, have distinct roles in cell growth control. *Molecular cell*. 2002;10(3):457-68.
63. Lee CM, Nantel A, Jiang L, Whiteway M, Shen SH. The serine/threonine protein phosphatase Sit4 modulates yeast-to-hypha morphogenesis and virulence in *Candida albicans*. *Molecular microbiology*. 2004;51(3):691-709.
64. Rohde JR, Campbell S, Zurita-Martinez SA, Cutler NS, Ashe M, Cardenas ME. TOR controls transcriptional and translational programs via Sap-Sit4 protein phosphatase signaling effectors. *Molecular and cellular biology*. 2004;24(19):8332-41.
65. Yan G, Lai Y, Jiang Y. The TOR complex 1 is a direct target of Rho1 GTPase. *Molecular cell*. 2012;45(6):743-53.
66. Beck T, Hall MN. The TOR signalling pathway controls nuclear localization of nutrient-regulated transcription factors. *Nature*. 1999;402(6762):689-92.
67. Cardenas ME, Cutler NS, Lorenz MC, Di Como CJ, Heitman J. The TOR signaling cascade regulates gene expression in response to nutrients. *Genes & development*. 1999;13(24):3271-9.
68. Bertram PG, Choi JH, Carvalho J, Ai W, Zeng C, Chan TF, et al. Tripartite regulation of Gln3p by TOR, Ure2p, and phosphatases. *The Journal of biological chemistry*. 2000;275(46):35727-33.
69. Wei Y, Tsang CK, Zheng XF. Mechanisms of regulation of RNA polymerase III-dependent transcription by TORC1. *The EMBO journal*. 2009;28(15):2220-30.
70. Michels AA. MAF1: a new target of mTORC1. *Biochemical Society transactions*. 2011;39(2):487-91.
71. Jorgensen P, Nishikawa JL, Breikreutz BJ, Tyers M. Systematic identification of pathways that couple cell growth and division in yeast. *Science (New York, NY)*. 2002;297(5580):395-400.
72. Cipollina C, Alberghina L, Porro D, Vai M. SFP1 is involved in cell size modulation in respiro-fermentative growth conditions. *Yeast (Chichester, England)*. 2005;22(5):385-99.
73. Urban J, Souldard A, Huber A, Lippman S, Mukhopadhyay D, Deloche O, et al. Sch9 is a major target of TORC1 in *Saccharomyces cerevisiae*. *Molecular cell*. 2007;26(5):663-74.

74. Huber A, French SL, Tekotte H, Yerlikaya S, Stahl M, Perepelkina MP, et al. Sch9 regulates ribosome biogenesis via Stb3, Dot6 and Tod6 and the histone deacetylase complex RPD3L. *The EMBO journal*. 2011;30(15):3052-64.
75. Zhang A, Shen Y, Gao W, Dong J. Role of Sch9 in regulating Ras-cAMP signal pathway in *Saccharomyces cerevisiae*. *FEBS letters*. 2011;585(19):3026-32.
76. Zhang A, Gao W. Mechanisms of protein kinase Sch9 regulating Bcy1 in *Saccharomyces cerevisiae*. *FEMS microbiology letters*. 2012;331(1):10-6.
77. Blumberg H, Silver P. A split zinc-finger protein is required for normal yeast growth. *Gene*. 1991;107(1):101-10.
78. Xu Z, Norris D. The SFP1 gene product of *Saccharomyces cerevisiae* regulates G2/M transitions during the mitotic cell cycle and DNA-damage response. *Genetics*. 1998;150(4):1419-28.
79. Fingerman I, Nagaraj V, Norris D, Vershon AK. Sfp1 plays a key role in yeast ribosome biogenesis. *Eukaryotic cell*. 2003;2(5):1061-8.
80. Singh J, Tyers M. A Rab escort protein integrates the secretion system with TOR signaling and ribosome biogenesis. *Genes & development*. 2009;23(16):1944-58.
81. Lempiainen H, Uotila A, Urban J, Dohnal I, Ammerer G, Loewith R, et al. Sfp1 interaction with TORC1 and Mrs6 reveals feedback regulation on TOR signaling. *Molecular cell*. 2009;33(6):704-16.
82. Liao WL, Ramon AM, Fonzi WA. GLN3 encodes a global regulator of nitrogen metabolism and virulence of *C. albicans*. *Fungal genetics and biology : FG & B*. 2008;45(4):514-26.
83. Zacchi LF, Gomez-Raja J, Davis DA. Mds3 regulates morphogenesis in *Candida albicans* through the TOR pathway. *Molecular and cellular biology*. 2010;30(14):3695-710.
84. Dabas N, Morschhauser J. Control of ammonium permease expression and filamentous growth by the GATA transcription factors GLN3 and GAT1 in *Candida albicans*. *Eukaryotic cell*. 2007;6(5):875-88.
85. Liu W, Zhao J, Li X, Li Y, Jiang L. The protein kinase CaSch9p is required for the cell growth, filamentation and virulence in the human fungal pathogen *Candida albicans*. *FEMS yeast research*. 2010.
86. Bastidas RJ, Heitman J, Cardenas ME. The protein kinase Tor1 regulates adhesin gene expression in *Candida albicans*. *PLoS pathogens*. 2009;5(2):e1000294.
87. Lu Y, Su C, Liu H. A GATA transcription factor recruits Hda1 in response to reduced Tor1 signaling to establish a hyphal chromatin state in *Candida albicans*. *PLoS Pathog*. 2012;8(4):e1002663. PubMed PMID: 22536157. Pubmed Central PMCID: PMC3334898. eng.
88. Care RS, Trevethick J, Binley KM, Sudbery PE. The MET3 promoter: a new tool for *Candida albicans* molecular genetics. *Molecular microbiology*. 1999;34(4):792-8.
89. Homann OR, Dea J, Noble SM, Johnson AD. A phenotypic profile of the *Candida albicans* regulatory network. *PLoS genetics*. 2009;5(12):e1000783.
90. Csank C, Haynes K. *Candida glabrata* displays pseudohyphal growth. *FEMS microbiology letters*. 2000;189(1):115-20.
91. Yang L, Ukil L, Osmani A, Nahm F, Davies J, De Souza CP, et al. Rapid production of gene replacement constructs and generation of a green fluorescent protein-tagged centromeric marker in *Aspergillus nidulans*. *Eukaryotic cell*. 2004;3(5):1359-62.
92. Noble SM, Johnson AD. Strains and strategies for large-scale gene deletion studies of the diploid human fungal pathogen *Candida albicans*. *Eukaryotic cell*. 2005;4(2):298-309.
93. Rose MD, Winston F, Hieter P. *Laboratory Course Manual*. Cold Spring Harbor, NY.: Cold Spring Harbor Laboratory Press; 1990.

94. Ling M, Merante F, Robinson BH. A rapid and reliable DNA preparation method for screening a large number of yeast clones by polymerase chain reaction. *Nucleic acids research*. 1995;23(23):4924-5.
95. Köhrer K, Domdey H. Preparation of high molecular weight RNA. *Methods Enzymol*. 1991;194:398-405. PubMed PMID: 1706459. eng.
96. Nantel A, Dignard D, Bachewich C, Harcus D, Marcil A, Bouin AP, et al. Transcription profiling of *Candida albicans* cells undergoing the yeast-to-hyphal transition. *Molecular biology of the cell*. 2002;13(10):3452-65.
97. Bachewich C, Nantel A, Whiteway M. Cell cycle arrest during S or M phase generates polarized growth via distinct signals in *Candida albicans*. *Molecular microbiology*. 2005;57(4):942-59.
98. Balan I, Alarco AM, Raymond M. The *Candida albicans* CDR3 gene codes for an opaque-phase ABC transporter. *Journal of Bacteriology*. 1997;179(23):7210-8.
99. Jorgensen P, Rupes I, Sharom JR, Schnepfer L, Broach JR, Tyers M. A dynamic transcriptional network communicates growth potential to ribosome synthesis and critical cell size. *Genes & development*. 2004;18(20):2491-505.
100. Marion RM, Regev A, Segal E, Barash Y, Koller D, Friedman N, et al. Sfp1 is a stress- and nutrient-sensitive regulator of ribosomal protein gene expression. *Proceedings of the National Academy of Sciences of the United States of America*. 2004;101(40):14315-22.
101. Biswas S, Van Dijck P, Datta A. Environmental sensing and signal transduction pathways regulating morphopathogenic determinants of *Candida albicans*. *Microbiology and molecular biology reviews : MMBR*. 2007;71(2):348-76.
102. Tsao CC, Chen YT, Lan CY. A small G protein Rhb1 and a GTPase-activating protein Tsc2 involved in nitrogen starvation-induced morphogenesis and cell wall integrity of *Candida albicans*. *Fungal genetics and biology : FG & B*. 2009;46(2):126-36.
103. Lu Y, Su C, Wang A, Liu H. Hyphal development in *Candida albicans* requires two temporally linked changes in promoter chromatin for initiation and maintenance. *PLoS biology*. 2011;9(7):e1001105.
104. Su C, Lu Y, Liu H. Reduced TOR signaling sustains hyphal development in *Candida albicans* by lowering Hog1 basal activity. *Molecular biology of the cell*. 2013;24(3):385-97.
105. Cruz MC, Cavallo LM, Gorlach JM, Cox G, Perfect JR, Cardenas ME, et al. Rapamycin antifungal action is mediated via conserved complexes with FKBP12 and TOR kinase homologs in *Cryptococcus neoformans*. *Molecular and cellular biology*. 1999;19(6):4101-12.
106. Chen YT, Lin CY, Tsai PW, Yang CY, Hsieh WP, Lan CY. Rhb1 regulates the expression of secreted aspartic protease 2 through the TOR signaling pathway in *Candida albicans*. *Eukaryotic cell*. 2012;11(2):168-82.
107. Feng J, Zhao Y, Duan Y, Jiang L. Genetic interactions between protein phosphatases CaPtc2p and CaPph3p in response to genotoxins and rapamycin in *Candida albicans*. *FEMS yeast research*. 2012.
108. Wong GK, Griffith S, Kojima I, Demain AL. Antifungal activities of rapamycin and its derivatives, prolylrapamycin, 32-desmethylrapamycin, and 32-desmethoxyrapamycin. *The Journal of antibiotics*. 1998;51(5):487-91.
109. Spellman PT, Sherlock G, Zhang MQ, Iyer VR, Anders K, Eisen MB, et al. Comprehensive identification of cell cycle-regulated genes of the yeast *Saccharomyces cerevisiae* by microarray hybridization. *Molecular biology of the cell*. 1998;9(12):3273-97.
110. Lopez AD, Tar K, Krugel U, Dange T, Ros IG, Schmidt M. Proteasomal degradation of Sfp1 contributes to the repression of ribosome biogenesis during starvation and is mediated by the proteasome activator Blm10. *Molecular biology of the cell*. 2011;22(5):528-40.

111. Sudbery PE. Growth of *Candida albicans* hyphae. *Nature reviews Microbiology*. 2011;9(10):737-48.
112. Gertz J, Riles L, Turnbaugh P, Ho SW, Cohen BA. Discovery, validation, and genetic dissection of transcription factor binding sites by comparative and functional genomics. *Genome research*. 2005;15(8):1145-52.
113. Hemenway CS, Heitman J. Immunosuppressant target protein FKBP12 is required for P-glycoprotein function in yeast. *The Journal of biological chemistry*. 1996;271(31):18527-34.
114. Gunther J, Nguyen M, Hartl A, Kunkel W, Zipfel PF, Eck R. Generation and functional in vivo characterization of a lipid kinase defective phosphatidylinositol 3-kinase Vps34p of *Candida albicans*. *Microbiology (Reading, England)*. 2005;151(Pt 1):81-9.
115. Uwamahoro N, Qu Y, Jelacic B, Lo TL, Beaurepaire C, Bantun F, et al. The functions of Mediator in *Candida albicans* support a role in shaping species-specific gene expression. *PLoS genetics*. 2012;8(4):e1002613.
116. Ariyachet C, Solis NV, Liu Y, Prasadarao NV, Filler SG, McBride AE. SR-like RNA-binding protein Slr1 affects *Candida albicans* filamentation and virulence. *Infection and immunity*. 2013.
117. Bates S, MacCallum DM, Bertram G, Munro CA, Hughes HB, Buurman ET, et al. *Candida albicans* Pmr1p, a secretory pathway P-type Ca²⁺/Mn²⁺-ATPase, is required for glycosylation and virulence. *The Journal of biological chemistry*. 2005;280(24):23408-15.
118. Veses V, Casanova M, Murgui A, Dominguez A, Gow NA, Martinez JP. ABG1, a novel and essential *Candida albicans* gene encoding a vacuolar protein involved in cytokinesis and hyphal branching. *Eukaryotic cell*. 2005;4(6):1088-101.
119. Chen X, Chen JY. Cloning and Functional Analysis of ALS Family Genes from *Candida albicans*. *Sheng wu hua xue yu sheng wu wu li xue bao Acta biochimica et biophysica Sinica*. 2000;32(6):586-94.
120. Zheng XD, Lee RT, Wang YM, Lin QS, Wang Y. Phosphorylation of Rga2, a Cdc42 GAP, by CDK/Hgc1 is crucial for *Candida albicans* hyphal growth. *The EMBO journal*. 2007;26(16):3760-9.
121. Carlisle PL, Kadosh D. *Candida albicans* Ume6, a filament-specific transcriptional regulator, directs hyphal growth via a pathway involving Hgc1 cyclin-related protein. *Eukaryotic cell*. 2010;9(9):1320-8.
122. Wu W, Pujol C, Lockhart SR, Soll DR. Chromosome loss followed by duplication is the major mechanism of spontaneous mating-type locus homozygosity in *Candida albicans*. *Genetics*. 2005 Mar;169(3):1311-27. PubMed PMID: 15654090. Pubmed Central PMCID: PMC1449533.
123. Pendrak ML, Yan SS, Roberts DD. Hemoglobin regulates expression of an activator of mating-type locus alpha genes in *Candida albicans*. *Eukaryotic cell*. 2004;3(3):764-75.
124. Zheng XF, Schreiber SL. Target of rapamycin proteins and their kinase activities are required for meiosis. *Proceedings of the National Academy of Sciences of the United States of America*. 1997;94(7):3070-5.
125. Weisman R, Finkelstein S, Choder M. Rapamycin blocks sexual development in fission yeast through inhibition of the cellular function of an FKBP12 homolog. *The Journal of biological chemistry*. 2001;276(27):24736-42.
126. Colomina N, Liu Y, Aldea M, Gari E. TOR regulates the subcellular localization of Ime1, a transcriptional activator of meiotic development in budding yeast. *Molecular and cellular biology*. 2003;23(20):7415-24.
127. Alvarez B, Moreno S. Fission yeast Tor2 promotes cell growth and represses cell differentiation. *Journal of cell science*. 2006;119(Pt 21):4475-85.
128. Valbuena N, Moreno S. TOR and PKA pathways synergize at the level of the Ste11 transcription factor to prevent mating and meiosis in fission yeast. *PloS one*. 2010;5(7):e11514.

129. Bruckner S, Kern S, Birke R, Saugar I, Ulrich HD, Mosch HU. The TEA transcription factor Tec1 links TOR and MAPK pathways to coordinate yeast development. *Genetics*. 2011;189(2):479-94.
130. Xu G, Jansen G, Thomas DY, Hollenberg CP, Ramezani Rad M. Ste50p sustains mating pheromone-induced signal transduction in the yeast *Saccharomyces cerevisiae*. *Molecular microbiology*. 1996;20(4):773-83.
131. Wu C, Leberer E, Thomas DY, Whiteway M. Functional characterization of the interaction of Ste50p with Ste11p MAPKKK in *Saccharomyces cerevisiae*. *Molecular biology of the cell*. 1999;10(7):2425-40.
132. Chen J, Chen J, Lane S, Liu H. A conserved mitogen-activated protein kinase pathway is required for mating in *Candida albicans*. *Molecular microbiology*. 2002;46(5):1335-44.
133. Hoose SA, Rawlings JA, Kelly MM, Leitch MC, Ababneh QO, Robles JP, et al. A systematic analysis of cell cycle regulators in yeast reveals that most factors act independently of cell size to control initiation of division. *PLoS genetics*. 2012;8(3):e1002590.
134. Stichernoth C, Fraund A, Setiadi E, Giasson L, Vecchiarelli A, Ernst JF. Sch9 kinase integrates hypoxia and CO₂ sensing to suppress hyphal morphogenesis in *Candida albicans*. *Eukaryotic cell*. 2011;10(4):502-11.
135. Wade CH, Umbarger MA, McAlear MA. The budding yeast rRNA and ribosome biosynthesis (RRB) regulon contains over 200 genes. *Yeast (Chichester, England)*. 2006;23(4):293-306.
136. Bernstein KA, Bleichert F, Bean JM, Cross FR, Baserga SJ. Ribosome biogenesis is sensed at the Start cell cycle checkpoint. *Molecular biology of the cell*. 2007;18(3):953-64.
137. Busti S, Gotti L, Balestrieri C, Querin L, Drovandi G, Felici G, et al. Overexpression of Far1, a cyclin-dependent kinase inhibitor, induces a large transcriptional reprogramming in which RNA synthesis senses Far1 in a Sfp1-mediated way. *Biotechnology Advances*. 2012;30(1):185-201.
138. Li X, Huang X, Zhao J, Zhao J, Wei Y, Jiang L. The MAP kinase-activated protein kinase Rck2p plays a role in rapamycin sensitivity in *Saccharomyces cerevisiae* and *Candida albicans*. *FEMS yeast research*. 2008;8(5):715-24.
139. Monge RA, Roman E, Nombela C, Pla J. The MAP kinase signal transduction network in *Candida albicans*. *Microbiology (Reading, England)*. 2006;152(Pt 4):905-12.
140. Petkova MI, Pujol-Carrion N, de la Torre-Ruiz MA. Signal flow between CWI/TOR and CWI/RAS in budding yeast under conditions of oxidative stress and glucose starvation. *Communicative & integrative biology*. 2010;3(6):555-7.
141. Lengeler KB, Davidson RC, D'Souza C, Harashima T, Shen WC, Wang P, et al. Signal transduction cascades regulating fungal development and virulence. *Microbiology and molecular biology reviews : MMBR*. 2000;64(4):746-85.
142. Valenzuela L, Aranda C, Gonzalez A. TOR modulates GCN4-dependent expression of genes turned on by nitrogen limitation. *Journal of Bacteriology*. 2001;183(7):2331-4.
143. Orlova M, Kanter E, Krakovich D, Kuchin S. Nitrogen availability and TOR regulate the Snf1 protein kinase in *Saccharomyces cerevisiae*. *Eukaryotic cell*. 2006;5(11):1831-7.
144. Rai R, Tate JJ, Nelson DR, Cooper TG. gln3 mutations dissociate responses to nitrogen limitation (nitrogen catabolite repression) and rapamycin inhibition of TorC1. *The Journal of biological chemistry*. 2013;288(4):2789-804.
145. Hsu PC, Chao CC, Yang CY, Ye YL, Liu FC, Chuang YJ, et al. Diverse Hap43-independent functions of the *Candida albicans* CCAAT-binding Complex. *Eukaryotic cell*. 2013.
146. Wang Y, Zou H, Fang HM, Zhu Y. Linking cellular actin status with cAMP signaling in *Candida albicans*. *Virulence*. 2010;1(3):202-5.

147. Miwa T, Takagi Y, Shinozaki M, Yun CW, Schell WA, Perfect JR, et al. Gpr1, a putative G-protein-coupled receptor, regulates morphogenesis and hypha formation in the pathogenic fungus *Candida albicans*. *Eukaryotic cell*. 2004;3(4):919-31.
148. Midkiff J, Borochoff-Porte N, White D, Johnson DI. Small molecule inhibitors of the *Candida albicans* budded-to-hyphal transition act through multiple signaling pathways. *PLoS one*. 2011;6(9):e25395.
149. Leberer E, Harcus D, Broadbent ID, Clark KL, Dignard D, Ziegelbauer K, et al. Signal transduction through homologs of the Ste20p and Ste7p protein kinases can trigger hyphal formation in the pathogenic fungus *Candida albicans*. *Proceedings of the National Academy of Sciences of the United States of America*. 1996;93(23):13217-22.
150. Pulver R, Heisel T, Gonia S, Robins R, Norton J, Haynes P, et al. Rsr1 Focuses Cdc42 Activity at Hyphal Tips and Promotes Maintenance of Hyphal Development in *Candida albicans*. *Eukaryotic cell*. 2013;12(4):482-95.
151. Bennett RJ, Johnson AD. Mating in *Candida albicans* and the search for a sexual cycle. *Annual Review of Microbiology*. 2005;59:233-55.
152. Takahara T, Maeda T. TORC1 of fission yeast is rapamycin-sensitive. *Genes to cells : devoted to molecular & cellular mechanisms*. 2012;17(8):698-708.
153. Gola S, Martin R, Walther A, Dunkler A, Wendland J. New modules for PCR-based gene targeting in *Candida albicans*: rapid and efficient gene targeting using 100 bp of flanking homology region. *Yeast (Chichester, England)*. 2003;20(16):1339-47.

8.0 APPENDIX

Table S1: Length by width ratios of the *sfp1Δ/sfp1Δ* strain compared to the control strain in media containing different carbon sources¹.

Strain	Carbon Source	Incubation Time (h)	Mean LxW ² (μm ²) ± S.E. M.	W value ³	P value ⁴
HHCa1 (n= 113)	Glucose	10	15.49 ±0.23	15501.5	p < 0.001
HHCa28 (n= 114)			13.57 ±0.24		
HHCa1 (n= 101)		24	16.81 ±0.34	13004.5	p < 0.001
HHCa28 (n= 105)			13.97 ±0.24		
HHCa1 (n= 118)	Galactose	10	13.41 ±0.27	15021	p = 0.0256
HHCa28 (n= 116)			12.31 ±0.19		
HHCa1 (n= 109)		24	15.30 ±0.31	15500	p < 0.001
HHCa28 (n= 112)			11.94 ±0.27		
HHCa1 (n= 114)	Raffinose	10	11.30 ±0.31	12988	p = 0.9879
HHCa28 (n= 113)			11.24 ±0.21		
HHCa1 (n= 111)		24	9.47 ±0.33	12013	p = 0.5176

HHCa28 (n= 110)		9.58 ±0.25		
HHCa1 (n= 114)		11.83 ±0.28		
	10		12426.5	p = 0.9011
HHCa28 (n= 102)		11.85 ±0.34		
	Glycerol			
HHCa1 (n= 105)		11.58 ±0.28		
	24		13311	p < 0.001
HHCa28 (n= 104)		9.56 ±0.26		

¹ Strains HHCa1 (*SFP1/SFP1*, *URA3*, *HIS1*) and HHCa28 (*sfp1::URA3/sfp1::HIS1*) were incubated in MM medium containing either 2% glucose, galactose, raffinose or glycerol, incubated for 10 or 24 h at 30°C, fixed in 70% EtOH, and length and width measurements were recorded from images. Results represent two separate trials.

² A minimum of 100 cells were measured, and values represent mean length by width ratios.

³ Mann-Whitney test W value for statistical analysis of non-normally distributed samples

⁴ Mann-Whitney test P value for difference between control and knock-out samples.

Table S2: List of modulated genes of the *sfp1Δ/sfp1Δ* microarray expression experiment¹

Systematic Name²	Standard Name³	CGD Description⁴	Normalized Expression⁵	t-test p value⁶
orf19.255	<i>ZCF1</i>	Predicted zinc-cluster protein; possibly transcriptionally regulated upon hyphal formation; late-stage biofilm-induced; intron in 5'-UTR; mutants display decreased colonization of mouse kidneys	-0.01	no replicates
orf19.3145.4		ORF Predicted by Annotation Working Group; removed from Assembly 20	-0.0125	0.000147
orf19.6116	<i>GLK4</i>	Putative glucokinase; decreased expression in hyphae compared to yeast-form cells	-0.0153	7.89E-05
orf19.3182	<i>GIS2</i>	Putative transcription factor; expression is increased in high iron and reduced upon yeast-hyphal switch; null mutant exhibits sensitivity to sorbitol, 5-fluorocytosine, and cold temperatures	-0.0163	2.81E-07
orf19.3521	<i>ARH2</i>	Putative adrenodoxin-NADPH oxidoreductase; role in heme biosynthesis	-0.017	0.001528
orf19.1860	<i>LSC2</i>	Putative succinate-CoA ligase beta subunit; transcription regulated by Mig1p and Tup1p; transcriptionally regulated by iron; expression greater in high iron; filament; protein present in exponential and stationary growth phase yeast cells	-0.0176	0.000293
orf19.7278		Similar to a region of the Tca2 (pCal) retrotransposon, which is present in strain hOG1042 as 50 to 100 copies of a linear dsDNA	-0.0205	0.001656
orf19.2374		Predicted ORF from Assembly 19; removed from Assembly 20	-0.0216	0.000341
orf19.1152		Late-stage biofilm-induced gene; regulated by Gcn2p and Gcn4p; induced in core stress response	-0.0217	4.84E-06
orf19.6817	<i>FCRI</i>	Zinc cluster transcription factor; negative regulator of fluconazole, ketoconazole, brefeldin A resistance; transposon mutation increases filamentous growth; partially suppresses <i>S. cerevisiae</i> pdr1 pdr3 mutant fluconazole sensitivity	-0.0225	0.001812

orf19.45		Predicted ORF from Assembly 19; merged with orf19.5742 in Assembly 20	-0.0327	0.159485
orf19.675		Putative cell wall protein; induced in core stress response and core caspofungin response; iron-regulated; amphotericin B, ketoconazole, and hypoxia induced; regulated by Cyr1p, Ssn6p; induced in oropharyngeal candidiasis	-0.0339	5.90E-07
orf19.5861	<i>KRE9</i>	Protein of beta-1,6-glucan biosynthesis; required for serum-induced hyphal growth; required for efficient utilization of galactose and for growth on glucose; similar to <i>S. cerevisiae</i> Kre9p and Knh1p; O-glycosylated by Pmt1p	-0.0353	0.00013
orf19.2551	<i>MET6</i>	Essential 5-methyltetrahydropteroyltriglutamate-homocysteine methyltransferase (cobalamin-independent methionine synthase); antigenic during murine or human systemic infection; heat shock, estrogen, possibly biofilm, and GCN-induced	-0.0376	0.000219
orf19.1716	<i>URA3</i>	Orotidine-5'-phosphate decarboxylase, enzyme of pyrimidine biosynthesis; gene used as a molecular genetic marker, but decreased expression when integrated at ectopic chromosomal locations can cause defects in hyphal growth and virulence	-0.0391	0.000304
orf19.3775	<i>SSK2</i>	MAP kinase kinase kinase (MAPKKK) that regulates Hog1p activation and signaling; transcription is downregulated in response to treatment with ciclopirox olamine	-0.0397	0.00125
orf19.5383	<i>PMA1</i>	Plasma membrane H(+)-ATPase; highly expressed, comprising 20-40% of total plasma membrane protein; abundance increases at stationary phase transition; fluconazole induced; caspofungin repressed; upregulated in RHE model	-0.0416	0.001297
orf19.2866		Has domain(s) with predicted DNA binding activity	-0.0476	0.002343
orf19.6078	<i>POL93</i>	Predicted ORF in retrotransposon Tca8 with similarity to the Pol region of retrotransposons encoding reverse transcriptase, protease and integrase; downregulated in response to ciclopirox olamine; induced upon biofilm formation	-0.0479	0.002905
orf19.7265		Hap43p-repressed gene	-0.0485	0.001241
orf19.1164	<i>GARI</i>	Putative H/ACA snoRNP pseudouridylylase complex protein; mutation confers hypersensitivity to tubercidin (7-deazaadenosine); macrophage/pseudohyphal-induced	-0.0517	6.20E-06
orf19.3712		Predicted ORF in Assemblies 19, 20 and 21; transcriptionally activated by Mnl1p under weak acid stress; late-stage biofilm-induced gene	-0.0538	0.000504

orf19.2765	<i>PGA62</i>	Adhesin-like cell wall protein; putative GPI-anchor; fluconazole-induced; regulated by iron; expression greater in high iron; induced during cell wall regeneration; Cyr1p or Ras1p downregulated; positively regulated by Tbf1p	-0.0541	0.003068
orf19.1105.2	<i>PGA56</i>	Regulator of sorbose utilization; putative GPI-anchor; predicted helix-loop helix domain; hyphal induced; induced during cell wall regeneration; colony morphology-related gene regulation by Ssn6p; transcription activated by Tbf1p, Hap43p	-0.0544	0.00535
orf19.7350	<i>RCT1</i>	Fluconazole-induced protein; elevated mRNA levels in a <i>cyr1</i> or <i>ras1</i> null mutant and decreased mRNA abundance in <i>efg1</i> null mutant; regulated by Nrg1p, Tup1p, Tbf1p, Ssn6p; induced in oralpharyngeal candidiasis	-0.0574	0.000912
orf19.3038	<i>TPS2</i>	Trehalose-6-phosphate (Tre6P) phosphatase; mutant heat sensitive, has Tre6P accumulation, decreased mouse virulence; possible drug target; two conserved phosphohydrolase motifs; no mammalian homolog; Hap43p-repressed gene; biofilm-induced	-0.0577	3.99E-06
orf19.5749	<i>SBA1</i>	Similar to co-chaperones; transcriptionally regulated by iron; expression greater in high iron; farnesol-, heavy metal (cadmium) stress-induced; protein level decreases in stationary phase cultures; Hap43p-repressed gene	-0.0578	5.08E-06
orf19.5591	<i>ADO1</i>	Adenosine kinase; heterozygous null mutant exhibits resistance to cordycepin in the <i>C. albicans</i> fitness test; ketoconazole-induced; protein level decreased in stationary phase cultures; sumoylation target	-0.0624	0.000634
orf19.7219	<i>FTRI</i>	High-affinity iron permease; required for mouse virulence, low-iron growth; iron, amphotericin B, caspofungin, ciclopirox, Hog1p, Sef1p, Sfu1p, and Hap43p regulated; complements <i>S. cerevisiae</i> <i>frl1</i> iron transport; Hap43p-repressed	-0.0673	0.001295
orf19.6187		Predicted ORF in Assemblies 19, 20 and 21; overlaps orf19.6185 and orf19.6188	-0.0681	0.003652
orf19.1889		Putative phosphoglycerate mutase family protein; stationary phase enriched protein; early-stage biofilm-induced	-0.0689	0.000253
orf19.3334	<i>RPS21</i>	Predicted ribosomal protein; genes encoding cytoplasmic ribosomal subunits, translation factors, and tRNA synthetases are downregulated upon phagocytosis by murine macrophage; transcription is positively regulated by Tbf1p	-0.0695	0.001073
orf19.3911	<i>SAHI</i>	Putative S-adenosyl-L-homocysteine hydrolase; predicted enzyme of sulfur amino acid metabolism; antigenic in human; biofilm-, alkaline-, fluconazole-induced expression; Gcn4p-regulated; amino acid starvation (3-AT) repressed	-0.0722	8.57E-08
orf19.710		Putative beta subunit of succinate-CoA ligase; transcription regulated by Mig1p and Tup1p; transcriptionally regulated by iron; expression greater in high iron; merged with orf19.1860 in Assembly 20	-0.0731	0.00547

orf19.1407		Predicted ORF from Assembly 19; merged with orf19.6117 in Assembly 20	-0.0774	0.000814
orf19.5445	<i>GLO3</i>	Ortholog(s) have ARF GTPase activator activity and role in COPI coating of Golgi vesicle, ER to Golgi vesicle-mediated transport, retrograde vesicle-mediated transport, Golgi to ER	-0.0816	0.000233
orf19.5451		Ortholog of <i>Candida guilliermondii</i> ATCC 6260 : PGUG_05321, <i>Candida lusitanae</i> ATCC 42720 : CLUG_00887 and <i>Candida albicans</i> WO-1 : CAWG_02354	-0.0837	0.000769
orf19.5459		Putative mRNA polyadenylation regulating protein; Hap43p-repressed gene, transcription is upregulated in an RHE model of oral candidiasis and in clinical isolates from HIV+ patients with oral candidiasis	-0.0837	0.002607
orf19.47		Predicted ORF from Assembly 19; removed from Assembly 20	-0.0962	4.36E-07
orf19.84	<i>CAN3</i>	Hap43p-repressed gene; expression is regulated upon white-opaque switching	-0.098	1.36E-05
orf19.338		Putative protein of unknown function; stationary phase enriched protein; Hog1p-downregulated; shows colony morphology-related gene regulation by Ssn6p	-0.0992	3.15E-07
orf19.6190	<i>SRB1</i>	Essential GDP-mannose pyrophosphorylase; synthesizes GDP-mannose for protein glycosylation; functional homolog of <i>S. cerevisiae</i> Psa1p; on yeast-form cell surface, not hyphal cells; alkaline upregulated; induced on adherence to polystyrene	-0.0996	1.97E-05
orf19.4055		Protein similar to <i>S. cerevisiae</i> Ybr075wp; transposon mutation affects filamentous growth; clade-associated gene expression	-0.1021	7.35E-07
orf19.5636	<i>RBT5</i>	GPI-anchored cell wall protein involved in hemoglobin utilization; regulated by Rfg1p, Rim101p, Tbf1p, iron; repressed by Sfu1p, Hog1p, Tup1p; induced by serum, alkaline pH, ketoconazole, ciclopirox olamine, geldamycin, Hap43p, biofilm	-0.108	0.004829
orf19.968	<i>PGA14</i>	Putative GPI-anchored protein; induced during cell wall regeneration; regulated by Ssn6p	-0.1101	0.002642
orf19.1162		Predicted ORF in Assemblies 19, 20 and 21; increased transcription is observed upon benomyl treatment	-0.1118	0.005595

orf19.2685	<i>PGA54</i>	Putative GPI-anchored protein; hyphal induced; Hog1p-downregulated; induced in a <i>cyr1</i> or <i>efg1</i> homozygous null mutant; shows colony morphology-related gene regulation by Ssn6p; upregulated in an RHE model; mRNA binds to She3p	-0.1143	0.000923
orf19.316	<i>SEC13</i>	Putative protein transport factor; antigenic during murine systemic infection; macrophage-downregulated protein abundance; protein level decreases in stationary phase cultures	-0.1162	4.85E-06
orf19.5809		Putative arylformamidase, enzyme of the NAD biosynthesis pathway; Gcn4p-regulated	-0.1196	0.000774
orf19.3713		Late-stage biofilm-induced gene; transcriptionally activated by Mnl1p under weak acid stress; transcription detected in high-resolution tiling array experiments	-0.1253	0.00048
orf19.7398.1	<i>TSA1B</i>	Putative peroxidase; orf19.7398.1 is contig-truncated fragment of gene identical to TSA1; Tsa1p and Tsa1Bp role under oxidative/reductive stress, hyphal cell wall formation; in hyphal nucleus, cell wall; yeast-form nucleus, cytoplasm	-0.1256	0.00087
orf19.5989		Ortholog(s) have mRNA binding activity, role in mRNA cleavage, mRNA polyadenylation and cytoplasmic stress granule, mRNA cleavage factor complex localization	-0.1261	0.003692
orf19.5678		Has domain(s) with predicted role in peptidyl-diphthamide biosynthetic process from peptidyl-histidine and cytoplasm localization	-0.1267	no replicates
orf19.4540	<i>UBC8</i>	Protein similar to <i>S. cerevisiae</i> Ubc8p; transcription is induced in response to alpha pheromone in SpiderM medium	-0.1275	0.002011
orf19.1180		Ortholog(s) have 2-aminoadipate transaminase activity and cytoplasm, nucleus localization	-0.1284	0.000135
orf19.7405		Predicted ORF in Assemblies 19, 20 and 21; transcriptionally activated by Mnl1p under weak acid stress	-0.1287	0.000884
orf19.7635	<i>DRS1</i>	Putative nucleolar DEAD-box protein; Hap43p-induced gene; mutation confers hypersensitivity to 5-fluorouracil (5-FU), tubercidin (7-deazaadenosine); transcription is positively regulated by Tbf1p; downregulated during core stress response	-0.1338	0.002283
orf19.4845		Putative integral membrane protein; fluconazole-induced	-0.1348	2.09E-06

orf19.4702		Biofilm-induced gene; expression regulated during planktonic growth; similarity to mutator-like element (MULE) transposase	-0.1384	0.001432
orf19.2371		Putative Gag protein of retrotransposon Tca2; separated by a stop codon from Pol protein orf19.2372; both likely translated as single polyprotein that includes nucleocapsid-like protein (Gag), reverse transcriptase, protease, and integrase	-0.1385	8.45E-05
orf19.4263		Ortholog of <i>Candida albicans</i> WO-1 : CAWG_04633	-0.139	0.000306
orf19.7446	<i>OPI3</i>	Phosphatidylethanolamine N-methyltransferase of phosphatidylcholine biosynthesis; downregulation correlates with clinical development of fluconazole resistance; amphotericin B repressed; caspofungin repressed; Hap43p-induced gene	-0.1394	2.67E-05
orf19.535	<i>RBR1</i>	Glycosylphosphatidylinositol (GPI)-anchored cell wall protein required for filamentous growth at acidic pH; expression is repressed by Rim101p and activated by Nrg1p; Hap43p-induced gene	-0.1402	0.000609
orf19.2163		Ortholog(s) have cytosol localization	-0.1405	0.000407
orf19.1154	<i>EGD1</i>	Putative GAL4 DNA-binding enhancer protein; soluble protein in hyphae; biofilm induced; macrophage/pseudohyphal-induced; the same level of protein present in exponential and stationary growth phase yeast cultures	-0.1436	9.92E-05
orf19.1857		Protein not essential for viability	-0.1471	0.00324
orf19.7308	<i>TUB1</i>	Alpha-tubulin; gene has intron; complements cold-sensitivity of <i>S. cerevisiae</i> tub1 mutant; <i>C. albicans</i> has single alpha-tubulin gene, whereas <i>S. cerevisiae</i> has two (TUB1, TUB3); farnesol-upregulated in biofilm; sumoylation target	-0.1481	0.000217
orf19.4040	<i>ILV3</i>	Putative dihydroxyacid dehydratase; upregulated in biofilm; repressed by nitric oxide; macrophage-induced protein; farnesol-downregulated; protein present in exponential and stationary growth phase; Sef1p-, Sfulp-, and Hap43p-regulated	-0.1494	2.65E-05
orf19.5710		Putative protein of unknown function; mRNA binds to She3p	-0.1501	6.09E-06
orf19.3822	<i>SCS7</i>	Putative ceramide hydroxylase; transcription is regulated by Nrg1p; transcriptionally regulated by iron; expression greater in high iron; fluconazole-induced; Hap43p-repressed (-0.1527	0.005269

orf19.5372		Predicted ORF from Assembly 19; orf19.5372 and orf19.5373 are similar to the Tca2 (pCal) retrotransposon, which is present in strain hOG1042 as 50 to 100 copies of a linear dsDNA; removed from Assembly 20; transcription is Tbf1p-activated	-0.1561	0.000737
orf19.1591	<i>ERG10</i>	Acetyl-CoA acetyltransferase; role in ergosterol biosynthesis; soluble in hyphae; changes in protein abundance associated with azole resistance; fluconazole or ketoconazole induced; macrophage-downregulated protein; GlcNAc-induced protein	-0.1593	4.76E-08
orf19.2451	<i>PGA45</i>	Cell wall protein; putative GPI-anchor; downregulated in core caspofungin response; Hog1p-induced; regulated by Ssn6p; Mob2p-dependent hyphal regulation; biofilm-induced	-0.1615	0.006851
orf19.7188	<i>RPP1B</i>	Conserved acidic ribosomal protein, likely to be involved in regulation of translation elongation; interacts with Rpp2Ap; one of four similar <i>C. albicans</i> ribosomal proteins (Rpp1Ap, Rpp1Bp, Rpp2Ap, Rpp2Bp); transcription activated by Tbf1p	-0.1622	4.95E-07
orf19.3400	<i>COQ3</i>	Protein with a predicted role in coenzyme Q biosynthesis; transcriptionally induced by interaction with macrophages; possibly an essential gene, disruptants not obtained by UAU1 method	-0.1632	7.47E-05
orf19.1631	<i>ERG6</i>	Delta(24)-sterol C-methyltransferase, converts zymosterol to fecosterol, ergosterol biosynthesis; mutation confers nystatin resistance; Hap43, GlcNAc-, fluconazole-induced; upregulated in azole-resistant strain	-0.1634	0.002597
orf19.1536		Putative vacuolar transporter; Hap43p-induced gene, required for normal filamentous growth; mRNA binds to She3p and is localized to hyphal tips	-0.1657	0.004456
orf19.993		Ortholog of <i>C. parapsilosis</i> CDC317 : CPAR2_502110, <i>Candida tenuis</i> NRRL Y-1498 : CANTEDRAFT_105930, <i>Candida dubliniensis</i> CD36 : CD36_09890 and <i>Pichia stipitis</i> Pignal : PICST_30848	-0.1681	0.000188
orf19.7076	<i>GBP2</i>	Putative single-strand telomeric DNA-binding protein; protein level decreases in stationary phase cultures	-0.1684	0.001537
orf19.7005		Predicted ORF from Assembly 19; removed from Assembly 20	-0.1701	0.003206
orf19.327	<i>HTA3</i>	Putative histone H2A; amphotericin B repressed; flucytosine induced; RNA abundance regulated by tyrosol and cell density	-0.1725	3.45E-05
orf19.1082.1		Ortholog(s) have cytochrome-c oxidase activity, role in mitochondrial respiratory chain complex IV assembly and cytosol, mitochondrial respiratory chain complex IV, nucleus localization	-0.1767	1.18E-06

orf19.3449.2		Ortholog(s) have phosphatidylglycerophosphatase activity, role in cardiolipin biosynthetic process, phosphorylated carbohydrate dephosphorylation and mitochondrial matrix localization	-0.1794	0.00017
orf19.1785		Hap43p-repressed gene; biofilm-induced	-0.1818	0.001
orf19.6160		Ortholog(s) have role in eisosome assembly and eisosome, membrane raft, mitochondrion localization	-0.1822	9.79E-08
orf19.2116	<i>NAT2</i>	Putative N-terminal acetyltransferase; Hap43p-repressed gene; mutation confers hypersensitivity to toxic ergosterol analog	-0.187	1.40E-05
orf19.339	<i>NDE1</i>	Putative NADH dehydrogenase that could act alternatively to complex I in respiration; caspofungin repressed; fungal-specific (no human or murine homolog); transcription is upregulated in both intermediate and mature biofilms	-0.1889	0.002443
orf19.1357	<i>FCY21</i>	High affinity, high capacity, hypoxanthine-adenine-guanine-cytosine/ H ⁺ symporter; purine-cytosine permease of pyrimidine salvage; similar to <i>S. cerevisiae</i> Fcy2p; mutation confers resistance to 5-fluorocytosine (5-FC); biofilm-induced gene	-0.1907	0.001654
orf19.2864.1	<i>RPL28</i>	Putative ribosomal protein; Plc1p-regulated; genes encoding cytoplasmic ribosomal subunits, translation factors, and tRNA synthetases are downregulated upon phagocytosis by murine macrophage	-0.1947	0.002595
orf19.2775	<i>ID11</i>	Ortholog(s) have isopentenyl-diphosphate delta-isomerase activity, role in farnesyl diphosphate biosynthetic process and cytosol, nucleus localization	-0.1949	0.004145
orf19.5684		Ortholog(s) have structural constituent of ribosome activity and mitochondrial large ribosomal subunit localization	-0.1982	0.002809
orf19.3076		Ortholog(s) have role in vesicle-mediated transport and COPI-coated vesicle, integral to Golgi membrane localization	-0.1991	0.00634
orf19.2346		Putative protein of unknown function, transcription is positively regulated by Tbf1p	-0.1993	8.72E-05
orf19.3430		Plasma membrane-associated protein; physically interacts with TAP-tagged Nop1p	-0.2077	0.003132

orf19.1170	<i>ARO7</i>	Putative chorismate mutase; fungal-specific (no human or murine homolog); alkaline upregulated	-0.2082	0.000659
orf19.4051	<i>HTSI</i>	Putative tRNA-His synthetase; genes encoding ribosomal subunits, translation factors, tRNA synthetases are downregulated upon phagocytosis by murine macrophage; stationary phase enriched protein	-0.2083	0.003186
orf19.6529	<i>CDC34</i>	Putative ubiquitin-protein ligase; transcription is regulated by Nrg1p and Tup1p, and by Gcn2p and Gcn4p; planktonic growth-induced gene	-0.2099	0.001073
orf19.2953	<i>TOM20</i>	Putative mitochondrial primary import receptor	-0.2132	0.000711
orf19.7613	<i>HCRI</i>	Putative translation initiation factor; genes encoding ribosomal subunits, translation factors, and tRNA synthetases are downregulated upon phagocytosis by murine macrophage	-0.2139	0.000411
orf19.7173		Ortholog of <i>C. parapsilosis</i> CDC317 : CPAR2_702310, <i>Lodderomyces elongisporus</i> NRLL YB-4239 : LELG_04029, <i>Candida dubliniensis</i> CD36 : CD36_73730 and <i>Candida orthopsilosis</i> Co 90-125 : CORT0G02490	-0.2165	0.000171
orf19.1144		Early-stage biofilm-induced gene	-0.2165	0.000461
orf19.4438	<i>RME1</i>	Protein similar to <i>S. cerevisiae</i> meiotic regulator Rme1p; white-specific transcription; upregulation correlates with clinical development of fluconazole resistance; biofilm and planktonic growth-induced gene; Upc2p-regulated in hypoxia	-0.2211	0.001999
orf19.4311	<i>YNKI</i>	Nucleoside diphosphate kinase (NDP kinase); homo-hexameric; soluble protein in hyphae; flucytosine induced; biofilm induced; macrophage-induced protein; stationary phase enriched protein	-0.2227	0.002824
orf19.6105	<i>MVD</i>	Mevalonate diphosphate decarboxylase; functional homolog of <i>S. cerevisiae</i> Erg19p; possible drug target; transcriptionally regulated by carbon source, yeast-hyphal switch, growth phase, antifungals; gene has intron	-0.2264	0.004583
orf19.7643		Ortholog(s) have 4-hydroxybenzoate octaprenyltransferase activity, antioxidant activity and role in polyprenol biosynthetic process, ubiquinone biosynthetic process	-0.2335	2.92E-09
orf19.5305	<i>RHD3</i>	GPI-anchored cell wall protein; yeast-associated protein; transcriptionally regulated by iron; expression greater in high iron; clade-associated gene expression; not essential for cell wall integrity; fluconazole-repressed	-0.2345	0.002633

orf19.6202	<i>RBT4</i>	Pry family protein; required for virulence in mouse systemic/rabbit corneal infections; not required for filamentation; mRNA binds She3 and is localized to hyphal tips; Hap43-induced; detected in both yeast and hyphal culture supernatants	-0.2369	5.74E-05
orf19.5112	<i>TKL1</i>	Putative transketolase; localizes to surface of yeast-form cells, but not hyphae; soluble protein in hyphae; transcription regulated by Nrg1p, Mig1p, and Tup1p; antigenic in human or murine infection; possibly essential (by UAU1 method)	-0.2371	0.00017
orf19.7097		Putative cytoplasmic RNA-binding protein; heterozygous null mutant exhibits hypersensitivity to parnafungin and cordycepin in the <i>C. albicans</i> fitness test	-0.2383	0.002479
orf19.1030		Putative peptidyl-prolyl cis-trans isomerase	-0.2392	0.001135
orf19.5463	<i>SEC6</i>	Predicted subunit of the exocyst complex, involved in exocytosis; localizes to a crescent on the surface of the hyphal tip; Hap43p-repressed gene, overlaps orf19.5464 and orf19.5465	-0.2411	2.89E-05
orf19.220	<i>PIR1</i>	1,3-beta-glucan-linked structural cell wall protein; N-mannosylated, O-glycosylated by Pmt1p; tandem repeats; cell wall defect in heterozygous mutant; hyphal repressed; Hog1p, fluconazole, hypoxia induced; iron, Efg1p, Plc1p, temp regulated	-0.2435	0.000399
orf19.5437	<i>RHR2</i>	Glycerol 3-phosphatase; roles in osmotic tolerance, glycerol accumulation in response to salt; required for biofilm formation; biofilm-induced; regulated by macrophage, stress response, yeast-hyphal switch, pheromone, GCN4, HOG1, NRG1, TUP1	-0.2444	0.001051
orf19.3302		Putative type-1 protein phosphatase targeting subunit; late-stage biofilm-induced gene; transcription downregulated upon yeast-hyphal switch; transcriptionally activated by Mnl1p under weak acid stress	-0.2491	0.00046
orf19.6081	<i>PHR2</i>	Glycosidase; role in cell wall structure; may act on beta-1,3-glucan prior to beta-1,6-glucan linkage; role in vaginal not systemic virulence (low pH not neutral); low pH, high iron, fluconazole, Hap43p-induced; Rim101p-downregulated at Ph8	-0.2493	0.000445
orf19.4980	<i>HSP70</i>	Putative hsp70 chaperone; role in entry into host cells; heat-shock, amphotericin B, cadmium, ketoconazole-induced; farnesol-downregulated in biofilm; surface localized in yeast-form and hyphal cells; antigenic in host	-0.25	0.000818
orf19.4523		Ortholog(s) have 5-formyltetrahydrofolate cyclo-ligase activity, role in folic acid-containing compound biosynthetic process and mitochondrion localization	-0.2504	3.06E-05
orf19.6676		Has domain(s) with predicted diphthine synthase activity and role in peptidyl-diphthamide biosynthetic process from peptidyl-histidine	-0.2505	0.00692

orf19.2967	<i>TIF34</i>	Putative translation initiation factor eIF3, p39 subunit; mutation confers hypersensitivity to roridin A and verrucarin A; ribosomal subunits, translation factors, tRNA synthetases are downregulated upon phagocytosis by murine macrophages	-0.2505	0.003255
orf19.7399	-	ORF Predicted by Annotation Working Group; removed from Assembly 21	-0.2508	0.000277
orf19.5157		Predicted ORF in Assemblies 19, 20 and 21; six putative membrane-spanning regions; similar to <i>S. cerevisiae</i> Yjl097p, which is required for growth	-0.2532	1.31E-06
orf19.698		Ortholog(s) have role in endoplasmic reticulum inheritance and integral to endoplasmic reticulum membrane localization	-0.2536	0.000276
orf19.2954		Hap43p-repressed gene; repressed by nitric oxide	-0.2538	1.98E-05
orf19.3470		Putative flavodoxin; similar to <i>S. cerevisiae</i> Ypl207p; predicted Kex2p substrate	-0.2549	0.000356
orf19.1234	<i>FGR6-10</i>	Protein lacking an ortholog in <i>S. cerevisiae</i> ; member of a family encoded by FGR6-related genes in the RB2 repeat sequence; transposon mutation affects filamentous growth	-0.2574	0.005448
orf19.6400		Ortholog(s) have role in inositol metabolic process and cytosol, nuclear envelope localization	-0.2619	1.10E-05
orf19.6041	<i>RPO41</i>	Putative mitochondrial RNA polymerase; downregulated during core stress response	-0.2626	6.82E-05
orf19.5117	<i>OLE1</i>	Fatty acid desaturase, essential protein involved in oleic acid synthesis; required for aerobic hyphal growth and chlamydospore formation; subject to hypoxic regulation; fluconazole-induced; caspofungin repressed; Hap43p-induced	-0.264	4.48E-05
orf19.2392		Protein not essential for viability	-0.2643	0.000547
orf19.3459		Putative serine/threonine/tyrosine (dual-specificity) kinase; disruptants not obtained by UAU1 method	-0.2667	1.28E-05

orf19.4336	<i>RPS5</i>	Ribosomal protein S5; macrophage/pseudohyphal-induced after 16 h; genes encoding cytoplasmic ribosomal subunits, translation factors, tRNA synthetases are downregulated upon phagocytosis by murine macrophage; Hap43p-induced gene	-0.2671	0.005503
orf19.4565	<i>BGL2</i>	Cell wall 1,3-beta-glucosyltransferase; one of many 1,3-beta-glucosyltransferases; mutant has cell-wall and growth defects, but wild-type 1,3- or 1,6-beta-glucan content; antigenic; virulence role in mouse systemic infection	-0.2675	0.000566
orf19.5443	<i>BNA4</i>	Putative kynurenine 3-monooxygenase, involved in NAD biosynthesis; transposon mutation affects filamentous growth; Hap43p-repressed gene; oral infection upregulated; mutants have reduced capacity to damage oral epithelial cells	-0.268	0.001598
orf19.1085		Ortholog(s) have ubiquitin-protein ligase activity and role in ER-associated protein catabolic process, protein ubiquitination involved in ubiquitin-dependent protein catabolic process, vesicle organization	-0.2716	3.02E-05
orf19.6146	<i>CLG1</i>	Putative cyclin-like protein; transcription is regulated upon yeast-hyphal switch	-0.2766	0.000376
orf19.5191	<i>FGR6-1</i>	Protein lacking an ortholog in <i>S. cerevisiae</i> ; member of a family encoded by FGR6-related genes in the RB2 repeat sequence; transposon mutation affects filamentous growth	-0.2768	0.000844
orf19.735		Putative DNA-binding transcription factor; putative TFIID subunit; flucytosine repressed; merged with orf19.6193 in Assembly 20	-0.2791	2.53E-06
orf19.2372		Putative Pol protein of retrotransposon Tca2; separated by a stop codon from Gag protein orf19.2371; both likely translated as single polyprotein that includes nucleocapsid-like protein (Gag), reverse transcriptase, protease, and integrase	-0.2799	0.000475
orf19.6113		Predicted ORF in Assemblies 19, 20 and 21; transcription detected in high-resolution tiling array experiments	-0.2808	0.002013
orf19.2208		Ortholog(s) have role in response to salt stress and cytoplasm localization	-0.2842	5.25E-05
orf19.1392		Ortholog(s) have chaperone binding, protein disulfide isomerase activity, unfolded protein binding activity, role in ER-associated protein catabolic process, protein retention in ER lumen and endoplasmic reticulum membrane localization	-0.285	0.003188
orf19.448		Ortholog(s) have ubiquitin binding activity and cytoplasm localization	-0.2862	0.001658

orf19.5373		Predicted ORF from Assembly 19; orf19.5372 and orf19.5373 are similar to the Tca2 (pCal) retrotransposon, which is present in strain HOG1042 as 50 to 100 copies of a linear dsDNA; clade-associated gene expression; removed from Assembly 20	-0.2869	0.001824
orf19.5027	<i>LCB2</i>	Putative serine palmitoyltransferase component; mutation confers hypersensitivity to aureobasidin A	-0.2879	3.65E-05
orf19.2966		Predicted ORF in Assemblies 19, 20 and 21; clade-associated gene expression; farnesol-downregulated	-0.2881	7.81E-05
orf19.2571	<i>SEC4</i>	Small GTPase of Rab family; role in post-Golgi secretion; possible C-terminal palmitoylation; downregulated on adherence to polystyrene; localizes to the Spitzenkorper during hyphal growth; functional homolog of <i>S. cerevisiae</i> Sec4p	-0.2884	5.71E-05
orf19.3895	<i>CHT2</i>	GPI-linked chitinase required for normal filamentous growth; downregulated in core caspofungin response; fluconazole, Cyr1p-, Efg1p-, pH-regulated; mRNA binds She3p, is localized to yeast-form buds and hyphal tips	-0.2926	0.006682
orf19.7625	<i>PGA1</i>	Putative GPI-anchored protein; induced during cell wall regeneration; required for normal adhesion to host cells and for adherence during biofilm formation	-0.296	0.004391
orf19.1560	<i>POB3</i>	Protein similar to <i>S. cerevisiae</i> Pob3p, which is involved in chromatin assembly and disassembly; transposon mutation affects filamentous growth	-0.297	6.72E-08
orf19.561		Predicted ORF from Assembly 19; removed from Assembly 20	-0.2979	0.00461
orf19.5101	<i>CCR4</i>	Component of the Ccr4-Pop2 mRNA deadenylase; transposon mutation affects filamentous growth	-0.3036	0.00094
orf19.6459	<i>DPP3</i>	Protein similar to <i>S. cerevisiae</i> pyrophosphate phosphatase Dpp1p; required for farnesol biosynthesis; downregulated in response to 17-beta-estradiol, ethynyl estradiol	-0.3056	0.006126
orf19.783		Ortholog(s) have role in endocytosis, retrograde vesicle-mediated transport, Golgi to ER, vacuole organization and COPI-coated vesicle, Golgi membrane, endosome localization	-0.3082	0.000227
orf19.7003		Predicted ORF from Assembly 19; removed from Assembly 20	-0.3085	0.001297

orf19.7658	<i>RFC4</i>	Putative heteropentameric replication factor C subunit; flucytosine induced; periodic mRNA expression, peak at cell-cycle G1/S phase	-0.3095	0.005541
orf19.6716	<i>ABD1</i>	RNA (guanine-N7-)-methyltransferase, SAM-dependent; methylates mRNA 5' cap; binds phosphorylated RNA Pol II C-terminal domain peptide; does not bind mRNA TPase and mRNA GTase (Cet1p and Cgt1p); functional homolog of <i>S. cerevisiae</i> Abd1p	-0.3118	0.004228
orf19.4907		Putative protein of unknown function; Hap43p-repressed gene; increased transcription is observed upon fluphenazine treatment; possibly transcriptionally regulated by Tac1p; induced by nitric oxide; fungal-specific (no human/murine homolog)	-0.3159	0.005417
orf19.7673		Ortholog(s) have mRNA binding activity, role in mRNA splicing, via spliceosome and U1 snRNP, U2-type prespliceosome, U4/U6 x U5 tri-snRNP complex, U5 snRNP, commitment complex localization	-0.3182	3.65E-06
orf19.1378	<i>SUP35</i>	Translation factor eRF3; shows prion-like aggregation in some, not all, studies; partially complements <i>S. cerevisiae</i> sup35 mutant translation defect; species barrier with <i>S. cerevisiae</i> Sup35p prion; gene not regulated by yeast-hyphal switch	-0.3182	0.003662
orf19.568	<i>SPE2</i>	Putative S-adenosylmethionine decarboxylase; Hap43p-induced gene; possibly adherence-induced	-0.3202	0.005077
orf19.3013	<i>CDC12</i>	Septin; essential for viability; forms ring at sites of cell division and also forms filaments in mature chlamydospore; filamentous growth induced; regulated by Nrg1p, Tup1p, tyrosol and cell density	-0.3217	0.000135
orf19.1401	<i>EAP1</i>	GPI-anchored cell wall adhesin; cell-cell adhesion, biofilm formation; Efg1p-regulated; mutant suppresses polystyrene or cell adhesion, filamentation, invasive growth defects of <i>S. cerevisiae</i> flo8 or flo11 mutant; biofilm-induced	-0.3225	0.002204
orf19.3292		Ortholog(s) have peptide-methionine (R)-S-oxide reductase activity, role in cellular response to oxidative stress and cytosol, mitochondrion, nucleus localization	-0.3231	0.001751
orf19.4732	<i>SEC24</i>	Protein with a possible role in ER to Golgi transport; induced upon yeast-hyphal switch; sumoylation target	-0.3246	0.000447
orf19.6287	<i>AAT21</i>	Putative aspartate aminotransferase; higher protein amounts present in stationary phase; Gcn4p-regulated	-0.3275	0.002211
orf19.1065	<i>SSA2</i>	HSP70 family chaperone; found in cell wall fractions; antigenic; role in import of beta-defensin peptides; ATPase domain binds histatin 5; at surface of hyphae, not yeast-form cells; farnesol-downregulated in biofilm; caspofungin repressed	-0.3291	0.000436

orf19.391	<i>UPC2</i>	Zn ² -Cys ⁶ transcriptional regulator of ergosterol biosynthetic genes and sterol uptake; binds ERG2 promoter; induced upon ergosterol depletion, by azoles, anaerobicity, in biofilms; macrophage/pseudohyphal-repressed	-0.3307	0.002808
orf19.2396	<i>IFR2</i>	Zinc-binding dehydrogenase; upregulated by benomyl, ciclopirox olamine or alpha pheromone; regulated by oxidative stress (via Cap1p) and osmotic stress (via Hog1p); protein present in exponential and stationary phase; Hap43p-induced gene	-0.3327	6.92E-05
orf19.340		Ortholog(s) have role in protein targeting to membrane, protein targeting to vacuole and ESCRT I complex localization	-0.3355	7.45E-05
orf19.6229	<i>CAT1</i>	Catalase; resistance to oxidative stress, neutrophils, peroxide; role in virulence; regulated by iron, ciclopirox, fluconazole, carbon source, pH, Rim101p, Ssn6p, Hog1p, Hap43p, Sfulp, Sef1p, farnesol, core stress response	-0.3371	0.000504
orf19.2926		Ortholog(s) have 5'-3' exonuclease activity, damaged DNA binding activity, role in DNA repair and nucleus localization	-0.3385	0.002795
orf19.3051		Predicted ORF in Assemblies 19, 20 and 21; shows colony morphology-related gene regulation by Ssn6p	-0.3406	0.004975
orf19.3152	<i>AMO2</i>	Protein similar to <i>A. niger</i> predicted peroxisomal copper amino oxidase; mutation confers hypersensitivity to toxic ergosterol analog; induced upon biofilm formation	-0.3425	0.002618
orf19.7231	<i>FTR2</i>	High-affinity iron permease; probably interacts with ferrous oxidase; regulated by iron level, ciclopirox olamine, amphotericin B, caspofungin; complements <i>S. cerevisiae</i> ftr1 iron transport defect; Hap43p-repressed	-0.3444	0.002716
orf19.4959		Ortholog of <i>C. parapsilosis</i> CDC317 : CPAR2_202690, <i>Candida tenuis</i> NRRL Y-1498 : CANTEDRAFT_112521, <i>Debaryomyces hansenii</i> CBS767 : DEHA2E16434g and <i>Candida dubliniensis</i> CD36 : CD36_12360	-0.3454	0.002093
orf19.6538	<i>VMA11</i>	Predicted ortholog of <i>S. cerevisiae</i> Tfp3p, which is the c' subunit of the V0 subcomplex of the vacuolar ATPase; required for hemoglobin-iron utilization	-0.3471	3.75E-05
orf19.1661	<i>DBP5</i>	Ortholog(s) have RNA helicase activity, RNA-dependent ATPase activity, inositol hexakisphosphate binding activity and role in mRNA export from nucleus, translational termination	-0.3486	0.006691
orf19.5528	<i>MOB1</i>	Putative mitotic exit network component; periodic mRNA expression, peak at cell-cycle G2/M phase	-0.349	0.000119

orf19.1050		Ortholog of <i>S. cerevisiae</i> : YMR087W, <i>C. glabrata</i> CBS138 : CAGL0J01397g, <i>C. parapsilosis</i> CDC317 : CPAR2_107150, <i>Candida dubliniensis</i> CD36 : CD36_03920 and <i>Pichia stipitis</i> Pignal : PICST_61741	-0.3505	0.000108
orf19.3965		Ortholog(s) have role in double-strand break repair via homologous recombination, meiotic gene conversion, reciprocal meiotic recombination, replication fork protection and Smc5-Smc6 complex, cytosol, nucleus localization	-0.3568	0.006917
orf19.7329		Ortholog(s) have ubiquitin-protein ligase activity	-0.3584	0.001917
orf19.7080	<i>LEU2</i>	Isopropyl malate dehydrogenase; enzyme of leucine biosynthesis; upregulated in the presence of human whole blood or polymorphonuclear (PMN) cells; protein level decreases in stationary phase; GlcNAc-induced protein	-0.3598	0.000152
orf19.7128	<i>SYS1</i>	Putative Golgi integral membrane protein; transcription is regulated by Mig1p	-0.3603	5.29E-07
orf19.7270		Ortholog of <i>C. parapsilosis</i> CDC317 : CPAR2_808740, <i>Candida tenuis</i> NRRL Y-1498 : CANTEDRAFT_95761, <i>Debaryomyces hansenii</i> CBS767 : DEHA2G11946g and <i>Candida dubliniensis</i> CD36 : CD36_70220	-0.3614	0.003452
orf19.4853	<i>HCM1</i>	Protein with forkhead domain; similar to <i>S. cerevisiae</i> Hcm1p; Hap43p-induced gene	-0.3615	0.001803
orf19.1227	<i>ZCF4</i>	Putative transcription factor with zinc cluster DNA-binding motif	-0.3622	0.004788
orf19.916		Ortholog(s) have role in apoptotic process, calcium-mediated signaling, endoplasmic reticulum unfolded protein response and Golgi apparatus, endoplasmic reticulum, fungal-type vacuole membrane, mitochondrion localization	-0.3636	3.81E-06
orf19.1613	<i>ILV2</i>	Putative acetolactate synthase; regulated by Gcn4p; induced by amino acid starvation (3-AT treatment); stationary phase enriched protein	-0.3637	0.00138
orf19.1193	<i>GNP1</i>	Protein similar to asparagine and glutamine permease; fluconazole or caspofungin induced; transcription is regulated by Nrg1p, Mig1p, Tup1p, Gcn2p, Gcn4p, and alkaline regulated by Rim101p; biofilm-induced; fungal-specific	-0.3659	0.003187
orf19.5071	<i>NRP1</i>	Ortholog(s) have cytoplasmic stress granule, nucleolus localization	-0.3663	0.00091

orf19.6536	<i>IQG1</i>	Component of actomyosin ring at bud neck; cell-cycle regulated serine phosphorylation at CDK sites regulates association with formins Bni1p and Bnr1p, Iqg1p degradation, and ring disassembly; mutation causes severe cytokinetic defects	-0.3692	0.003408
orf19.6078.1	<i>RFC52</i>	Putative replication factor C complex protein; periodic mRNA expression, peak at cell-cycle G1/S phase; overlaps orf19.6079	-0.3704	0.000116
orf19.797	<i>BAT21</i>	Putative branched chain amino acid aminotransferase; regulated by Gcn4p, Gcn2p; induced in response to amino acid starvation (3-aminotriazole treatment); early-stage biofilm-induced	-0.3721	0.000496
orf19.5493	<i>GSP1</i>	Small RAN G-protein; essential; prenylation not predicted; overproduction rescues <i>S. cerevisiae</i> <i>gsp1</i> viability; macrophage/pseudohyphal-induced; not transcriptionally regulated by white-opaque or yeast-hyphal switching; GlcNAc-induced	-0.3733	0.003743
orf19.5217	<i>TES1</i>	Putative acyl-CoA thioesterase	-0.3734	0.002023
orf19.820	<i>SDS22</i>	Putative protein serine-threonine phosphatase; macrophage/pseudohyphal-repressed	-0.3744	0.001677
orf19.953.1	<i>COF1</i>	Putative cofilin; macrophage-induced protein; protein present in exponential and stationary-phase yeast cells, but higher amounts in stationary phase	-0.3749	0.000785
orf19.6927	<i>PEP8</i>	Protein similar to <i>S. cerevisiae</i> Pep8p, which is involved in retrograde transport; transposon mutation affects filamentous growth	-0.3761	0.000136
orf19.1397		Has domain(s) with predicted heme binding activity	-0.3787	0.001213
orf19.5400		ORF Predicted by Annotation Working Group; merged with orf19.5399 in Assembly 20	-0.3808	no replicates
orf19.837	<i>GNA1</i>	Glucosamine-6-phosphate acetyltransferase; enzyme of UDP-GlcNAc biosynthesis; required for viability in absence of GlcNAc supplementation; required for persistent infection and wild-type virulence in mouse systemic infection	-0.3824	5.75E-05
orf19.2489		Putative karyopherin beta; repressed by nitric oxide	-0.3825	0.004358

orf19.2560	<i>CDC60</i>	Cytosolic leucyl tRNA synthetase; conserved amino acid and ATP binding class I signature, tRNA binding, proofreading motifs; likely essential for growth; interacts with benzoxaborole antifungals; present in exponential and stationary phase	-0.383	0.000443
orf19.5788	<i>EFT2</i>	Elongation Factor 2 (eEF2); GTPase; essential; highly expressed; target of sordarin antifungals; antigenic in human/mouse; lacks site for regulatory phosphorylation by eEF2 kinase; GCN-regulated; higher protein amount in stationary phase	-0.3866	0.005191
orf19.4262		Ortholog(s) have mRNA binding activity and role in cellular protein complex localization, establishment of mitochondrion localization, nuclear-transcribed mRNA catabolic process, deadenylation-dependent decay	-0.3888	0.000435
orf19.5779	<i>RNR1</i>	Ribonucleotide reductase large subunit; expression greater in low iron; transposon mutation affects filamentous growth; farnesol upregulated in biofilm; regulated by cell cycle, tyrosol, cell density; regulated by Sef1p, Sfu1p, and Hap43p	-0.3895	0.001137
orf19.4485		Predicted ORF from Assembly 19; removed from Assembly 20	-0.3896	0.001184
orf19.6756		Ortholog(s) have Rab GTPase binding activity and Golgi apparatus, endoplasmic reticulum localization	-0.39	0.000107
orf19.1883	<i>YCS4</i>	Putative condensin complex subunit; cell-cycle regulated periodic mRNA expression	-0.3905	2.12E-05
orf19.3010.1	<i>ECM33</i>	GPI-anchored cell wall protein; mutants show cell-wall defects and reduced adhesion, host cell damage, and endocytosis; mutant infection is immunoprotective in murine model; fluconazole-induced; caspofungin repressed	-0.391	0.002401
orf19.6399	<i>ATSI</i>	Putative protein required for modification of wobble nucleosides in tRNA; induced upon adherence to polystyrene; regulated by Sef1p-, Sfu1p-, and Hap43p	-0.3916	0.007043
orf19.4633		Ortholog(s) have carbonyl reductase (NADPH) activity, oxidoreductase activity, acting on the aldehyde or oxo group of donors, NAD or NADP as acceptor activity and cytosol, nucleus, ribosome localization	-0.3934	2.47E-06
orf19.3043		Ortholog(s) have triglyceride lipase activity, role in triglyceride catabolic process and mitochondrion localization	-0.3934	7.69E-05
orf19.4651	<i>PGA53</i>	GPI-anchored cell surface protein of unknown function; greater mRNA abundance observed in a <i>cyr1</i> homozygous null mutant than in wild type	-0.3962	3.86E-05

orf19.2124		Has domain(s) with predicted nucleotide binding, oxidoreductase activity, transferase activity, transferring acyl groups other than amino-acyl groups, zinc ion binding activity and role in oxidation-reduction process	-0.3978	0.001363
orf19.3518		Ortholog(s) have dicarboxylic acid transmembrane transporter activity, role in mitochondrial transport and mitochondrial inner membrane localization	-0.3981	0.004887
orf19.951		Hap43p-repressed gene; transcription downregulated upon yeast-hyphal switch; fluconazole-induced; biofilm-induced	-0.3983	7.64E-06
orf19.3333		Ortholog(s) have poly(A) RNA binding activity, role in mRNA polyadenylation, poly(A)+ mRNA export from nucleus, regulation of mRNA stability and cytoplasm, nucleus localization	-0.3995	0.001181
orf19.7079		Ortholog(s) have role in cytokinesis and cellular bud neck localization	-0.4022	0.000306
orf19.1054		Ortholog(s) have structural constituent of nuclear pore activity	-0.4026	0.000991
orf19.4026	<i>HIS1</i>	ATP phosphoribosyl transferase; enzyme of histidine biosynthesis; fungal-specific (no human, murine homolog); upregulated in biofilm; acid upregulated/alkaline downregulated by Rim101p; regulated by Gcn2p, Gcn4p; strain CA9 is a his1 mutant	-0.4028	0.003814
orf19.3259		Ortholog(s) have peptidase activity, role in protein targeting to ER, signal peptide processing and signal peptidase complex localization	-0.403	9.53E-05
orf19.1814	<i>STT4</i>	Putative phosphatidylinositol-4-kinase	-0.4045	0.003051
orf19.1414		Protein of unknown function, transcription is upregulated in an RHE model of oral candidiasis; Hap43p-repressed gene	-0.4064	7.52E-07
orf19.1195		Ortholog(s) have metalloendopeptidase activity, role in cellular iron ion homeostasis, protein processing involved in protein targeting to mitochondrion and mitochondrion localization	-0.4101	0.00634
orf19.4677		Putative protein of unknown function, transcription is upregulated in clinical isolates from HIV+ patients with oral candidiasis	-0.4106	0.002862

orf19.7144		Ortholog(s) have GTPase activity, ribosome binding activity, role in nonfunctional rRNA decay, nuclear-transcribed mRNA catabolic process, no-go decay, ribosome disassembly and cytosol localization	-0.4111	0.002507
orf19.2222		Putative casein kinase; plasma membrane-localized	-0.4112	0.000585
orf19.532	<i>RBR2</i>	Cell wall protein; expression is repressed by Rim101p; expression is regulated upon white-opaque switching; transcription is repressed in response to alpha pheromone in SpiderM medium; macrophage-induced gene	-0.4123	0.002007
orf19.5741	<i>ALS1</i>	Adhesin; ALS family of cell-surface glycoproteins; adhesion, virulence roles; immunoprotective; band at hyphal base; amyloid domain; biofilm-induced; Rfg1p, Ssk1p; strain background affects expression; N-term binds fucose-containing glycans	-0.4136	0.013313
orf19.511		Ortholog(s) have ribosylnicotinamide kinase activity, role in NAD biosynthesis via nicotinamide riboside salvage pathway, nicotinamide riboside metabolic process and cytosol, nucleus localization	-0.4147	5.69E-06
orf19.5083	<i>DRG1</i>	Member of the DRG family of GTP-binding proteins; involved in regulation of invasive filamentous growth	-0.4173	0.001403
orf19.301	<i>PGA18</i>	Putative GPI-anchored protein; regulated by Nrg1p, Tup1p	-0.4176	0.00176
orf19.6034	<i>TUB2</i>	Beta-tubulin; functional homolog of ScTub2p; overproduction causes <i>S. cerevisiae</i> inviability; has two introns; hyphal-induced; fluconazole-induced; slow growth, ectopic expression causes increased white-to opaque switching; GlcNAc-induced	-0.4279	0.006582
orf19.749		Protein likely to be essential for growth, based on an insertional mutagenesis strategy; merged with orf19.48 in Assembly 20	-0.4332	0.004128
orf19.4437		Ortholog(s) have ATPase activity, DNA binding, nucleosome binding, rDNA binding activity	-0.4371	0.001938
orf19.6524	<i>TOM40</i>	Protein involved in mitochondrial protein import	-0.4375	0.00483
orf19.3479		Predicted ORF in Assemblies 19, 20 and 21; merged with orf19.3477	-0.4384	0.00089

orf19.7522		Hap43p-repressed gene; mutation confers hypersensitivity to amphotericin B	-0.4426	0.002038
orf19.6086	<i>LEU4</i>	Putative 2-isopropylmalate synthase; regulated by Nrg1p, Mig1p, Tup1p, Gcn4p; upregulated in the presence of human whole blood or polymorphonuclear (PMN) cells; macrophage/pseudohyphal-repressed after 16h; fungal-specific	-0.4427	0.002821
orf19.3031	<i>SEC62</i>	Putative endoplasmic reticulum (ER) protein-translocation complex subunit	-0.4477	8.45E-05
orf19.2093	<i>RFA1</i>	Putative DNA replication factor A; RNA abundance regulated by cell cycle, tyrosol and cell density	-0.4481	0.000147
orf19.2601	<i>HEM1</i>	Putative 5-aminolevulinatase synthase; transcriptionally regulated by iron; caspofungin repressed; expression greater in high iron; regulated by Ssn6p; induced by nitric oxide; Hap43p-repressed	-0.4486	9.73E-05
orf19.6838		Putative protein of unknown function, transcription is upregulated in clinical isolates from HIV+ patients with oral candidiasis	-0.45	0.00019
orf19.7215.3		Ortholog(s) have chaperone binding, unfolded protein binding activity, role in protein refolding and mitochondrial matrix localization	-0.4509	0.002562
orf19.5734	<i>POP2</i>	Component of the Ccr4-Pop2 mRNA deadenylase; heterozygous null mutant exhibits resistance to parnafungin and cordycepin in the <i>C. albicans</i> fitness test	-0.4509	0.003309
orf19.1684		Ortholog of <i>C. parapsilosis</i> CDC317 : CPAR2_503620, <i>Debaryomyces hansenii</i> CBS767 : DEHA2D15268g, <i>Candida dubliniensis</i> CD36 : CD36_81500 and <i>Pichia stipitis</i> Pignal : PICST_66925	-0.4513	0.003022
orf19.7519		Ortholog of <i>C. parapsilosis</i> CDC317 : CPAR2_800030, <i>Candida tenuis</i> NRRL Y-1498 : CANTEDRAFT_125790, <i>Debaryomyces hansenii</i> CBS767 : DEHA2E18260g and <i>Candida dubliniensis</i> CD36 : CD36_25180	-0.452	0.001341
orf19.5873	<i>POL1</i>	Putative DNA directed DNA polymerase alpha; RNA abundance regulated by cell cycle, tyrosol and cell density	-0.4535	0.007533
orf19.7298	<i>CHS2</i>	Chitin synthase; nonessential; required for wild-type chitin deposition in hyphae; transcription is regulated during dimorphic transition; Chs1p and Chs2p, but not Chs3p, are inhibited by the protoberberine HWY-289; fungal-specific	-0.4537	0.003182

orf19.2146	<i>HAT2</i>	Putative subunit of the Hat1p-Hat2p histone acetyltransferase complex, involved in DNA damage repair and morphogenesis; mutations cause constitutive pseudohyphal growth, caspofungin sensitivity	-0.4549	0.00123
orf19.1597	<i>ABG1</i>	Vacuolar membrane protein of yeast and hyphae; depletion causes abnormal vacuolar morphology, cell separation defect, sensitivity to cell wall perturbation, increased hyphal branching; essential gene, no mammalian homolog; Cyr1p-regulated	-0.4558	1.81E-05
orf19.390	<i>CDC42</i>	Rho-type GTPase; required for budding and maintenance of hyphal growth; GGTase I geranylgeranylated; misexpression blocks hyphal growth, causes avirulence in mouse IV infection; shows actin-dependent localization to hyphal tip	-0.457	0.001021
orf19.3312		Ortholog(s) have mitochondrion localization	-0.4621	0.005706
orf19.5775		Predicted ORF in Assemblies 19, 20 and 21; member of a family encoded by FGR6-related genes in the RB2 repeat sequence	-0.4623	0.007642
orf19.1116		Planktonic growth-induced gene	-0.4627	0.000176
orf19.4309	<i>GRP2</i>	Methylglyoxal reductase; regulation associated with azole resistance; induced in core stress response or by oxidative stress (via Cap1p), fluphenazine, benomyl, or with long term fluconazole treatment; Hap43p-induced; antigenic in humans	-0.4628	0.00116
orf19.5893	<i>RIP1</i>	Putative ubiquinol cytochrome c-reductase; transcriptionally regulated by iron; expression greater in high iron; alkaline downregulated; repressed by nitric oxide; Hap43p-repressed	-0.4638	7.69E-05
orf19.2013	<i>KAR2</i>	Similar to chaperones of Hsp70p family; role in translocation of proteins into the ER; transcriptionally regulated by iron; expression greater in high iron; protein present in exponential and stationary growth phase yeast cultures	-0.4641	2.82E-05
orf19.2065		Ortholog(s) have role in allantoin catabolic process and cytosol, nucleus localization	-0.4645	0.00035
orf19.7108		D-ribulose-5-phosphate 3-epimerase; stationary phase enriched protein	-0.4659	0.000164
orf19.5246		Hap43p-repressed gene	-0.4669	0.001645

orf19.429		Putative non-canonical poly(A) polymerase; repressed by nitric oxide	-0.4687	0.000213
orf19.317		Ortholog(s) have inosine nucleosidase activity, nicotinamide riboside hydrolase activity, purine-nucleoside phosphorylase activity	-0.4714	3.61E-05
orf19.6219		Ortholog of <i>C. parapsilosis</i> CDC317 : CPAR2_208960, <i>Candida tenuis</i> NRRL Y-1498 : CANTEDRAFT_114040, <i>Candida dubliniensis</i> CD36 : CD36_06470 and <i>Pichia stipitis</i> Pignal : PICST_51125	-0.4726	0.064153
orf19.3921		Ortholog(s) have cell division site, cell tip, cytosol, nucleus localization	-0.4751	0.000564
orf19.2761		Putative glycosylphosphatidylinositol (GPI) anchor assembly protein; transposon insertion causes decreased colony wrinkling but does not block true hyphal growth; induced by nitric oxide independent of Yhb1p	-0.4757	0.000216
orf19.956		Ortholog(s) have role in fermentation and mitochondrion localization	-0.4761	0.003261
orf19.3873	<i>ARC40</i>	Protein similar to <i>S. cerevisiae</i> Arc40p, which is involved in actin filament organization in <i>S. cerevisiae</i> ; transposon mutation affects filamentous growth	-0.4765	1.19E-05
orf19.6702	<i>DED81</i>	Putative tRNA-Asn synthetase; genes encoding ribosomal subunits, translation factors, tRNA synthetases are downregulated upon phagocytosis by murine macrophage; protein enriched in stationary phase yeast cultures	-0.4772	0.002796
orf19.1634		Has domain(s) with predicted fatty-acyl-CoA binding activity	-0.4797	0.002212
orf19.3947		Ortholog(s) have rDNA binding activity	-0.4813	0.00546
orf19.7056		Putative protein of unknown function, transcription is upregulated in clinical isolates from HIV+ patients with oral candidiasis; regulated by Sef1p-, Sfu1p-, and Hap43p	-0.483	0.008001
orf19.6944	<i>PHB1</i>	Putative prohibitin; identified in detergent-resistant membrane fraction (possible lipid raft component); predicted N-terminal acetylation; Hap43p-repressed gene	-0.4868	2.81E-06

orf19.1522		Ortholog of <i>C. parapsilosis</i> CDC317 : CPAR2_211990, <i>Debaryomyces hansenii</i> CBS767 : DEHA2G03036g, <i>Candida dubliniensis</i> CD36 : CD36_16850 and <i>Pichia stipitis</i> Pignal : psti_CGOB_00069	-0.4868	0.000285
orf19.374		Ortholog(s) have role in protein targeting to vacuole involved in ubiquitin-dependent protein catabolic process via the multivesicular body sorting pathway	-0.4876	6.83E-06
orf19.6923		Ortholog(s) have chromatin binding activity, role in RNA polymerase II transcriptional preinitiation complex assembly and transcription factor TFIID complex localization	-0.4938	7.33E-06
orf19.2730		Has domain(s) with predicted zinc ion binding activity	-0.4942	0.001757
orf19.5589		Predicted ORF in Assemblies 19, 20 and 21; transcription detected in high-resolution tiling array experiments	-0.4943	0.000355
orf19.267		Protein required for normal filamentous growth; mRNA binds to She3p	-0.4983	0.001
orf19.3045		Predicted ORF in Assemblies 19, 20 and 21; virulence-group-correlated expression	-0.4983	0.001966
orf19.6063	<i>UBP6</i>	Putative ubiquitin-specific protease of the 26S proteasome; oxidative stress-induced via Cap1p	-0.4996	1.47E-05
orf19.6856		Predicted ORF from Assembly 19; merged with orf19.748 in Assembly 20	-0.4996	0.002649
orf19.3794	<i>CSRI</i>	Zinc-finger transcription factor involved in zinc homeostasis and in regulation of biofilm matrix; mutation affects filamentous growth; can suppress <i>S. cerevisiae</i> rok1 mutant inviability	-0.5024	6.14E-05
orf19.6975	<i>YST1</i>	Ribosome-associated protein; antigenic in mice; complements <i>S. cerevisiae</i> yst1 yst2 mutant; similar to laminin-binding proteins, does not bind laminin; predicted S/T phosphorylation, N-glycosylation, myristoylation, Hap43p-, Gcn4p-regulated	-0.5031	0.002671
orf19.1833		Ortholog(s) have pseudouridine synthase activity, role in box H/ACA snoRNA 3'-end processing, rRNA pseudouridine synthesis, snRNA pseudouridine synthesis and 90S preribosome, box H/ACA snoRNP complex, cytosol localization	-0.5064	4.12E-07

orf19.6090		Putative nucleolar protein with a predicted role in pre-rRNA processing and ribosome biogenesis; required for biofilm formation; repressed by nitric oxide	-0.5082	0.000272
orf19.5685	<i>THS1</i>	Putative threonyl-tRNA synthetase; transcription regulated by Mig1p and Tup1p; downregulated upon phagocytosis by murine macrophages; stationary phase enriched protein	-0.5095	0.003126
orf19.3391	<i>ADK1</i>	Putative adenylate kinase; decreased expression in hyphae compared to yeast; macrophage-induced protein; adenylate kinase release used as a marker for cell lysis; possibly an essential gene (UAU1 method); biofilm-induced gene	-0.5096	0.007393
orf19.2960	<i>FRS2</i>	Putative tRNA-Phe synthetase; genes encoding ribosomal subunits, translation factors, tRNA synthetases are downregulated upon phagocytosis by murine macrophage; protein present in exponential and stationary growth phase yeast cultures	-0.5097	0.000136
orf19.3944	<i>GRR1</i>	Protein involved in the negative control of pseudohyphal growth; ortholog of <i>S. cerevisiae</i> Grr1p, which is an F-box protein component of the SCF ubiquitin-ligase complex required for cell cycle progression	-0.5136	0.001778
orf19.5360	<i>RPC11</i>	Putative RNA polymerase III subunit C11; downregulated in core caspofungin response	-0.5144	0.003941
orf19.5321		Ortholog(s) have methylenetetrahydrofolate reductase (NADPH) activity and role in methionine biosynthetic process, oxidation-reduction process	-0.5146	0.000148
orf19.5849	<i>CWT1</i>	Zn2Cys6 transcription factor involved in negative regulation of nitrosative stress response; mutant has cell wall defects; transcription increased at stationary phase; has predicted PAS domain; similar to <i>S. cerevisiae</i> Rds2p	-0.5151	0.00017
orf19.441	<i>RPT1</i>	Putative 26S proteasome regulatory subunit 7; Hap43p-repressed gene; regulated by Gcn2p and Gcn4p; overlaps orf19.442	-0.519	0.001255
orf19.1723		Ortholog(s) have role in response to purine-containing compound and cytoplasm, nucleus localization	-0.5199	0.001287
orf19.7057		Putative glutamine-tRNA ligase; stationary phase enriched protein	-0.5211	0.000527
orf19.3050	<i>AGE1</i>	Putative GTPase activator; transcriptionally regulated by iron; expression greater in low iron	-0.5252	4.10E-05

orf19.7654	<i>CPR6</i>	Putative peptidyl-prolyl cis-trans isomerase; macrophage/pseudohyphal-repressed; heavy metal (cadmium) stress-induced; heterozygous null mutant displays sensitivity to virgineone	-0.5284	8.02E-06
orf19.5136		Putative pyridoxamine 5'-phosphate oxidase; early-stage biofilm- and planktonic growth-induced gene	-0.5297	0.006077
orf19.5844		Ortholog(s) have role in meiotic DNA recombinase assembly, reciprocal meiotic recombination and condensed nuclear chromosome localization	-0.5309	0.022685
orf19.2289	<i>ARP3</i>	Protein with Myo5p-dependent localization to cortical actin patches at hyphal tip; mutation confers hypersensitivity to cytochalasin D	-0.5311	0.001073
orf19.5871	<i>SNF5</i>	SWI/SNF chromatin remodeling complex subunit involved in transcriptional regulation; mutants have defects in silicone adherence, biofilm formation, hyphal morphogenesis, cell wall defects; increased cell aggregation during yeast form growth	-0.5408	0.001928
orf19.2573	<i>FRS1</i>	Phenylalanyl-tRNA synthetase; possible role in early cell wall biosynthesis; downregulated by phagocytosis by macrophages; possibly essential gene, disruptants not obtained by UAU1 method; protein present in exponential and stationary phase	-0.5409	0.002139
orf19.3919		Early-stage biofilm-induced gene	-0.5415	0.005751
orf19.7232	<i>IRR1</i>	Putative cohesin complex subunit; cell-cycle regulated periodic mRNA expression	-0.5423	0.004511
orf19.3268	<i>TMA19</i>	Cell wall protein, ortholog of <i>S. cerevisiae</i> Tma19p (Ykl065cp)	-0.5432	1.33E-05
orf19.1652	<i>POx1-3</i>	Predicted acyl-CoA oxidase; farnesol regulated; stationary phase enriched protein	-0.5443	0.003325
orf19.5776	<i>TOM1</i>	Putative E3 ubiquitin ligase; transcription is regulated by Nrg1p and Mig1p	-0.5479	0.001585
orf19.6628		Ortholog of <i>C. parapsilosis</i> CDC317 : CPAR2_206070, <i>Candida tenuis</i> NRRL Y-1498 : CANTEDRAFT_100837, <i>Debaryomyces hansenii</i> CBS767 : DEHA2E20262g and <i>Candida dubliniensis</i> CD36 : CD36_31230	-0.5493	0.00244

orf19.1952		Protein not essential for viability; merged with orf19.1953 in Assembly 21	-0.5564	0.004271
orf19.3803	<i>MNN22</i>	Putative Golgi alpha-1,2-mannosyltransferase; regulated by Tsa1p, Tsa1Bp in minimal media at 37 deg; Hog1p-induced; induced by nitric oxide; downregulated in core stress response; planktonic growth-induced gene	-0.5615	8.41E-05
orf19.5641	<i>CAR2</i>	Ornithine aminotransferase; role in arginine metabolism; alkaline upregulated; mutation confers hypersensitivity to toxic ergosterol analog and to amphotericin B; present in exponential and stationary phase yeast cultures; biofilm-induced	-0.565	0.00015
orf19.2151	<i>NAG6</i>	Protein required for wild-type mouse virulence and wild-type cycloheximide resistance; putative GTP-binding motif; similar to <i>S. cerevisiae</i> Yor165Wp; in gene cluster that encodes enzymes of GlcNAc catabolism; no human or murine homolog	-0.5665	0.000408
orf19.151	<i>TPO5</i>	Putative polyamine transporter; mutation confers hypersensitivity to toxic ergosterol analog; hyphal induced; macrophage induced	-0.567	0.005276
orf19.4831	<i>MTS1</i>	Sphingolipid C9-methyltransferase, catalyzes methylation of the 9th carbon in the long chain base component of glucosylceramides; glucosylceramide biosynthesis is important for virulence	-0.5691	0.003156
orf19.109		Probable mitochondrial tyrosyl-tRNA synthetase, based on conservation in other fungi	-0.5701	0.018821
orf19.240	<i>PAM17</i>	Predicted component of the presequence translocase-associated import motor (PAM complex) involved in protein import into mitochondrial matrix	-0.5702	6.63E-05
orf19.5897		Ortholog(s) have Seh1-associated complex, cytosol, extrinsic to fungal-type vacuolar membrane localization	-0.5758	0.000347
orf19.4211	<i>FET3</i>	Multicopper oxidase; required for growth in low iron, for prostaglandin E2 production; ketoconazole, caspofungin, amphotericin B repressed; regulated by Sef1p, Sfu1p, and Hap43p; reports differ if functional homolog of <i>S. cerevisiae</i> Fet3	-0.5759	0.006034
orf19.6170		Ortholog(s) have microtubule binding, protein heterodimerization activity, protein homodimerization activity	-0.577	0.006115
orf19.3573	<i>PEX6</i>	Ortholog(s) have ATPase activity, protein heterodimerization activity, role in protein import into peroxisome matrix, receptor recycling, replicative cell aging and cytosol, nucleus, peroxisome localization	-0.5773	0.001403

orf19.6684	<i>PNC1</i>	Putative nicotinamidase, involved in NAD salvage pathway; decreased transcription is observed in an azole-resistant strain that overexpresses MDR1	-0.5793	0.002564
orf19.967		Ortholog(s) have endodeoxyribonuclease activity, exodeoxyribonuclease activity, ribonuclease activity and role in DNA catabolic process, DNA recombination, RNA catabolic process, apoptotic process, cellular response to nitrogen starvation	-0.5816	1.70E-05
orf19.6967	<i>USO6</i>	Putative vesicular transport protein; transcription is induced upon filamentous growth	-0.5844	6.17E-06
orf19.5858	<i>EGD2</i>	Putative nascent polypeptide associated complex protein alpha subunit; soluble protein in hyphae; macrophage/pseudohyphal-induced; protein level decrease in stationary phase cultures; GlcNAc-induced protein	-0.5846	0.000842
orf19.1007		Putative transcription factor with bZIP DNA-binding motif	-0.5851	0.002275
orf19.7506		Ortholog(s) have ATPase activity, DNA binding, nucleosome binding activity, role in chromatin remodeling and ISW1 complex localization	-0.5897	0.000773
orf19.5076	<i>PFY1</i>	Profilin, functional homolog of <i>S. cerevisiae</i> Pfy1p; hyphal-induced; macrophage/pseudohyphal-induced; regulated by Nrg1p, Tup1p; gene lacks intron (unlike <i>S. cerevisiae</i> PFY1); complements growth of <i>S. cerevisiae</i> srv2 mutant; nonessential	-0.5911	0.000211
orf19.5032	<i>SIMI</i>	Putative adhesin-like protein involved in cell wall maintenance, redundant with Sun41p; possibly secreted; macrophage-downregulated gene; transcription is negatively regulated by Rim101p, Cyr1p, Ras1p	-0.5913	0.001765
orf19.1637		Ortholog(s) have cytosol, nucleus localization	-0.5915	1.30E-06
orf19.586	<i>ERV46</i>	Putative ER-derived vesicle protein, COPII-coated vesicle complex subunit; transcription is induced upon filamentous growth	-0.592	0.006967
orf19.3169		Ortholog(s) have role in establishment of mitotic sister chromatid cohesion and cytosol, nucleus localization	-0.5937	0.004061
orf19.7312	<i>ERG13</i>	3-hydroxy-3-methylglutaryl coenzyme A synthase; ergosterol biosynthesis protein; sumoylation target; transposon mutation affects filamentous growth; amphotericin B, caspofungin repressed; exponential and stationary growth phase expressed	-0.5944	0.000267

orf19.898	<i>HEM2</i>	Putative porphobilinogen synthase; transcriptionally regulated by iron; expression greater in high iron; protein level decrease in stationary phase cultures	-0.5947	0.001364
orf19.1843	<i>ALG6</i>	Putative glucosyltransferase involved in cell wall mannan biosynthesis; transcription is elevated in <i>chk1</i> , <i>nik1</i> , and <i>sln1</i> homozygous null mutants; repressed by nitric oxide; possibly essential gene, disruptants not obtained by UAU1 method	-0.5975	0.003575
orf19.589	<i>VPS21</i>	Late endosomal Rab small monomeric GTPase involved in transport of endocytosed proteins to the vacuole; involved in filamentous growth and virulence	-0.5977	6.84E-05
orf19.287		Putative NADH-ubiquinone oxidoreductase subunit; Hap43p-repressed gene; repressed by nitric oxide; identified in detergent-resistant membrane fraction (possible lipid raft component)	-0.6007	0.002845
orf19.5665		Ortholog(s) have D-arabinose 1-dehydrogenase [NAD(P)+] activity and role in dehydro-D-arabinono-1,4-lactone biosynthetic process	-0.6016	0.002818
orf19.5689		Ortholog(s) have role in ER to Golgi vesicle-mediated transport, late endosome to vacuole transport via multivesicular body sorting pathway, vesicle coating and COPI vesicle coat, endosome localization	-0.6048	0.001849
orf19.3681		Ortholog(s) have Ran guanyl-nucleotide exchange factor activity, protein transporter activity	-0.6093	0.005764
orf19.6339	<i>NRG2</i>	Protein similar to <i>S. cerevisiae</i> Nrg2p transcription factor, which regulates invasive growth in <i>S. cerevisiae</i> ; transposon mutation affects filamentous growth	-0.614	0.001106
orf19.3294	<i>MBF1</i>	Putative transcriptional coactivator; caspofungin repressed	-0.6145	0.00025
orf19.426		Ortholog of <i>C. parapsilosis</i> CDC317 : CPAR2_107740, <i>Candida tenuis</i> NRRL Y-1498 : CANTEDRAFT_136277, <i>Debaryomyces hansenii</i> CBS767 : DEHA2A02266g and <i>Candida dubliniensis</i> CD36 : CD36_05120	-0.6177	1.21E-05
orf19.3702		Predicted ORF from Assembly 19; merged with orf19.6452 in Assembly 20	-0.6187	0.000348
orf19.4901		Has domain(s) with predicted methyltransferase activity and role in metabolic process	-0.6275	0.004792

orf19.5996.1	<i>RPS19A</i>	Putative ribosomal protein S19; protein level decreases in stationary phase cultures	-0.6283	2.44E-05
orf19.2426		Ortholog(s) have cytosol, nucleus localization	-0.629	0.005993
orf19.4865		Ortholog(s) have phosphatidylinositol-3,5-bisphosphate 5-phosphatase activity, phosphatidylinositol-3-phosphatase activity, phosphatidylinositol-4-phosphate phosphatase activity and role in phosphatidylinositol dephosphorylation	-0.6296	0.00581
orf19.1999		Predicted ORF in Assemblies 19, 20 and 21; transcription detected in high-resolution tiling array experiments	-0.6314	0.001306
orf19.7030	<i>SSRI</i>	Beta-glucan associated ser/thr rich cell-wall protein with a role in cell wall structure; GPI anchor; similar mRNA abundance in yeast-form and germ tubes; detected at germ tube plasma membrane; repressed in cells treated with Congo Red	-0.6342	0.001212
orf19.3324	<i>TIF</i>	Translation initiation factor; upregulated in highly virulent strain compared to less virulent strain; antigenic in human; flucytosine induced; translation-related genes are downregulated upon phagocytosis	-0.6348	0.004267
orf19.3399		Ortholog(s) have histone binding activity, role in histone exchange and Swr1 complex, cytoplasm localization	-0.6357	0.00363
orf19.7114	<i>CSAI</i>	Surface antigen on elongating hyphae and buds; no obvious hyphal defects in mutant; strain variation in repeat domain number; upregulated in filaments; alkaline upregulated by Rim101p; ciclopirox induced; Efg1p-, Cph1p, Hap43p-regulated	-0.6368	0.000341
orf19.1095		Putative nuclear pore complex; possibly an essential gene, disruptants not obtained by UAU1 method	-0.638	8.14E-05
orf19.5806	<i>ALD5</i>	NAD-aldehyde dehydrogenase; decreased expression in fluconazole-resistant isolate, or in hyphae; biofilm induced; fluconazole-downregulated; protein abundance is affected by URA3 expression in the CAI-4 strain; stationary phase enriched	-0.6403	0.000146
orf19.3735		Predicted ORF in Assemblies 19, 20 and 21; transcription is induced in response to alpha pheromone in SpiderM medium	-0.6416	0.002907
orf19.5964	<i>ARF2</i>	Putative ADP-ribosylation factor; mutation confers hypersensitivity to Brefeldin A	-0.6423	0.001419

orf19.7067		Ortholog(s) have RNA polymerase II core binding, RNA polymerase II transcription factor binding transcription factor activity, triplex DNA binding activity	-0.646	0.005788
orf19.3466		Predicted ORF in Assemblies 19, 20 and 21; decreased transcription is observed upon fluphenazine treatment or in an azole-resistant strain that overexpresses CDR1 and CDR2	-0.6511	0.000912
orf19.6293	<i>EMP24</i>	COPII-coated vesicle component	-0.6518	0.005227
orf19.2016		Ortholog(s) have protein binding, bridging activity, role in ergosterol biosynthetic process and endoplasmic reticulum membrane localization	-0.6555	0.002855
orf19.2077	<i>ZCF9</i>	Putative transcription factor with zinc cluster DNA-binding motif; hypersensitive to toxic ergosterol analog ECC69 and/or ECC1384	-0.6562	0.001278
orf19.2974	<i>YKT6</i>	Putative protein of the vacuolar SNARE complex with a predicted role in vacuolar fusion	-0.657	4.00E-05
orf19.6057		Ortholog(s) have 3-methyl-2-oxobutanoate hydroxymethyltransferase activity, role in pantothenate biosynthetic process and mitochondrion localization	-0.6616	0.000548
orf19.412	<i>SSH1</i>	Protein with a role in protein translocation across membranes	-0.6618	0.000121
orf19.6376	<i>PTC5</i>	Mitochondrial protein phosphatase of the Type 2C-related family (serine/threonine-specific), involved in drug response and cadmium tolerance	-0.6649	0.004598
orf19.2618	<i>MET2</i>	Homoserine acetyltransferase; Hap43p-, Gcn4p-regulated; macrophage/pseudohyphal-repressed; not highly biofilm induced, in contrast to many sulfur amino acid metabolic genes; no human or murine homolog; virulence-group-correlated expression	-0.6649	0.00604
orf19.6046	<i>APC1</i>	Putative Anaphase-Promoting Complex/Cyclosome subunit; essential for growth; periodic mRNA expression, peak at cell-cycle S/G2 phase	-0.6678	0.000172
orf19.458		Ortholog(s) have protein transmembrane transporter activity and role in chaperone-mediated protein complex assembly, mitochondrial respiratory chain complex III assembly, protein insertion into mitochondrial membrane from inner side	-0.6691	0.00041

orf19.6526		Ortholog(s) have COPI-coated vesicle, Golgi apparatus localization	1.44028	0.000496
orf19.3057		Ortholog(s) have role in mitochondrial genome maintenance and endoplasmic reticulum localization	1.50105	0.000368
orf19.2315		Putative transcription factor with bZIP DNA-binding motif	1.50168	0.000859
orf19.2895	<i>VMA8</i>	Protein similar to the <i>S. cerevisiae</i> Vma8p subunit of vacuolar H ⁺ -ATPase; transcription is regulated by Nrg1p and Mig1p; transcription is increased in populations of cells exposed to fluconazole over multiple generations	1.50247	1.70E-05
orf19.1681		Ortholog of <i>C. parapsilosis</i> CDC317 : CPAR2_503590, <i>Candida tenuis</i> NRRL Y-1498 : CANTEDRAFT_115755, <i>Debaryomyces hansenii</i> CBS767 : DEHA2D15334g and <i>Candida dubliniensis</i> CD36 : CD36_81530	1.50447	0.000112
orf19.6893		Ortholog(s) have role in ER to Golgi vesicle-mediated transport	1.50707	0.007554
orf19.2733		Putative subunit of phosphatidylinositol 3-kinase complexes I and II; transcription is activated in the presence of elevated CO ₂	1.50794	0.003168
orf19.5177		Ortholog of <i>Candida albicans</i> WO-1 : CAWG_05627	1.50832	0.00152
orf19.1764		Ortholog of <i>C. parapsilosis</i> CDC317 : CPAR2_407390, <i>Candida tenuis</i> NRRL Y-1498 : CANTEDRAFT_95056, <i>Debaryomyces hansenii</i> CBS767 : DEHA2F09504g and <i>Candida dubliniensis</i> CD36 : CD36_24220	1.50936	0.00733
orf19.3736	<i>KAR4</i>	Protein similar to <i>S. cerevisiae</i> Kar4p, which has a role in karyogamy; transcription is opaque-specific, a-specific, and induced by alpha factor	1.51383	0.000878
orf19.138	<i>FIG1</i>	Probable ortholog of <i>S. cerevisiae</i> Fig1p, which is an integral membrane protein required for mating; role in thigmotropism; transcription is opaque-specific, a-specific, and activated by Cph1p or alpha pheromone	1.51396	0.004938
orf19.2915		Ortholog(s) have nucleoside-diphosphatase activity, nucleoside-triphosphatase activity, nucleoside-triphosphate diphosphatase activity, role in protein mannosylation and COPI-coated vesicle, Golgi membrane localization	1.51426	0.002535

orf19.335		Sef1p-, Sfu1p-, and Hap43p-regulated gene (1.51486	0.001752
orf19.3955	<i>MES1</i>	Cytoplasmic methionyl-tRNA synthetase; zinc-binding motif; ribosomal subunits, translation factors, tRNA synthetases are downregulated upon phagocytosis by murine macrophage; protein present in exponential and stationary phase yeast	1.51587	0.000741
orf19.5666		Ortholog(s) have transcription coactivator activity	1.51773	4.23E-05
orf19.5440	<i>RPT2</i>	Putative ATPase of the 19S regulatory particle of the 26S proteasome; oxidative stress-induced via Cap1p	1.51859	0.002285
orf19.5727		Ortholog of <i>C. parapsilosis</i> CDC317 : CPAR2_601230, <i>Candida tenuis</i> NRRL Y-1498 : CANTEDRAFT_115908, <i>Debaryomyces hansenii</i> CBS767 : DEHA2E12540g and <i>Candida dubliniensis</i> CD36 : CD36_64130	1.51926	0.000926
orf19.5855	<i>MBP1</i>	Putative component of the MBF transcription complex involved in G1/S cell-cycle progression; non-periodic mRNA expression; predicted, conserved MBF binding sites upstream of G1/S-regulated genes	1.52234	0.003568
orf19.5680		Predicted ORF in Assemblies 19, 20 and 21; possibly an essential gene, disruptants not obtained by UAU1 method	1.52412	0.000413
orf19.4620	<i>TIM12</i>	Predicted component of the TIM22 complex, involved in protein import into mitochondrial inner membrane	1.52486	0.000587
orf19.6667		Ortholog(s) have histone deacetylase activity	1.52525	0.005099
orf19.2742		Ortholog of <i>C. parapsilosis</i> CDC317 : CPAR2_400095, <i>Candida tenuis</i> NRRL Y-1498 : CANTEDRAFT_113280, <i>Lodderomyces elongisporus</i> NRLL YB-4239 : LELG_04166 and <i>Candida dubliniensis</i> CD36 : CD36_42560	1.52787	0.000979
orf19.729	<i>SHE3</i>	Protein similar to <i>S. cerevisiae</i> She3p, an adaptor protein required for specific mRNA transport; transposon mutation affects filamentous growth	1.52861	0.004997
orf19.6875	<i>VPS35</i>	Putative role in vacuolar sorting; downregulated in biofilm; induced upon adherence to polystyrene	1.53491	0.001206

orf19.5029	<i>MODF</i>	Ortholog(s) have mitochondrion localization	1.53592	0.007607
orf19.261		Ortholog(s) have dolichol kinase activity, role in protein glycosylation and endoplasmic reticulum membrane localization	1.53785	0.002624
orf19.4225	<i>LEU3</i>	Zinc-finger protein; putative role in regulating branched-chain amino acid biosynthesis genes; alkaline upregulated; transcriptionally activated by Mnl1p under weak acid stress; required for yeast cell adherence to silicone substrate	1.53798	4.22E-05
orf19.981		Predicted ORF from Assembly 19; merged with orf19.4911 in Assembly 20	1.53883	0.000796
orf19.542.2	<i>MIMI</i>	Predicted mitochondrial protein involved in outer membrane protein import	1.54033	6.27E-06
orf19.1606		Predicted ORF in Assemblies 19, 20 and 21; Plc1p-regulated	1.54041	0.004848
orf19.5850	<i>NOC2</i>	Putative nucleolar complex protein; Hap43p-induced gene; transposon mutation affects filamentous growth; mutation confers hypersensitivity to 5-fluorouracil (5-FU), tubercidin (7-deazaadenosine); downregulated during core stress response	1.5405	0.002972
orf19.5901	<i>PKC1</i>	Protein kinase C; functional homolog of <i>S. cerevisiae</i> Pkc1p; mutant has abnormal yeast-form cell morphology and increased cell lysis; activated by phosphatidylserine; target of antifungal, cercosporamide; R400P mutant is activated	1.5435	0.000354
orf19.5035		Ortholog(s) have DNA binding, nucleosome binding activity	1.54561	0.006531
orf19.4163		Ortholog(s) have role in protein targeting to vacuole, receptor-mediated endocytosis, response to pheromone and actin cortical patch, cytosol, endosome, plasma membrane, ribosome localization	1.54701	4.40E-05
orf19.5572		Ortholog of <i>C. parapsilosis</i> CDC317 : CPAR2_600660, <i>Candida tenuis</i> NRRL Y-1498 : CANTEDRAFT_104804, <i>Debaryomyces hansenii</i> CBS767 : DEHA2C11902g and <i>Candida dubliniensis</i> CD36 : CD36_63110	1.54994	6.87E-06
orf19.4057		Ortholog of <i>Candida dubliniensis</i> CD36 : CD36_04885 and <i>Candida albicans</i> WO-1 : CAWG_00885	1.54995	0.003525

orf19.6239		Putative serine/threonine protein kinase; possibly an essential gene, disruptants not obtained by UAU1 method	1.55229	0.001229
orf19.3956		Ortholog(s) have glutaminyl-tRNA synthase (glutamine-hydrolyzing) activity and role in endoplasmic reticulum organization, glutaminyl-tRNAGln biosynthesis via transamidation	1.55429	0.000323
orf19.5276		Putative nuclear pore-associated protein; Hap43p-induced gene; induced upon low-level peroxide stress; possibly an essential gene, disruptants not obtained by UAU1 method	1.55472	0.004273
orf19.1464	<i>BMT5</i>	Putative beta-mannosyltransferase involved in beta-1,2-mannosylation of phospholipomannan; member of a 9-member family that includes Bmt1p, Bmt2p, Bmt3p, and Bmt4p with roles in mannosylation of cell wall phosphopeptidomannan	1.55577	3.09E-05
orf19.5605		Ortholog(s) have protein binding, bridging, ubiquitin protein ligase binding activity and role in positive regulation of ubiquitin-dependent endocytosis, regulation of intracellular transport	1.55711	0.002581
orf19.56	<i>ARG2</i>	Putative enzyme of arginine biosynthesis; transcription of genes of arginine biosynthesis pathway, except for ARG2, is induced upon phagocytosis by macrophage	1.56069	0.000303
orf19.4874	<i>MNN3</i>	Predicted Golgi alpha-1,2-mannosyltransferase; mutation confers hypersensitivity to toxic ergosterol analog, and to amphotericin B; late-stage biofilm-induced gene	1.56173	0.000242
orf19.1185		Ortholog(s) have ubiquitin-protein ligase activity and role in establishment of mitotic spindle orientation, mitotic cell cycle spindle assembly checkpoint, protein autoubiquitination, septin ring assembly	1.56256	0.000496
orf19.2799	<i>GPI8</i>	Protein similar to <i>S. cerevisiae</i> Gpi8p, which is a subunit of the GPI transamidase complex that adds GPI anchors to proteins; likely to be essential for growth, based on an insertional mutagenesis strategy	1.56441	1.68E-05
orf19.621		Predicted ORF from Assembly 19; removed from Assembly 20	1.56683	0.004212
orf19.1750	<i>SLR1</i>	Protein similar to mammalian SR-like RNA splicing factor, involved in filamentous growth and virulence; gene has intron	1.56914	0.000409
orf19.2190	<i>VRP1</i>	Verprolin-related protein involved in actin cytoskeleton organization and polarized morphogenesis; interacts with Wallp and Myo5p; downregulated upon adherence to polystyrene	1.57178	9.91E-05

orf19.4869	<i>SFUI</i>	Transcriptional regulator of iron-responsive genes; represses iron utilization genes if iron is present; Hap43p-repressed; promotes gastrointestinal commensalism in mice	1.57436	0.000222
orf19.6780	<i>MET8</i>	Putative bifunctional dehydrogenase and ferrochelatase with a predicted role in siroheme biosynthesis; regulated by Gcn2p and Gcn4p	1.57838	0.00596
orf19.3237		Ortholog(s) have cytosol, mitochondrion, nucleus localization	1.57992	0.00023
orf19.157		Predicted ORF from Assembly 19; merged with orf19.156 in Assembly 20	1.58138	0.000214
orf19.2400		Ortholog(s) have role in mRNA splicing, via spliceosome, maturation of SSU-rRNA, positive regulation of ATPase activity, positive regulation of helicase activity	1.5832	0.000299
orf19.6991	<i>PRE3</i>	Putative beta-1 proteasome subunit; macrophage-induced protein; regulated by Gcn2p and Gcn4p; GlcNAc-induced protein	1.58413	4.62E-05
orf19.4812		Ortholog(s) have holo-[acyl-carrier-protein] synthase activity, role in protein-cofactor linkage and mitochondrion localization	1.58671	0.004891
orf19.2507	<i>ARP9</i>	Protein similar to <i>S. cerevisiae</i> Arp3p, a component of the Arp2/3 complex involved in actin-dependent processes; likely to be essential for growth, based on an insertional mutagenesis strategy	1.58798	0.000255
orf19.6639		Hap43p-repressed gene	1.58988	0.002243
orf19.882	<i>HSP78</i>	Putative heat-shock protein; transcriptionally regulated by macrophage response; transcription is regulated by Nrg1p, Mig1p, Gcn2p, Gcn4p, Mnl1p; heavy metal (cadmium) stress-induced; stationary phase enriched protein	1.60091	0.002241
orf19.3445	<i>HOC1</i>	Protein with similarity to mannosyltransferases; similar to <i>S. cerevisiae</i> Hoc1p and <i>C. albicans</i> Och1p	1.60092	0.000798
orf19.6284		Ortholog(s) have GTP binding, signal recognition particle binding activity, role in protein targeting to ER and integral to endoplasmic reticulum membrane localization	1.60093	0.000196

orf19.486	<i>NIP100</i>	p150 subunit of dynactin; required for normal spindle formation and position	1.60107	0.066069
orf19.3768		Predicted ORF from Assembly 19; merged with orf19.736 in Assembly 20	1.60315	0.000321
orf19.5777		Predicted ORF in Assemblies 19, 20 and 21; induced upon biofilm formation	1.60512	0.000126
orf19.2269		Putative 3-phosphoserine phosphatase; fungal-specific (no human or murine homolog); increased transcription observed upon benomyl treatment or in an azole-resistant strain that overexpresses MDR1; early-stage biofilm-induced	1.60538	0.000917
orf19.1848.1		Ortholog of <i>S. cerevisiae</i> : KSH1, <i>C. parapsilosis</i> CDC317 : CPAR2_203260, <i>Candida tenuis</i> NRRL Y-1498 : CANTEDRAFT_116778 and <i>Debaryomyces hansenii</i> CBS767 : DEHA2A10604g	1.60693	9.81E-06
orf19.1949	<i>VPS1</i>	Dynamamin-family GTPase-related protein; induced upon adherence to polystyrene; regulated by Gcn2p and Gcn4p	1.60762	0.000972
orf19.609		Predicted ORF in Assemblies 19, 20 and 21; transcription is specific to white cell type	1.60874	0.001478
orf19.5841		Ortholog of <i>C. parapsilosis</i> CDC317 : CPAR2_212340, <i>Candida tenuis</i> NRRL Y-1498 : CANTEDRAFT_101113, <i>Debaryomyces hansenii</i> CBS767 : DEHA2G03784g and <i>Candida dubliniensis</i> CD36 : CD36_17700	1.61256	0.004665
orf19.2637		Ortholog(s) have Golgi apparatus, fungal-type vacuole membrane localization	1.61418	0.001504
orf19.1531		Ortholog(s) have RNA binding, protein heterodimerization activity, role in mRNA cleavage, mRNA polyadenylation and mRNA cleavage factor complex, mitochondrion localization	1.61719	0.003711
orf19.7547		Ortholog(s) have phosphatidylinositol-3-phosphate binding, ubiquitin-protein ligase activity, role in protein ubiquitination and cytosol, fungal-type vacuole membrane, late endosome, nucleus localization	1.61747	0.000746
orf19.3884	<i>FGR50</i>	Protein lacking an ortholog in <i>S. cerevisiae</i> ; transposon mutation affects filamentous growth	1.61777	1.70E-06

orf19.1451	<i>SRB9</i>	Subunit of the RNA polymerase II mediator complex; transposon mutation affects filamentous growth; suppresses <i>S. cerevisiae</i> diploid filamentous (<i>flo8</i> , <i>ste7</i> , <i>ste12</i> , <i>tec1</i>) or haploid invasive (<i>flo8</i>) mutant growth defects	1.61854	0.006181
orf19.2972	<i>PDE2</i>	Cyclic nucleotide phosphodiesterase, high affinity; role in moderating signaling via cAMP; required for wild-type virulence, hyphal growth, switching, and cell wall, but not for pseudohyphal growth; expressed shortly after hyphal induction	1.61877	0.007419
orf19.7089	<i>PMR1</i>	Putative secretory pathway P-type Ca ²⁺ /Mn ²⁺ -ATPase; required for protein glycosylation and cell wall maintenance; required for hyphal tip oscillation in semisolid substrate; putative ortholog of <i>S. cerevisiae</i> PMR1	1.62062	0.000229
orf19.6712		Ortholog(s) have COPI-coated vesicle, Golgi apparatus localization	1.62069	0.002819
orf19.1465		Has domain(s) with predicted N-acetyltransferase activity and role in metabolic process	1.62133	0.002837
orf19.6416		Ortholog(s) have role in cellular response to oxidative stress, protein N-linked glycosylation and endoplasmic reticulum membrane localization	1.62545	0.000133
orf19.1636	<i>STE50</i>	Protein with sterile alpha motif (SAM) and Ras-associated domain (RAD); similar to <i>S. cerevisiae</i> Rad50p, which is involved in signal transduction via interaction with and regulation of MAPKKK	1.62671	7.35E-05
orf19.5213.2	<i>COx9</i>	Putative subunit VIIa of cytochrome c oxidase; flucytosine induced	1.62889	5.66E-05
orf19.6338		Ortholog of <i>Candida albicans</i> WO-1 : CAWG_05352	1.63025	0.001952
orf19.1604		Protein with a Gal4p-like DNA-binding domain	1.63027	0.003226
orf19.4134		Ortholog(s) have plasma membrane localization	1.63047	0.003651
orf19.6706	<i>GYP7</i>	Protein similar to <i>S. cerevisiae</i> Gyp7p (GTPase-activating protein for Ypt1p); caspofungin-induced	1.63363	0.000817

orf19.5821		Ortholog of <i>S. cerevisiae</i> : YML002W, <i>C. glabrata</i> CBS138 : CAGL0L07634g, <i>C. parapsilosis</i> CDC317 : CPAR2_212430 and <i>Candida tenuis</i> NRRL Y-1498 : CANTEDRAFT_128807	1.63458	0.001856
orf19.1078	<i>HBR2</i>	Putative alanine glyoxylate aminotransferase; regulated by Gcn4p and hemoglobin; stationary phase enriched protein	1.63503	0.001018
orf19.3132		Predicted ORF in Assemblies 19, 20 and 21; induced by nitric oxide	1.64053	0.002169
orf19.7317	<i>UGA33</i>	Zinc-finger transcription factor; similar to <i>S. cerevisiae</i> Uga3p which regulates gamma-aminobutyrate metabolism gene expression; required for yeast cell adherence to silicone substrate	1.64255	5.52E-05
orf19.6382		Putative MRP/CFTR-subfamily ABC transporter; member of multidrug resistance-associated protein (MRP) subfamily of ABC family; similar to <i>S. cerevisiae</i> Bpt1p	1.64313	0.002555
orf19.4172		Has domain(s) with predicted hydrolase activity and role in metabolic process	1.6436	0.005859
orf19.1821		Predicted ORF in Assemblies 19, 20 and 21; transcription is repressed in response to alpha pheromone in SpiderM medium	1.64455	0.006538
orf19.1360		Ortholog(s) have role in mitochondrial genome maintenance and mitochondrion localization	1.64646	0.000781
orf19.5967	<i>FGR44</i>	Protein lacking an ortholog in <i>S. cerevisiae</i> ; transposon mutation affects filamentous growth	1.64997	0.003837
orf19.7115	<i>SAC7</i>	Putative GTPase activating protein (GAP) for RHO1; downregulated upon adherence to polystyrene; macrophage/pseudohyphal-repressed; transcription is upregulated in RHE model of oral candidiasis and in clinical oral candidiasis	1.65229	0.000561
orf19.7581		Ortholog(s) have role in spliceosomal complex assembly and U2 snRNP, U2-type prespliceosome localization	1.65292	0.001354
orf19.2196		Ortholog(s) have ubiquitin binding activity and cytoplasm localization	1.65482	0.005971

orf19.1621	<i>GPA2</i>	G-protein alpha subunit; regulates filamentous growth, copper resistance; involved in cAMP-mediated glucose signaling; reports differ on role in cAMP-PKA pathway, MAP kinase cascade; Gpr1p C terminus binds Gpa2p; regulates HWP1 and ECE1	1.65676	0.001159
orf19.4757	<i>NARI</i>	Putative cytosolic iron-sulfur (FeS) protein assembly machinery protein; induced by nitric oxide; oxidative stress-induced via Cap1p	1.6579	0.002459
orf19.3767		Ortholog(s) have signal sequence binding activity, role in protein targeting to vacuole and Golgi apparatus localization	1.65844	0.006934
orf19.7244		Putative fumarylacetoacetate hydrolase; biofilm-induced gene; induced by nitric oxide independent of Yhb1p; regulated by Sef1p-, Sfu1p-, and Hap43p	1.66561	0.000406
orf19.28		Putative thiamine transmembrane transporter; biofilm-induced	1.66691	0.084545
orf19.5614		Putative ribonuclease H1; biofilm-induced gene; possibly an essential gene, disruptants not obtained by UAU1 method	1.66792	0.000325
orf19.2896	<i>SOU1</i>	Enzyme involved in utilization of L-sorbose; has sorbitol dehydrogenase, fructose reductase, and sorbose reductase activities; NAD-binding site motif; transcriptional regulation affected by chromosome 5 copy number; Hap43p-induced gene	1.66812	3.87E-06
orf19.4294		Ortholog(s) have oxidoreductase activity, role in cytochrome c-heme linkage, mitochondrial membrane organization and extrinsic to mitochondrial inner membrane localization	1.66964	0.00014
orf19.105	<i>HAL22</i>	Putative phosphoadenosine-5'-phosphate (PAP) or 3'-phosphoadenosine 5'-phosphosulfate (PAPS) phosphatase; possible role in sulfur recycling; induced upon biofilm formation; Hap43p-repressed gene	1.67035	0.001214
orf19.6464		Predicted ORF in Assemblies 19, 20 and 21; induced upon adherence to polystyrene; oxidative stress-induced via Cap1p	1.67258	0.004459
orf19.5174	<i>TAF19</i>	Putative TFIID subunit; mutation confers hypersensitivity to amphotericin B	1.67349	0.004794
orf19.6606		Ortholog of <i>C. parapsilosis</i> CDC317 : CPAR2_201040, <i>Candida tenuis</i> NRRL Y-1498 : CANTEDRAFT_112677, <i>Debaryomyces hansenii</i> CBS767 : DEHA2E02420g and <i>Pichia stipitis</i> Pignal : PICST_37559	1.6746	4.35E-06

orf19.2675		Ortholog(s) have mRNA binding activity, role in spliceosomal complex assembly and U2 snRNP, U2-type prespliceosome localization	1.67498	0.003687
orf19.7678	<i>ATP16</i>	Subunit of the mitochondrial F1F0 ATP synthase; sumoylation target; protein newly produced during adaptation to the serum	1.67542	0.002419
orf19.4567		Catechol 1,2-dioxygenase (1,2-CTD), involved in degradation of aromatic compounds	1.67578	0.004963
orf19.4761	<i>HST1</i>	Putative histone deacetylase, involved in regulation of white-opaque switching	1.67649	0.005219
orf19.4307		Ortholog(s) have role in late endosome to vacuole transport via multivesicular body sorting pathway, protein targeting to vacuole and late endosome localization	1.68283	0.002341
orf19.6525		Predicted ORF in Assemblies 19, 20 and 21; transcriptionally activated by Mnl1p under weak acid stress	1.68397	3.99E-05
orf19.3674	<i>GAL102</i>	UDP-glucose 4,6-dehydratase with role in mannosylation of cell wall proteins; mutation confers hypersensitivity to toxic ergosterol analog; overlaps orf19.3673	1.68485	0.000151
orf19.1294		Predicted ORF from Assembly 19; merged with orf19.2629 in Assembly 20	1.68994	0.001625
orf19.1278		Predicted ORF from Assembly 19; merged with orf19.4403 in Assembly 20	1.69286	0.006664
orf19.274	<i>TFC4</i>	Putative RNA polymerase III transcription initiation factor complex (TFIIIC) subunit; transcriptionally activated by Mnl1p under weak acid stress; possibly an essential gene, disruptants not obtained by UAU1 method	1.69701	0.000129
orf19.7183		Ortholog(s) have role in protein folding in endoplasmic reticulum and ER membrane protein complex localization	1.70006	0.001198
orf19.3340	<i>SOD2</i>	Mitochondrial Mn-containing superoxide dismutase; protection against oxidative stress; homotetramer active; N-terminal 34 amino acids removed on mitochondrial import; H2O2-induced via Cap1p; Hap43p-, alkaline-downregulated, farnesol-induced	1.70121	0.000134

orf19.5194.1		Putative protein of unknown function; clade-associated gene expression	1.70152	0.007156
orf19.2180		Ortholog(s) have calcium ion binding, zinc ion binding activity, role in axial cellular bud site selection, bipolar cellular bud site selection, regulation of COPII vesicle coating and cellular bud neck, cytosol, nucleus localization	1.70406	0.001504
orf19.6864		Has domain(s) with predicted ubiquitin-protein ligase activity, role in protein ubiquitination and ubiquitin ligase complex localization	1.70496	0.006062
orf19.5302	<i>PGA31</i>	Cell wall protein; putative GPI anchor; expression is regulated upon white-opaque switching; induced by Congo Red and by cell wall regeneration	1.70521	0.001583
orf19.337		Ortholog(s) have SNAP receptor activity and role in Golgi to vacuole transport, intra-Golgi vesicle-mediated transport, vacuole fusion, non-autophagic, vesicle fusion	1.70564	0.001205
orf19.1655.3		Ortholog(s) have role in cation transport, regulation of membrane potential and plasma membrane localization	1.7081	1.67E-05
orf19.551		Ortholog of <i>C. parapsilosis</i> CDC317 : CPAR2_204170, <i>Candida tenuis</i> NRRL Y-1498 : CANTEDRAFT_110235, <i>Debaryomyces hansenii</i> CBS767 : DEHA2F17072g and <i>Candida dubliniensis</i> CD36 : CD36_29980	1.70971	0.001508
orf19.2785	<i>ATP7</i>	Putative subunit of the F1F0-ATPase complex; shows colony morphology-related gene regulation by Ssn6p; farnesol-, macrophage-downregulated protein abundance; protein present in exponential and stationary yeast growth phases; Hap43p-induced	1.71654	0.001234
orf19.7187	<i>MAM33</i>	Putative mitochondrial acidic matrix protein; regulated by Ssn6p; protein present in exponential and stationary growth phase yeast cultures	1.7198	0.005241
orf19.804		Ortholog(s) have mitochondrion localization	1.72247	0.005723
orf19.1659	<i>ALG8</i>	Putative glucosyltransferase involved in cell wall mannan biosynthesis; transcription is elevated in <i>nik1</i> and <i>sln1</i> homozygous null mutants, but not in the <i>chk1</i> null mutant; possibly an essential gene, disruptants not obtained by UAU1 method	1.72364	0.000133
orf19.1175		ORF, Deleted from Assembly 20	1.72377	0.002565

orf19.6861		Ortholog(s) have ubiquitin-protein ligase activity and role in anaphase-promoting complex-dependent proteasomal ubiquitin-dependent protein catabolic process, chromatin assembly, protein ubiquitination	1.7248	0.003192
orf19.7276.1	<i>TLO4</i>	Member of a family of telomere-proximal genes of unknown function; transcription is upregulated in an RHE model of oral candidiasis; Hap43p-repressed gene	1.72508	0.006475
orf19.1856		Ortholog(s) have histone deacetylase activity	1.7254	0.001915
orf19.6470	<i>AHP2</i>	Putative thiol-specific peroxiredoxin; macrophage-downregulated gene	1.72667	0.000839
orf19.3806		Ortholog(s) have role in negative regulation of gluconeogenesis, proteasomal ubiquitin-dependent protein catabolic process, traversing start control point of mitotic cell cycle and GID complex, cytoplasm, nucleus localization	1.72853	3.82E-06
orf19.6964		Predicted ORF from Assembly 19; removed from Assembly 20	1.73214	0.005635
orf19.3542	<i>LEM3</i>	Putative membrane protein; early-stage biofilm-induced gene; mutation causes increased resistance to miltefosine	1.73402	0.003359
orf19.6662		Putative coenzyme Q (ubiquinone) binding protein; transcription is upregulated in clinical isolates from HIV+ patients with oral candidiasis	1.73426	0.000101
orf19.2215	<i>GLE1</i>	Putative nucleoporin; moderately induced at 42 degrees C	1.7351	5.61E-05
orf19.844	<i>STE11</i>	Protein similar to <i>S. cerevisiae</i> Ste11p; mutants are sensitive to growth on H2O2 medium (1.7366	0.000293
orf19.3544		Putative protein of unknown function; Hap43p-repressed gene	1.73697	0.000575
orf19.639		Predicted ORF in Assemblies 19, 20 and 21; decreased transcription is observed upon fluphenazine treatment or in an azole-resistant strain that overexpresses CDR1 and CDR2	1.74812	0.00452

orf19.5335	<i>SGSI</i>	RecQ-related DNA helicase; Bloom's syndrome-related gene; haploinsufficient for wild-type lifespan; upregulated in farnesol treated biofilm	1.74815	0.00191
orf19.2252		Ortholog of <i>C. parapsilosis</i> CDC317 : CPAR2_406690, <i>Lodderomyces elongisporus</i> NRLL YB-4239 : LELG_02433, <i>Candida dubliniensis</i> CD36 : CD36_21270 and <i>Pichia stipitis</i> Pignal : PICST_33114	1.75062	3.50E-06
orf19.1756	<i>GPD1</i>	Putative glycerol-3-phosphate dehydrogenase; role in glycerol biosynthesis; biofilm-induced expression; regulated by Efg1p; regulated by Tsa1p, Tsa1Bp under H2O2 stress conditions	1.75606	0.001963
orf19.3364		Ortholog of <i>C. parapsilosis</i> CDC317 : CPAR2_403360, <i>Debaryomyces hansenii</i> CBS767 : DEHA2D00814g, <i>Candida dubliniensis</i> CD36 : CD36_43140 and <i>Pichia stipitis</i> Pignal : PICST_32156	1.75777	0.002545
orf19.5213		Putative protein of unknown function, transcription is upregulated in clinical isolates from HIV+ patients with oral candidiasis	1.75852	0.003926
orf19.7038		Ortholog(s) have phosphatidylinositol-3-phosphate binding activity, role in protein targeting to vacuole and cytoplasm, nucleus localization	1.76292	0.001813
orf19.3453		Ortholog(s) have cytoplasm localization	1.76639	0.006791
orf19.5311		Ortholog of <i>C. parapsilosis</i> CDC317 : CPAR2_402060, <i>Candida dubliniensis</i> CD36 : CD36_43850, <i>Pichia stipitis</i> Pignal : PICST_68242 and <i>Candida tropicalis</i> MYA-3404 : CTRG_00303	1.76694	0.003797
orf19.7444		Ortholog(s) have cytoplasm, holo TFIIF complex localization	1.77107	0.000377
orf19.5503		Putative protein of unknown function, transcription is upregulated in clinical isolates from HIV+ patients with oral candidiasis	1.77822	0.002464
orf19.1500		Ortholog of <i>C. parapsilosis</i> CDC317 : CPAR2_210210, <i>Candida tenuis</i> NRRL Y-1498 : CANTEDRAFT_128446, <i>Debaryomyces hansenii</i> CBS767 : DEHA2B04092g and <i>Candida dubliniensis</i> CD36 : CD36_16720	1.77859	0.006796
orf19.4242	<i>CST20</i>	Protein kinase of Ste20p/p65PAK family, required for wild-type mating efficiency and virulence in a mouse model; Cst20p-Hst7p-Cek1p-Cph1p MAPK pathway regulates some hyphal growth; involved in Cdc42p growth regulation	1.77963	0.00062

orf19.6731.1		Ortholog of <i>C. parapsilosis</i> CDC317 : CPAR2_808260, <i>Candida dubliniensis</i> CD36 : CD36_87460, <i>Candida tropicalis</i> MYA-3404 : CTRG_05596 and <i>Candida albicans</i> WO-1 : CAWG_03064	1.78124	0.001574
orf19.1159		Protein similar to <i>A. nidulans</i> CYSA serine O-trans-acetylase, suggesting that <i>C. albicans</i> uses an O-acetyl-serine (OAS) pathway of sulfur assimilation; induced upon biofilm formation	1.78245	0.001336
orf19.4375.1	<i>RPS30</i>	Putative 40S ribosomal protein S30; shows colony morphology-related gene regulation by Ssn6p	1.78291	0.003283
orf19.2191		Ortholog(s) have role in endocytic recycling, peptidyl-diphthamide biosynthetic process from peptidyl-histidine and cytosol, endosome, nucleus localization	1.78614	0.007039
orf19.1035	<i>WARI</i>	Zinc cluster transcription factor; plays a role in resistance to weak organic acids; required for yeast cell adherence to silicone substrate	1.78921	0.007313
orf19.1975		Ortholog(s) have role in mRNA splicing, via spliceosome, mitotic cell cycle G2/M transition checkpoint, regulation of mitotic metaphase/anaphase transition and U4/U6 x U5 tri-snRNP complex, U5 snRNP localization	1.79069	0.000136
orf19.4439.1		Ortholog(s) have role in nucleotide-excision repair, phosphorylation of RNA polymerase II C-terminal domain, transcription from RNA polymerase II promoter and core TFIID complex, cytosol, holo TFIID complex localization	1.79199	0.000151
orf19.1083		Putative protein of unknown function; macrophage-induced gene	1.79299	2.60E-05
orf19.2104		Ortholog(s) have chaperone binding activity, role in aerobic respiration, iron-sulfur cluster assembly and mitochondrion localization	1.79338	0.006465
orf19.2166		Putative vacuolar H(+)-ATPase; plasma membrane localized	1.79441	0.001861
orf19.876	<i>PGA33</i>	Putative GPI-anchored protein	1.79534	0.001525
orf19.2758	<i>PGA38</i>	Putative GPI-anchored protein; adhesin-like protein; repressed during cell wall regeneration; possibly an essential gene, disruptants not obtained by UAU1 method	1.80212	0.004919

orf19.4175	<i>TOK1</i>	Outwardly rectifying, noisily gated potassium channel; modulates sensitivity to human salivary histatin (Hst5); very similar to <i>S. cerevisiae</i> Tok1p	1.80288	5.28E-05
orf19.867		Ortholog(s) have ribosome localization	1.80635	0.000182
orf19.3146		Predicted ORF from Assembly 19; merged with orf19.2227 in Assembly 20	1.8075	0.010086
orf19.1548		Ortholog(s) have role in mRNA splicing, via spliceosome and U4/U6 x U5 tri-snRNP complex localization	1.80783	0.000246
orf19.4626		Ortholog(s) have role in TOR signaling cascade, positive regulation of transcription from RNA polymerase I promoter and cytosol, extrinsic to membrane, nucleus localization	1.80901	0.005561
orf19.3483		Putative phosphatidyl glycerol phospholipase C; late-stage biofilm-induced gene; Plc1p-regulated	1.81038	0.028086
orf19.3153	<i>MSS4</i>	Phosphatidylinositol-4-phosphate 5-kinase; activity induced by phosphatidic acid (Pld1p product); macrophage/pseudohyphal-repressed; mRNA binds to She3p and is localized to yeast cell buds and hyphal tips; Hap43p-induced gene	1.81425	0.003362
orf19.1417		Ortholog of <i>C. parapsilosis</i> CDC317 : CPAR2_401720, <i>Candida tenuis</i> NRRL Y-1498 : CANTEDRAFT_102588, <i>Debaryomyces hansenii</i> CBS767 : DEHA2G16698g and <i>Candida dubliniensis</i> CD36 : CD36_43970	1.81566	0.001323
orf19.3290		Plasma membrane-localized protein; repressed by nitric oxide; Hap43p-repressed gene	1.816	1.81E-05
orf19.3922		Possible pyrimidine 5' nucleotidase; protein present in exponential and stationary growth phase yeast cultures; Hap43p-repressed gene	1.81737	4.81E-05
orf19.1911	<i>PGA52</i>	GPI-anchored cell surface protein of unknown function; Hap43p-repressed gene; fluconazole-induced; possibly an essential gene, disruptants not obtained by UAU1 method	1.82397	0.002207
orf19.4187		Ortholog(s) have role in mitochondrial genome maintenance, phospholipid transport, protein import into mitochondrial outer membrane and ERMES complex, integral to endoplasmic reticulum membrane localization	1.82475	0.000752

orf19.4534		Putative UBx-domain (ubiquitin-regulatory domain) protein; macrophage-downregulated gene	1.83254	6.23E-05
orf19.2612		Putative zinc finger DNA-binding transcription factor; expression downregulated in an <i>ssr1</i> null mutant; late-stage biofilm-induced gene	1.83855	0.064755
orf19.5751	<i>ORM1</i>	Putative endoplasmic reticulum membrane protein; Hap43p-repressed gene; mutation confers hypersensitivity to aureobasidin A	1.84394	0.001056
orf19.7127.1		Putative protein of unknown function, transcription is upregulated in an RHE model of oral candidiasis	1.84424	2.13E-07
orf19.3535		Ortholog(s) have cellular bud neck, fungal-type vacuole localization	1.84649	0.000258
orf19.4250		Ortholog of <i>C. parapsilosis</i> CDC317 : CPAR2_502480, <i>Candida tenuis</i> NRRL Y-1498 : CANTEDRAFT_115972, <i>Debaryomyces hansenii</i> CBS767 : DEHA2G19976g and <i>Candida dubliniensis</i> CD36 : CD36_52200	1.84665	0.000359
orf19.7044	<i>RIM15</i>	Ortholog(s) have protein kinase activity, role in age-dependent response to oxidative stress involved in chronological cell aging, protein phosphorylation, regulation of meiosis and cytosol, nucleus localization	1.85386	0.001158
orf19.4590	<i>RFx2</i>	Transcriptional repressor; regulator of filamentation, response to DNA damage, adhesion, virulence in murine mucosal, systemic infections; RFx domain; regulated by Nrg1p, UV-induced; partially complements <i>S. cerevisiae</i> rfx1 mutant defects	1.86068	0.001299
orf19.6308		Ortholog of <i>Candida albicans</i> WO-1 : CAWG_01818	1.86456	0.003177
orf19.3135		Ortholog(s) have protein binding, bridging activity and role in ER-associated protein catabolic process, lipid particle organization	1.86604	0.000192
orf19.7507		Has domain(s) with predicted oxidoreductase activity, role in antibiotic biosynthetic process and cytoplasm localization	1.86683	0.000115
orf19.3772		Predicted ORF in Assemblies 19, 20 and 21; merged with orf19.3773 in Assembly 21	1.86976	2.58E-05

orf19.3554	<i>AATI</i>	Aspartate aminotransferase; soluble protein in hyphae; macrophage-induced protein; alkaline upregulated; amphotericin B repressed; gene used for strain identification by multilocus sequence typing; farnesol-, Hap43p-induced; GlcNAc-induced	1.87091	0.001238
orf19.2988		Biofilm-induced gene	1.87247	0.003849
orf19.3122.2		Ortholog(s) have role in exocytosis, filamentous growth, mRNA export from nucleus, proteasomal ubiquitin-dependent protein catabolic process, proteasome assembly, regulation of cell cycle	1.87584	0.000268
orf19.1301		Ortholog(s) have cytoplasm, nucleus, ribosome localization	1.87813	0.005488
orf19.4349.6		ORF Predicted by Annotation Working Group; removed from Assembly 20	1.88423	0.005192
orf19.6625		Ortholog(s) have acetyltransferase activator activity, histone binding activity and role in double-strand break repair via nonhomologous end joining, nucleosome assembly, positive regulation of histone acetylation	1.88548	0.005798
orf19.1861		Late-stage biofilm-induced	1.88587	5.39E-06
orf19.642		Ortholog of <i>C. parapsilosis</i> CDC317 : CPAR2_203380, <i>Candida tenuis</i> NRRL Y-1498 : CANTEDRAFT_117493, <i>Debaryomyces hansenii</i> CBS767 : DEHA2G19228g and <i>Candida dubliniensis</i> CD36 : CD36_30470	1.88628	0.00058
orf19.203	<i>STB3</i>	Putative SIN3-binding protein 3 homolog; caspofungin induced; macrophage/pseudohyphal-repressed	1.88637	0.000514
orf19.4637		Ortholog(s) have role in SCF-dependent proteasomal ubiquitin-dependent protein catabolic process, cellular response to methylmercury and SCF ubiquitin ligase complex, cytosol localization	1.89233	0.003494
orf19.2863.1	<i>ERV1</i>	Predicted component of the mitochondrial intermembrane space (IMS), involved in protein import into mitochondrial intermembrane space	1.89935	0.00128
orf19.3421.1	<i>MED19</i>	RNA polymerase II mediator complex subunit	1.90558	0.00161

orf19.2061		Protein not essential for viability	1.90584	0.002252
orf19.6889	<i>MKK2</i>	Protein similar to <i>S. cerevisiae</i> Mkk2p, a MAP kinase kinase involved in signal transduction; macrophage-downregulated gene; mutant is hypersensitive to caspofungin; not essential for viability	1.90672	1.93E-05
orf19.2810	<i>AAP1</i>	Putative amino acid permease; fungal-specific (no human or murine homolog); possibly an essential gene, disruptants not obtained by UAU1 method	1.9082	0.006982
orf19.212	<i>VPS28</i>	ESCRT I protein sorting complex subunit involved in Rim8p processing and proteolytic activation of Rim101p, which regulates pH response; role in echinocandin, azole sensitivity	1.9119	0.000264
orf19.2173	<i>MAFI</i>	Putative negative regulator of RNA polymerase III; decreased expression in hyphae compared to yeast-form cells; caspofungin repressed	1.91531	0.000425
orf19.6753		Predicted ORF in Assemblies 19, 20 and 21; possibly an essential gene, disruptants not obtained by UAU1 method	1.91737	0.000634
orf19.6056		Ortholog(s) have phosphatase activity, role in dephosphorylation and cytosol, nucleus localization	1.91999	0.005787
orf19.2703		Protein similar to <i>S. cerevisiae</i> Ymr171cp; transcriptionally regulated by iron; induced in a <i>ssr1</i> null mutant; fungal-specific (no human or murine homolog)	1.92133	0.000364
orf19.5814		Ortholog of <i>C. parapsilosis</i> CDC317 : CPAR2_303800, <i>Candida tenuis</i> NRRL Y-1498 : CANTEDRAFT_110078, <i>Debaryomyces hansenii</i> CBS767 : DEHA2E21362g and <i>Candida dubliniensis</i> CD36 : CD36_17470	1.92845	0.000123
orf19.7517	<i>CHT1</i>	Chitinase; putative N-terminal catalytic domain; has secretory signal sequence; lacks S/T region and N-glycosylation motifs of Chs2p and Chs3p; alkaline downregulated; expression not detected in yeast-form or hyphal cells	1.93029	6.69E-07
orf19.1872		Plasma membrane protein; repressed by nitric oxide	1.9305	5.96E-05
orf19.5021	<i>PDx1</i>	Pyruvate dehydrogenase complex protein x, an essential component of the mitochondrial pyruvate dehydrogenase complex which is involved in the respiratory pathway; protein present in exponential and stationary growth phase yeast cultures	1.93244	0.000987

orf19.7449		Ortholog(s) have role in mitochondrial genome maintenance, plasmid maintenance and cytosol, mitochondrion localization	1.93805	0.00013
orf19.2411		Ortholog(s) have SNAP receptor activity, role in transport and endosome localization	1.93891	0.000486
orf19.4913		Ortholog(s) have ubiquitin binding activity, role in cellular protein localization, positive regulation of ubiquitin-specific protease activity and cell cortex of cell tip, cell division site, cytosol localization	1.94119	0.001751
orf19.1107		Ortholog(s) have cytoplasm localization	1.94165	0.000191
orf19.191	<i>KIC1</i>	Member of the GCK-III subfamily of eukaryotic Ste20p kinases; in RAM cell wall integrity signaling network; role in cell separation, azole sensitivity; required for hyphal growth; constitutive expression is MTL, white-opaque independent	1.94261	0.001239
orf19.7112	<i>FRP2</i>	Putative ferric reductase; alkaline upregulated by Rim101p; fluconazole-downregulated; upregulated in the presence of human neutrophils; possibly adherence-induced; regulated by Sef1p, Sfu1p, and Hap43p	1.94288	0.005902
orf19.2990	<i>xOG1</i>	Exo-1,3-beta-glucanase; 5 glycosyl hydrolase family member; affects sensitivity to chitin and glucan synthesis inhibitors; not required for yeast-to-hyphal transition or for virulence in mouse systemic infection; Hap43p-induced gene	1.95631	0.002205
orf19.5178	<i>ERG5</i>	Putative C-22 sterol desaturase; fungal C-22 sterol desaturases are cytochrome P450 enzymes of ergosterol biosynthesis, catalyze formation of the C-22(23) double bond in the sterol side chain; transposon mutation affects filamentous growth	1.95848	4.59E-05
orf19.6583		Predicted ORF in Assemblies 19, 20 and 21; transcription is induced in response to alpha pheromone in SpiderM medium	1.95996	0.001209
orf19.6013		Ortholog(s) have cytosol, nucleolus localization	1.96096	0.000708
orf19.6636		Ortholog of <i>S. cerevisiae</i> : YPR084W, <i>C. glabrata</i> CBS138 : CAGL0K07898g, <i>C. parapsilosis</i> CDC317 : CPAR2_702430, <i>Candida tenuis</i> NRRL Y-1498 : CANTEDRAFT_112957 and <i>Candida dubliniensis</i> CD36 : CD36_31160	1.96849	0.005704
orf19.4323		Ortholog(s) have phosphatidylinositol-3-phosphate binding activity and endosome localization	1.96934	0.001141

orf19.5299	<i>ECM1</i>	Putative pre-ribosomal factor; decreased mRNA abundance observed in <i>cyr1</i> homozygous mutant hyphae; induced by heavy metal (cadmium) stress; Hog1p regulated	1.97072	0.002568
orf19.2842	<i>GZF3</i>	Putative transcription factor; oxidative stress-induced via Cap1p; null mutant exhibits abnormal colony morphology and altered sensitivity to fluconazole, LiCl, and copper	1.97753	0.000568
orf19.3263	<i>ATO10</i>	Putative fungal-specific transmembrane protein	1.97952	0.000348
orf19.2711.1	<i>MED20</i>	Subunit of the RNA polymerase II mediator complex; involved in control of filamentous growth and biofilm formation	1.98056	0.004164
orf19.2245	<i>YPT72</i>	Vacuolar Rab small monomeric GTPase involved in vacuolar biogenesis; involved in filamentous growth and virulence	1.98525	0.000507
orf19.1936	<i>SNF1</i>	Essential protein; functional homolog of <i>S. cerevisiae</i> Snf1p regulator of sugar metabolism; constitutively expressed; Thr208 phosphorylation may have regulatory role; up-regulation associated with azole resistance; has polyhistidine tract	1.98544	0.000296
orf19.193		Ortholog of <i>C. parapsilosis</i> CDC317 : CPAR2_209710, <i>Candida tenuis</i> NRRL Y-1498 : CANTEDRAFT_113479, <i>Debaryomyces hansenii</i> CBS767 : DEHA2C15114g and <i>Candida dubliniensis</i> CD36 : CD36_19310	1.98701	0.032247
orf19.4284	<i>BUR2</i>	Protein with similarity to <i>S. cerevisiae</i> Bur2p, contains a cyclin domain; not required for wild-type hyphal growth, adherence to buccal epithelial cells, or virulence in mouse systemic infection	1.99593	0.007553
orf19.2378		Ortholog(s) have role in vacuolar proton-transporting V-type ATPase complex assembly and integral to endoplasmic reticulum membrane localization	1.99874	0.001054
orf19.2393		Putative transcription factor with zinc finger DNA-binding motif	1.99916	0.000194
orf19.4508		Ortholog of <i>Candida albicans</i> WO-1 : CAWG_04200	1.99933	0.000858
orf19.3936		Putative glycerophosphocholine phosphodiesterase; mutation confers hypersensitivity to 5-fluorouracil (5-FU); induced upon biofilm formation	1.99993	0.000579

orf19.7448	<i>LYS9</i>	Putative enzyme of lysine biosynthesis; soluble protein in hyphae; amphotericin B repressed; Gcn4p-regulated; shows colony morphology-related gene regulation by Ssn6p; protein present in exponential and stationary growth phase yeast cells	2.00505	0.000461
orf19.5474		Predicted ORF in Assemblies 19, 20 and 21; transcriptionally activated by Mnl1p under weak acid stress; transcription detected in high-resolution tiling array experiments	2.00778	0.003833
orf19.2026		Ortholog of <i>S. cerevisiae</i> UBP13, a putative ubiquitin carboxyl-terminal hydrolase; late-stage biofilm-induced gene	2.01061	0.000651
orf19.6132		Ortholog of <i>C. parapsilosis</i> CDC317 : CPAR2_701740, <i>Candida tenuis</i> NRRL Y-1498 : CANTEDRAFT_93887, <i>Debaryomyces hansenii</i> CBS767 : DEHA2E04554g and <i>Candida dubliniensis</i> CD36 : CD36_33000	2.01378	0.001583
orf19.852	<i>SAP98</i>	Glycosyl-phosphatidylinositol-anchored aspartic endopeptidase; regulated by Gcn2p and Gcn4p; expressed only in opaque MTLa/MTLa cells	2.02198	0.00071
orf19.6313	<i>MNT4</i>	Putative mannosyltransferase; transcriptionally regulated by iron; expression greater in low iron	2.02487	1.38E-05
orf19.3360		Hap43p-repressed gene; late-stage biofilm-induced	2.02492	8.58E-05
orf19.1121		Ortholog of <i>Candida dubliniensis</i> CD36 : CD36_53470, <i>Spathaspora passalidarum</i> NRRL Y-27907 : SPAPADRAFT_55715, <i>Candida tropicalis</i> MYA-3404 : CTRG_05538 and <i>Candida albicans</i> WO-1 : CAWG_04746	2.02556	2.86E-06
orf19.4006		Ortholog(s) have cytosol, nucleus localization	2.03708	3.02E-06
orf19.6795		Ortholog(s) have enzyme activator activity	2.0421	0.002929
orf19.3986	<i>PPR1</i>	Putative transcription factor with zinc cluster DNA-binding motif; has similarity to <i>S. cerevisiae</i> Ppr1p, which is a transcription factor involved in the regulation of uracil biosynthesis genes	2.05533	0.004412
orf19.3963		Ortholog(s) have mitochondrion localization	2.05558	1.70E-06

orf19.3176	<i>RIM21</i>	Plasma membrane pH-sensor involved in the Rim101p pH response pathway; required for processins and activation of Rim101p and for alkaline pH-induced hyphal growth	2.05721	0.004479
orf19.5906	<i>ADE2</i>	Phosphoribosylaminoimidazole carboxylase; role in adenine biosynthesis; required for normal growth and virulence in immunosuppressed mouse infection; not induced in GCN response, in contrast to <i>S. cerevisiae</i> ADE2; stationary phase-enriched	2.06508	0.001493
orf19.2005	<i>REG1</i>	Putative protein phosphatase regulatory subunit; Hap43p-repressed gene; macrophage/pseudohyphal-induced; possibly transcriptionally regulated upon hyphal formation; late-stage biofilm-induced	2.0699	0.000173
orf19.3711		Biofilm-induced gene	2.07743	2.11E-05
orf19.6552		Ortholog(s) have thiol oxidase activity, role in protein thiol-disulfide exchange and integral to endoplasmic reticulum membrane localization	2.07882	1.47E-05
orf19.1444		Ortholog(s) have phosphatidylinositol-4,5-bisphosphate binding activity, role in actin cortical patch assembly, actin filament organization, endocytosis and actin cortical patch, mating projection tip localization	2.08306	7.21E-05
orf19.4292		Ortholog(s) have SNAP receptor activity, role in Golgi to vacuole transport, vacuole inheritance and Golgi apparatus, endosome localization	2.09533	2.93E-05
orf19.194		Ortholog of <i>C. parapsilosis</i> CDC317 : CPAR2_209720, <i>Candida tenuis</i> NRRL Y-1498 : CANTEDRAFT_114035, <i>Debaryomyces hansenii</i> CBS767 : DEHA2E10494g and <i>Candida dubliniensis</i> CD36 : CD36_19300	2.09824	0.000175
orf19.4033	<i>PRP22</i>	Putative RNA-dependent ATPase; induced upon adherence to polystyrene; transcriptionally activated by Mnl1p under weak acid stress	2.11775	0.004089
orf19.6884	<i>GWT1</i>	Inositol acyltransferase with role in early steps of GPI anchor biosynthetic process; antifungal drug target	2.11867	0.00432
orf19.3971		Early-stage biofilm-induced gene	2.13346	4.12E-05
orf19.5467	<i>TLO7</i>	Member of a family of telomere-proximal genes of unknown function; may be spliced in vivo	2.147	0.004311

orf19.6596		Putative esterase; possibly transcriptionally regulated by Tac1p; transcriptionally activated by Mnl1p under weak acid stress; protein present in exponential and stationary growth phase yeast cultures	2.14775	0.001232
orf19.4950	<i>AKRI</i>	Ankyrin-repeat protein; increased transcription is observed upon fluphenazine treatment	2.15312	0.005519
orf19.7492	<i>SWC4</i>	Subunit of the NuA4 histone acetyltransferase complex	2.15378	5.78E-06
orf19.792		Ortholog(s) have protein serine/threonine kinase activity, protein serine/threonine/tyrosine kinase activity	2.15696	0.003323
orf19.5620		Stationary phase enriched protein; Gcn4p-regulated; induced by amino acid starvation (3-AT); increased transcription by benomyl treatment or in an azole-resistant strain that overexpresses MDR1; biofilm-induced; overlaps orf19.5621	2.15701	0.005449
orf19.618		Predicted ORF from Assembly 19; removed from Assembly 20	2.15864	0.001507
orf19.979	<i>FASI</i>	Beta subunit of fatty-acid synthase; multifunctional enzyme; fluconazole-induced; Hap43p-induced; amphotericin B, caspofungin repressed; macrophage/pseudohyphal-induced; fungal-specific (no human or murine homolog)	2.1639	0.004702
orf19.4492		Ortholog(s) have role in nuclear division, rRNA processing and nuclear periphery, nucleolus, preribosome, large subunit precursor, spindle pole body localization	2.16453	0.00705
orf19.6811		Ortholog(s) have iron ion binding activity, role in biotin biosynthetic process, iron-sulfur cluster assembly and mitochondrial intermembrane space localization	2.18273	0.00905
orf19.5094	<i>BUL1</i>	Protein not essential for viability; macrophage/pseudohyphal-induced; similar to <i>S. cerevisiae</i> Bul1p, which may be involved in selection of substrates for ubiquitination	2.18615	0.006736
orf19.4199		Ortholog(s) have role in ER to Golgi vesicle-mediated transport and endoplasmic reticulum localization	2.20422	2.26E-06
orf19.2317		Predicted ORF in Assemblies 19, 20 and 21; transcription is induced in response to alpha pheromone in SpiderM medium	2.20826	0.005771

orf19.5286	<i>YCP4</i>	Putative flavodoxin; fungal-specific (no human or murine homolog)	2.22434	0.003845
orf19.1108	<i>HAMI</i>	Putative deoxyribonucleoside triphosphate pyrophosphohydrolase; caspofungin repressed; regulated by Gcn2p and Gcn4p	2.22927	0.003477
orf19.1272		Ortholog(s) have role in regulation of cell size and cytoplasm, nucleus localization	2.23682	0.000938
orf19.5170	<i>ENA21</i>	Predicted ORF similar to <i>S. cerevisiae</i> sodium transporters Ena1p and Ena5p; Gcn4p-regulated; flucytosine, amphotericin B, or ketoconazole-induced; osmotic stress-induced; overlaps orf19.5170.1, which is annotated as a blocked reading frame	2.25231	0.0012
orf19.980		Ortholog(s) have inositol heptakisphosphate kinase activity, inositol hexakisphosphate 1-kinase activity, inositol hexakisphosphate 3-kinase activity, inositol hexakisphosphate 4-kinase activity, inositol hexakisphosphate 6-kinase activity	2.25443	0.000132
orf19.4566		Protein similar to <i>S. cerevisiae</i> Rot1p, which has roles in cytoskeletal dynamics and cell wall biosynthesis; predicted Kex2p substrate	2.25657	0.002783
orf19.3234.1	<i>SFT1</i>	Putative Golgi v-SNARE; Plc1p-regulated	2.25835	0.001316
orf19.637	<i>SDH2</i>	Succinate dehydrogenase, Fe-S subunit; localizes to surface of yeast cells, but not hyphae; transcriptionally regulated by iron; expression greater in high iron; repressed by nitric oxide, Hap43p; induced during log phase aerobic growth	2.26059	0.000639
orf19.7500	<i>PxA1</i>	Putative peroxisomal, half-size adrenoleukodystrophy protein (ALD or ALDp) subfamily ABC family transporter	2.27978	0.002357
orf19.117		Ortholog(s) have SNAP receptor activity, role in vesicle fusion and SNARE complex, extrinsic to plasma membrane localization	2.28877	0.000233
orf19.5022		Ortholog(s) have inorganic cation transmembrane transporter activity and role in cellular cobalt ion homeostasis, cellular manganese ion homeostasis, cobalt ion transport, manganese ion transport	2.28914	2.85E-09
orf19.6246		Ortholog(s) have peptide alpha-N-acetyltransferase activity, role in N-terminal peptidyl-methionine acetylation, cytoskeleton organization, mitochondrion inheritance and NatB complex, cytosol, nucleus localization	2.29137	6.15E-06

orf19.651	<i>LYP1</i>	Putative permease; amphotericin B induced; flucytosine repressed; possibly an essential gene, disruptants not obtained by UAU1 method	2.29589	0.005741
orf19.4653		Transcriptionally regulated by iron; expression greater in low iron; similar to GPI-linked cell-wall proteins	2.30628	0.001428
orf19.2111.2	<i>RPL38</i>	60S ribosomal ribosomal protein subunit; genes encoding cytoplasmic ribosomal subunits, translation factors, tRNA synthetases are downregulated upon phagocytosis by murine macrophage	2.30822	0.001791
orf19.6316.4		Putative nuclear protein; Hap43p-induced gene; ortholog of <i>S. cerevisiae</i> YLR363W-A	2.31031	0.005076
orf19.4445		Protein of unknown function; Plc1p-regulated; expression is upregulated early upon infection of reconstituted human epithelium (RHE), while expression of the <i>C. dubliniensis</i> ortholog is not upregulated; not required for viability	2.31048	7.55E-05
orf19.5639	<i>HIS4</i>	Multifunctional enzyme that catalyzes three steps of histidine biosynthesis, with phosphoribosyl-AMP cyclohydrolase, phosphoribosyl-ATP diphosphatase, and histidinol dehydrogenase activities; required for wild-type adhesion to human cells	2.33559	9.84E-05
orf19.7255	<i>RPC10</i>	Putative RNA polymerase subunit ABC10-alpha of RNA polymerase complexes I, II, and III; flucytosine induced	2.34217	8.80E-06
orf19.6544	<i>LPI9</i>	Ortholog(s) have protein phosphatase 1 binding, protein phosphatase type 1 regulator activity and role in chromosome segregation, regulation of phosphoprotein phosphatase activity	2.34244	8.42E-07
orf19.6635		Ortholog of <i>C. parapsilosis</i> CDC317 : CPAR2_205340, <i>Candida tenuis</i> NRRL Y-1498 : CANTEDRAFT_133521, <i>Debaryomyces hansenii</i> CBS767 : DEHA2E21868g and <i>Candida dubliniensis</i> CD36 : CD36_31170	2.34981	0.006022
orf19.7033		Putative dual specificity protein phosphatase, similar to <i>S. cerevisiae</i> Pps1p	2.36	no replicates
orf19.1766		Secreted protein; fluconazole-induced	2.37457	0.006406
orf19.7055		Ortholog of <i>Candida albicans</i> WO-1 : CAWG_05420	2.37589	0.000645

orf19.3198	<i>OBPA</i>	Similar to oxysterol binding protein; non-sex gene located within the MTL α mating-type-like locus; Plc1p-regulated	2.37675	0.000438
orf19.6881	<i>YTHI</i>	Putative mRNA cleavage and polyadenylation specificity factor; transcription is regulated upon yeast-hyphal switch; decreased expression in hyphae compared to yeast-form cells; fluconazole or flucytosine induced	2.37867	0.005781
orf19.1477		Putative protein of unknown function; Hap43p-repressed gene; <i>S. cerevisiae</i> ortholog YGL010W localizes to the endoplasmic reticulum	2.409	4.52E-07
orf19.278		Protein required for adhesion to abiotic substrate; biofilm-induced	2.42431	0.005689
orf19.1842	<i>BUD5</i>	Predicted GTP/GDP exchange factor for Rsr1p	2.43978	2.87E-06
orf19.6802		Ortholog(s) have palmitoyltransferase activity, role in protein palmitoylation, vacuole fusion, non-autophagic and Golgi apparatus, endoplasmic reticulum, fungal-type vacuole membrane localization	2.44542	0.000484
orf19.5519	<i>GCVI</i>	Putative T subunit of glycine decarboxylase; transcription is negatively regulated by Sfu1p	2.45233	0.000495
orf19.6869		Ortholog(s) have role in protein targeting to membrane and cytoplasm localization	2.46	0.000543
orf19.3742		Predicted ORF in Assemblies 19, 20 and 21; expression regulated during planktonic growth; greater mRNA abundance observed in a <i>cyr1</i> homozygous null mutant than in wild type	2.46949	0.030241
orf19.6782	<i>BMTI</i>	Beta-mannosyltransferase, required for addition of the 1st beta-mannose residue to acid-stable fraction of cell wall phosphopeptidomannan; 9-gene family member; mutants induce higher levels of inflammatory cytokines in mouse dendritic cells	2.47604	0.001793
orf19.2168.3		Ortholog(s) have role in cellular protein localization, endoplasmic reticulum inheritance, endoplasmic reticulum tubular network organization and nuclear pore complex assembly	2.47715	1.10E-05
orf19.6455		Putative protein of unknown function, transcription is upregulated in clinical isolates from HIV+ patients with oral candidiasis	2.49503	0.000167

orf19.72		Predicted ORF from Assembly 19; merged with orf19.4720 in Assembly 20	2.49896	5.58E-05
orf19.847	<i>YIM1</i>	Protein similar to protease of mitochondrial inner membrane; increased transcription is observed upon benomyl treatment; macrophage-downregulated gene	2.50751	0.00099
orf19.6594	<i>PLB3</i>	GPI-anchored cell surface phospholipase B; possibly secreted; fungal-specific (no mammalian homolog); transcription positively regulated by Tbf1p; possible essential gene (UAU1 method); late-stage biofilm-induced gene; fluconazole-induced	2.51507	0.001805
orf19.85	<i>GPx2</i>	Similar to glutathione peroxidase; expression greater in high iron; alkaline upregulated by Rim101p; transcriptionally induced by alpha factor or interaction with macrophage; regulated by Efg1p; caspofungin repressed	2.52121	0.000746
orf19.1562		Late-stage biofilm-induced gene; transcription is repressed in response to alpha pheromone in SpiderM medium	2.53551	7.40E-05
orf19.2050		Ortholog(s) have sterol esterase activity, role in cellular lipid metabolic process, sterol metabolic process and fungal-type vacuole, integral to membrane, lipid particle localization	2.54121	0.002352
orf19.6976		Predicted membrane transporter; member of the proton coupled folate transporter/heme carrier protein (PCFT/HCP) family, major facilitator superfamily (MFS); virulence-group-correlated expression	2.55065	6.98E-06
orf19.4720	<i>CTR2</i>	Putative low-affinity copper transporter of the vacuolar membrane; late-stage biofilm-induced gene; induced by nitric oxide; clade-associated gene expression	2.55668	1.77E-05
orf19.3826		Predicted ORF in Assemblies 19, 20 and 21; Plc1p-regulated	2.56852	0.000832
orf19.4369		Protein not essential for viability	2.58834	0.00023
orf19.2881	<i>MNN4</i>	Regulator of mannosylphosphorylation of N-linked mannans to cell wall proteins; not required for virulence/kidney burden in mice or normal interaction with macrophages; mutants induce high levels of inflammatory cytokines in dendritic cells	2.58953	0.004101
orf19.7374	<i>CTA4</i>	Zinc cluster transcription factor; involved in response to nitric oxide; induced by nitric oxide; transcriptionally activated by Mnl1p under weak acid stress; downregulated upon adherence to polystyrene; Hap43p-repressed	2.6276	0.000928

orf19.7014		Putative protein of unknown function; transcription is positively regulated by Tbf1p; overlaps orf19.7015	2.62791	0.001187
orf19.3893	<i>SCW11</i>	Cell wall protein; transcription decreased in mutant lacking ACE2; downregulated in core caspofungin response; expression greater in high iron; possibly an essential gene, disruptants not obtained by UAU1 method; planktonic growth-induced	2.64787	0.002442
orf19.4166	<i>ZCF21</i>	Predicted Zn2-Cys6 zinc-finger protein; mutants display increased colonization of mouse kidneys	2.66852	4.27E-06
orf19.2607		Ortholog of <i>C. parapsilosis</i> CDC317 : CPAR2_800670, <i>Candida tenuis</i> NRRL Y-1498 : CANTEDRAFT_112575, <i>Debaryomyces hansenii</i> CBS767 : DEHA2C16940g and <i>Candida dubliniensis</i> CD36 : CD36_26980	2.67118	0.004909
orf19.2474	<i>PRC3</i>	Putative carboxypeptidase Y precursor; transcription is regulated by Nrg1p and Mig1p; regulated by Gcn2p and Gcn4p	2.68186	7.41E-05
orf19.1480		Putative succinate dehydrogenase, enzyme of citric acid cycle; downregulated by Efg1p; repressed by nitric oxide; Hap43p-repressed gene	2.68592	0.00111
orf19.449		Putative phosphatidyl synthase; stationary phase enriched protein; transcription reduced upon yeast-hyphal switch; Hap43p-repressed gene; biofilm-induced	2.6864	0.000496
orf19.7670		Putative Ca ²⁺ /H ⁺ antiporter; oral infection upregulated gene; mutants have reduced capacity to damage oral epithelial cells	2.69841	0.001464
orf19.3222		Ortholog(s) have Golgi apparatus, endoplasmic reticulum, fungal-type vacuole membrane localization	2.7068	0.001099
orf19.697		Ortholog(s) have mitochondrial outer membrane localization	2.73118	0.001983
orf19.3448		Predicted ORF in Assemblies 19, 20 and 21; ketoconazole-repressed	2.73598	0.00015
orf19.2706	<i>CRH11</i>	GPI-anchored cell wall transglycosylase, putative ortholog of <i>S. cerevisiae</i> Crh1p; predicted glycosyl hydrolase domain; similar to Csf4p and to antigenic <i>A. fumigatus</i> AspF9; predicted Kex2p substrate; caspofungin-induced	2.74846	0.004043

orf19.4779		Putative transporter; slightly similar to the Sit1p siderophore transporter; Gcn4p-regulated; fungal-specific (no human or murine homolog); transcriptionally activated by Mnl1p under weak acid stress	2.75867	0.001205
orf19.5848		Late-stage biofilm-induced gene; oral infection upregulated gene; mutants have reduced capacity to damage oral epithelial cells	2.75912	0.007263
orf19.3568	<i>RxT3</i>	Putative transcriptional repressor	2.78897	2.69E-05
orf19.1356		Ortholog(s) have thiosulfate sulfurtransferase activity, role in tRNA wobble position uridine thiolation and mitochondrion localization	2.80903	7.57E-05
orf19.1509	<i>ROD1</i>	Protein not essential for viability; similar to <i>S. cerevisiae</i> Rod1p, which is a membrane protein with a role in drug tolerance; repressed by Rgt1p	2.82571	1.98E-06
orf19.2748	<i>ARG83</i>	Zinc-finger protein; clade-associated gene expression; null mutant shows abnormal regulation of invasive colony growth and is unable to utilize proline as a nitrogen source; late-stage biofilm-induced	2.84648	0.00039
orf19.5285	<i>PST3</i>	Putative flavodoxin; biofilm induced; fungal-specific (no human or murine homolog); stationary phase enriched protein	2.85231	0.006739
orf19.94		Ortholog of <i>C. parapsilosis</i> CDC317 : CPAR2_603030, <i>Candida tenuis</i> NRRL Y-1498 : CANTEDRAFT_113701, <i>Debaryomyces hansenii</i> CBS767 : DEHA2F10054g and <i>Candida dubliniensis</i> CD36 : CD36_60970	2.8783	3.52E-05
orf19.4372		Has domain(s) with predicted role in transmembrane transport and integral to membrane localization	2.8838	0.00081
orf19.7336		Predicted membrane transporter, member of the drug:proton antiporter (14 spanner) (DHA2) family, major facilitator superfamily (MFS)	2.91155	2.29E-05
orf19.3567	<i>BIO32</i>	Putative class III aminotransferase with a predicted role in biotin biosynthesis; induced during planktonic growth	2.9605	0.000667
orf19.1996	<i>CHA1</i>	Similar to catabolic serine/threonine dehydratases; negatively regulated by Rim101p; expression greater in low iron; regulated on white-opaque switching; filament induced; transposon mutation affects filamentous growth; biofilm-induced	2.96362	0.001639

orf19.5551	<i>MIF2</i>	Centromere-associated protein; similar to CENP-C proteins; Cse4p and Mif2p colocalize at <i>C. albicans</i> centromeres	2.98228	7.72E-09
orf19.2808	<i>ZCF16</i>	Predicted zinc-finger protein; not essential for viability	2.98848	0.006395
orf19.7198		Ortholog(s) have role in negative regulation of induction of conjugation with cellular fusion and negative regulation of transcription from RNA polymerase II promoter	3.06124	0.000197
orf19.4248		Predicted ORF in Assemblies 19, 20 and 21; regulated by Gcn4p; repressed in response to amino acid starvation (3-aminotriazole treatment)	3.07897	0.004934
orf19.2948	<i>SNO1</i>	Protein with a predicted role in pyridoxine metabolism; expressed during stationary phase; transcription is regulated by Tup1p, Efg1p;	3.10085	0.000673
orf19.1313	<i>CDR3</i>	Transporter of the Pdrp/Cdrp family of the ATP-binding cassette (ABC) superfamily; transports phospholipids in an out-to-in direction; expressed in opaque-phase cells; induced by macrophage interaction; fluconazole-downregulated	3.15883	0.00098
orf19.3190	<i>HAL9</i>	Protein with Zn(2)-Cys(6) binuclear cluster; gene in zinc cluster region of Chr. 5; transcriptionally activated by Mnl1p in weak acid; similar to <i>S. cerevisiae</i> Hal9p, which is a putative transcription factor involved in salt tolerance	3.16476	7.02E-05
orf19.4749		Hap43p-induced gene; hyphal-induced expression, regulated by Cyr1p, Ras1p, Efg1p	3.27669	0.001548
orf19.7106	<i>VPS70</i>	Ortholog(s) have role in protein targeting to vacuole and endoplasmic reticulum localization	3.32907	0.000677
orf19.4099	<i>ECM17</i>	Enzyme of sulfur amino acid biosynthesis; putative role in regulation of cell wall biogenesis; upregulated in biofilm; possibly adherence-induced; regulated by Tsa1p/Tsa1Bp in H2O2 stress; Gcn4p-regulated; Tbf1p-activated; Hap43p-repressed	3.46353	0.001074
orf19.3352		Has domain(s) with predicted nucleotide binding, oxidoreductase activity and role in oxidation-reduction process	3.50041	2.53E-05
orf19.4024	<i>RIB5</i>	Putative riboflavin synthase; fungal-specific (no human or murine homolog); farnesol-downregulated; protein present in exponential and stationary growth phase yeast cultures	3.58654	0.004206

orf19.3577.1		Ortholog(s) have mitochondrial intermembrane space localization	3.60791	0.000212
orf19.7436.1	<i>ECM15</i>	Protein with a predicted role in cell wall organization; Hap43p-repressed gene; caspofungin repressed	3.62313	0.000147
orf19.4593	<i>RGA2</i>	Putative GTPase-activating protein (GAP) for Rho-type GTPase Cdc42p; involved in cell signaling pathways controlling cell polarity; similar to <i>S. cerevisiae</i> Rga2p; induced upon low-level peroxide stress; late-stage biofilm-induced	3.7318	0.005128
orf19.5342		Ortholog(s) have cytosol, fungal-type vacuole, nucleus localization	4.09653	0.000434
orf19.3870	<i>ADE13</i>	Adenylosuccinate lyase; enzyme of adenine biosynthesis; soluble protein in hyphae; not induced during GCN response, in contrast to the <i>S. cerevisiae</i> ortholog; repressed by nitric oxide	4.10905	0.003707
orf19.7098		Putative protein of unknown function; Hap43p-repressed gene; repressed by nitric oxide	4.44856	0.002434
orf19.1641		Ortholog(s) have cytosol, nucleus localization	4.76057	0.00012
orf19.1855		Predicted membrane transporter, member of the anion:cation symporter (ACS) family, major facilitator superfamily (MFS); Gcn4p-regulated; flucytosine induced; ketoconazole-repressed; oxidative stress-induced via Cap1p	4.84589	0.00157
orf19.7514	<i>PCK1</i>	Phosphoenolpyruvate carboxykinase; regulated by hyphal switch, carbon source, Hap43p; repressed on glucose; induced by fluconazole, phagocytosis, H ₂ O ₂ , biofilm formation; induced in oralpharyngeal candidiasis	5.0044	0.005654
orf19.2738	<i>SUL2</i>	Putative sulfate transporter; transcription is negatively regulated by Sfu1p; induced upon biofilm formation; amphotericin B induced	5.73615	0.00022
orf19.670.2		Hap43p-repressed gene; hypoxia downregulated, ketoconazole induced; late-stage biofilm-induced; induced in oralpharyngeal candidiasis	6.0384	0.00158
orf19.2192	<i>GDH2</i>	Putative NAD-specific glutamate dehydrogenase; fungal-specific (no human or murine homolog); transcription is regulated by Nrg1p, Mig1p, Tup1p, and Gcn4p; stationary phase enriched protein; biofilm-induced	6.48147	0.005707

orf19.2991	<i>HOLI</i>	Putative MFS transporter; transcription regulated by Nrg1p; macrophage/pseudohyphal-repressed; transcription induced by alpha pheromone in SpiderM medium; possibly an essential gene, disruptants not obtained by UAU1 method	7.60748	0.002538
orf19.944	<i>IFG3</i>	Putative D-amino acid oxidase	7.82894	0.000759

¹ List of genes modulated differently in the *sfp1Δ/sfp1Δ* (HHCa28) and *SFPI/SFPI* (HHCa1) after incubation in minimal medium to an OD_{600nm} of 0.8. Modulated genes were selected from four independent microarray experiments with an expression cutoff at 1.5 folds and t-test with p < 0.05.

² Name assigned to open reading frame (orf) from assembly 19 of the *Candida albicans* genome.

³ Common name assigned to orf obtained from the Candida Genome Database (<http://www.candidagenome.org/>).

⁴ Description of orf function obtained from the Candida Genome Database (<http://www.candidagenome.org/>).

⁵ Normalized expression levels of orf obtained from the four microarray experiments using GeneSpring v.9.0.

⁶ t-test p value from four microarray experiments performed in GeneSpring v.9.0.